BIOGENESIS OF YEAST TELOMERASE OCCURS THROUGH TWO DIFFERENT NUCLEAR IMPORT PATHWAYS

By

Charlene Hawkins

Dissertation

Submitted to the Faculty of the

Graduate School of Vanderbilt University

in partial fulfillment of the requirements

for the degree of

DOCTOR OF PHILOSOPHY

in

Biological Sciences

August, 2014

Nashville, Tennessee

Approved:

Katherine L. Friedman, Ph.D.

Todd Graham, Ph.D.

Anita Corbett, Ph.D.

Neil Osheroff, Ph.D.

To the memories of my father, Mr. Charlie Smith and my godmother, Mrs. Imogene Essix, always full of loving encouragement, stern support, and great advice.

and

To the memory of Aunt Ruth—always full of laughter and a pleasant smile—though I knew her for a short while, we felt like family.

To my niece and nephew, future scientists in your own right; the buck doesn't stop here.

ACKNOWLEDGEMENTS

Funding for this work was provided by the Cellular, Biochemical, and Molecular Sciences training grant as well as grants 1F31CA154124-01A1 and R01-GM080393-01A1 to me and my mentor, respectively, from the National Institutes of Health. This work was also supported by the Vanderbilt University Department of Biological Sciences and the Gisela Mosig Graduate Student Travel Fund, which enabled me to attend several national meetings. I would like to especially thank the Initiative for Maximizing Student Diversity (IMSD) and its administrators, Drs. Linda Sealy and Roger Chalkley. I would not have been here without the chance provided me by IMSD and for that I will be forever grateful.

I would like to recognize the individuals I have worked with during this project. To the colleagues I have gained along the way, I appreciate your willingness to discuss science with me, to help me with experiments, and to let me borrow reagents. To the members of my dissertation committee, thank you all for your time and input during my tenure as a graduate student. I would be remiss if I did not acknowledge Dr. Wonder Drake to whom I am indebted for the advice, well wishes, and prayers over the years. If it were not for Dr. Drake, I would not have had the opportunity to become acquainted with the world of research. She has been a blessing to me and I am grateful that she continues to believe in me. I would also like to give special thanks to my advisor, Dr. Katherine Friedman. I sincerely appreciate your patience and willingness to help me. I have learned a great deal observing how you approach scientific problems and I am certain that I am a better scientist after having been a member of your lab.

Most of all, I would like to thank my family and friends for their endless love and support. It would not have been possible for me to get to this point without you. I am grateful for my mom's strength and boundless support, for the confidence in knowing that my brother would be there when I needed him, and for my sister's kindness, laughter, and unique perspective. To Barbara, thank you so much for adopting me into your life. Thank you for being there for me on the bad days when it seemed that nothing was going right and on good days to celebrate with me. To my friends, I have learned so much from you—life lessons that I will be with me always.

TABLE OF CONTENTS

Page

LIST OF TABLES

Table Page

LIST OF FIGURES

Figure Page

LIST OF ABBREVIATIONS

aa, amino acid
DC, dyskeratosis congenita (disease)
DKC1, dyskeratosis congenita 1 (gene)
EST, ever shorter telomere
GFP, green fluorescent protein
hTERT, human telomerase reverse transcriptase
hTR, human telomerase RNA
IGC, interchromatin granule cluster
IPF, idiopathic pulmonary fibrosis
kb, kilobase
MCS, multiple cloning site
Nab2NLS, NLS found in the Nab2 mRNA-binding protein in yeast
NAP, nucleotide addition processivity
NLS, nuclear localization sequence
nt, nucleotide
ORF, open reading frame
PY-NLS, proline/tyrosine-containing NLS
RAP, repeat addition processivity
RNP, ribonucleoprotein
SMN, survival motor neuron
snoRNA, small nucleolar RNA
snoRNP, small nucleolar ribonucleoprotein
SV40, simian virus 40
T_{Ag}, SV40 large T antigen protein
T_{Ag}NLS, classical NLS found in the SV40 large T antigen protein
TRF, telomere restriction fragment
U snRNP, Uridine-rich, small nuclear ribonucleoprotein

CHAPTER I

INTRODUCTION AND BACKGROUND

Chapter Overview

The cell uses complexes composed of proteins and RNA—termed ribonucleoproteins (RNP)—to execute vital functions. Such processes include DNA replication, gene splicing, protein translation, etc. [1,2]. Consequently, how the cell coordinates the assembly of ribonucleoproteins is an important biological question. In fact, mutations that disrupt the spatiotemporal associations between the components of certain RNP complexes have been observed to exhibit causal roles in a number of disease states. Such diseases include dyskeratosis congenita [3], poikiloderma with neutropenia [4], spinal muscular atrophy [5] and retinitis pigmentosa [6], and male infertility and Native American Indian childhood cirrhosis [7] among others. Therefore, the study of ribonucleoprotein biogenesis is very important to our understanding of human health and disease.

How are RNPs made? DNA is transcribed into RNA in the nucleus, however RNA is translated into proteins in the cytoplasm. How, then, does the cell regulate RNP assembly? When and where do the components of RNP complexes interact to form mature ribonucleoproteins capable of executing their diverse cellular functions? Given the significance of RNP function in the cell, these questions have shaped my interests and become the focus of my dissertation research. More specifically, my investigations have concentrated on the telomerase enzyme, a nuclear RNP whose activity is regulated in the

cell cycle [8]. Compared to the almost perpetual activity of the majority of other RNPs in the cell, the cell cycle regulation of telomerase activity is a feature that is fairly unique to this enzyme. Therefore, the study of telomerase biogenesis may reveal how the cell accomplishes the biogenesis of other such highly regulated RNPs as well as provide more insight into the general mechanisms modulating RNP assembly in the cell.

In this introductory chapter, I have chosen to highlight the significance of RNP biogenesis more comprehensively, with a particular focus on telomerase. Because telomerase—as well as a number of other cellular RNPs—functions in the nucleus, I address the problem of enzyme biogenesis starting at the source, the nucleus. After this brief discussion summarizing the features that allow the nucleus to execute its varied functions, I describe the process of nuclear localization. With an emphasis on the nuclear pore complex as a major regulator of protein (and RNA) traffic into and out of the nucleus, I include a description of the key proteins and sequence motifs involved in active nuclear transport.

To illustrate the significance of the process of nuclear localization to the cell, I present a discussion of how nuclear localization contributes to normal cell function. I also describe a number of disease states associated with disruptions in the nuclear localization of key proteins. I explain that viruses exploit endogenous nuclear transport mechanisms in their efforts to seize control of a cell. Using the SV40 monkey polyomavirus to exemplify such a virus, I summarize how SV40 was discovered as well as the consequence(s) associated with SV40 infection. This virus is of particular interest because the characterization of its mechanism of action revealed for the first time that the nuclear localization of a key viral protein, the SV40 Large Tumor Antigen protein, was

required for the virus to execute its cytopathic effects [9]. Furthermore, characterization of this critical protein from SV40 led to the identification of the first nuclear localization sequence[10]. Because nuclear localization is an integral step in the biogenesis of many cellular RNPs, the discussion provided in these initial sections of the introduction establish a solid foundation for understanding the mechanisms of RNP biogenesis and the significance of the study of this fundamental cellular process.

In subsequent sections, ribonucleoprotein biogenesis is specifically discussed, focusing on the ribosome and components of the spliceosome. I have chosen to present the biogenesis of these RNP complexes in an effort to describe the general mechanisms controlling RNP biogenesis in the cell and because telomerase biogenesis is hypothesized to occur in a manner similar to that utilized by RNP molecules that comprise the ribosome or the spliceosome[11-14]. The remainder of the chapter focuses on telomerase, beginning with a general description of the telomerase holoenzyme. The next few sections describe human telomerase, synthesizing current data regarding telomerase biogenesis in humans. I also present a discussion of disease states associated with errors in telomerase biogenesis.

As mentioned earlier, my research has focused on elucidating mechanisms of telomerase biogenesis and I have used budding yeast as the model system for my studies. Therefore, the chapter ends with a discussion of telomerase in *Saccharomyces cerevisiae*, including an explanation of how the components of the complex were identified and a summary of the functional role of the Est1p component of yeast telomerase in telomere maintenance. I also describe the current model of telomerase biogenesis in yeast, a model solely based upon studies of the localization of the RNA component of the enzyme [15].

The chapter ends with a description of how I have chosen to approach the problem of telomerase biogenesis: because Est1p is the only telomerase component whose abundance is regulated in the cell cycle [16], I have reasoned that the regulation of this protein may impart the cell cycle regulation of telomerase function. Furthermore, since the current model of telomerase trafficking in the cell is not based upon studies of the protein components of the telomerase RNP in yeast, I have sought to test this model by examining the nuclear localization of Est1p, data for which is included in chapter two.

The Nucleus

The nucleus is one of a number of specialized, membrane-bound organelles—absent in prokaryotes—that serves key functions in eukaryotic cells. Because the nucleus houses and protects the cell's genomic DNA, it can be considered the cell's hard drive, having roles in almost every process the cell executes. The nucleus is the site of DNA synthesis and transcription as well as ribosome biogenesis, serving to isolate these essential, complex cellular processes and, as such, providing a layer of regulation for how and when these processes occur [17].

In addition to chromosomal DNA, the nucleus contains a number of subcompartments and/or domains that facilitate its varied functions. The nuclear lamina consists of a network of filamentous proteins that provide structural support and integrity for the nucleus and help to anchor chromosomes within the nucleus [18]. The nucleolus is a dense assemblage of proteins, such as fibrillin and nucleolin, around the ribosomal DNA repeats and is the site of ribosome subunit assembly in the cell [19]. The nuclear envelope is made up of two concentric phospholipid bilayer membranes separated by up

to 50 nm. Nuclear pores within the nuclear envelope help to regulate macromolecular traffic between the nucleus and the cytoplasm [20]. Other nuclear substructures include Cajal bodies, Gemini of Cajal bodies (or gems), and interchromatin granule clusters (IGC)—each containing specific structural proteins organized around particular types of RNA, thereby aiding in the biogenesis of small nuclear ribonucleoproteins and ultimately helping to facilitate DNA transcription and RNA processing [21-23].

The nucleus is the site of the biogenesis of many RNP complexes that are critical for cell survival. However, the nucleus is encased in a protective barrier that limits its access to enzymes that must function in the nucleus to maintain and express the genome. To overcome this barrier and allow for the regulated entry of such key proteins, the cell uses the process of nuclear localization.

Nuclear Localization

The presence of membrane-bound organelles is a key difference between prokaryotes and eukaryotes. These semipermeable partitions serve to isolate the varied processes required for cell viability, thus helping to facilitate the survival of more complex organisms. The process of nuclear localization (and nuclear export) is an example of how the membrane associated with a particular organelle provides such essential functions—regulation of the types of molecules that enter (and exit) the nucleus. Because this process links the nucleus to the cytoplasm as well as other organelles, it allows the cell to preserve the crosstalk between these organelles while regulating how and when the crosstalk occurs [2].

The nuclear pore complex is a specialized structure that, through size limitations and/or the requirement for specific protein-protein interactions, regulates which molecules can localize to (or be exported from) the nucleus [20]. The nuclear pore complex is comprised of 30 to 50 distinct proteins—called nucleoporins—that interact to form a multi-domain superstructure that extends from the cytoplasm into the nucleoplasm, consisting of a basket-like structure on the nuclear face of the pore attached to a central transporter region and cytoplasmic filaments [24]. Although there is conflicting evidence in the literature regarding the exact size of the nuclear pore [25], most reports indicate that the nuclear pore in mammals has an outer diameter of greater than 100 nm and an inner diameter of approximately 10 nm. The difference in size results from the presence of nucleoporins and their associated filaments that occupy much of the space within the inner channel of the pore [26]. Thus, the nuclear pore forms an aqueous tunnel that allows for the free diffusion into the nucleus of molecules and ions less than 10 nm in diameter or with molecular masses of up to 100 kDa in vertebrates [27].

Although the limited size of the nuclear pore only permits the passive diffusion of small molecules into the nucleus, larger molecules and molecular complexes are able to enter the nucleus through an active transport mechanism, which allows the nuclear pore to stretch to 25 nm in diameter, 2.5 times its normal size [20]. Active transport through the nuclear pore into the nucleus is characterized by two different mechanisms of nuclear transport, classical nuclear import and non-classical nuclear import. Both are defined by specialized proteins termed karyopherins that interact with components of the nuclear pore complex. These pathways make use of a class of karyopherins—commonly called nuclear import receptors or importins—that function in the transport of molecules from

the cytoplasm into the nucleus [28,29]. There are also karyopherins that primarily function in the transport of molecules out of the nucleus (exportins) [30,31] as well a number of karyopherins that can facilitate bidirectional translocation into *and* out of the nucleus [32,33]. To identify particular cargo for transport, these karyopherins utilize special signals within proteins destined for the nucleus called nuclear localization sequences (NLS) [34].

The classical nuclear import machinery is estimated to participate in the nuclear localization of approximately 40% of nuclear proteins [35]. Transport via this pathway is generally first defined by binding of the adapter importin α to a cargo protein harboring a classical NLS [36-38]. Classical NLSs consist of a single cluster of basic residues such as the NLS found in the simian virus 40 (SV40) large T antigen protein (T_{Ag}NLS), comprised of the sequence PKKKRKV [10]. Alternatively, classical NLSs can consist of two clusters of basic residues separated by at least 9 to 29 amino acids (aa) such as the NLS found in nucleoplasmin, bearing the sequence KRPAATKKAGQKKKKLD (residues contributing to nuclear localization are underlined) [35,39]. The importin α-cargo complex also interacts with importin β, a member of the karyopherin family of proteins, to create a ternary protein complex for transport across the nuclear envelope [40-42]. To promote nuclear localization of the cargo protein, importin β then interacts with components of the nuclear pore complex, mediating the interaction between the nuclear pore complex and the import complex until the cargo-importin α-importin β heterotrimer reaches the nucleoplasm [43-46].

Nonclassical nuclear transport is similar to the classical pathway with a few exceptions. For molecules using this pathway, there is no requirement for importin α

binding to the cargo protein [47]. In addition, instead of a single β importin having the ability to facilitate nuclear transport, multiple importin βs in the cell function to directly recognize different cargo and transport them across the nuclear envelope. In fact, beyond the classical importin β, 13 other β karyopherins have been identified in yeast and at least 19 have been identified in mammalian cells [47]. Thus, there are a number of non-classical importins available to transport the remaining 60% of nuclear proteins and other macromolecules into the nucleus. Another key difference between the two types of import pathways is the signal used by the cargo protein. Nuclear proteins that undergo transport using the non-classical machinery can have varying types of NLSs. These include the extended asparagine/glycine-rich NLS found in the yeast homolog of fibrillin, Nop1p [48], the proline/tyrosine (PY) NLS of the Nab2 mRNA-binding protein [49], as well as other non-classical motifs that have been shown to be important for the nuclear localization of other nuclear proteins [50-52].

In addition to the direct protein-protein interactions required for nuclear translocation, the primary mechanism of active nuclear transport, through either the classical or non-classical pathways, also requires the exchange of Ran-GTP for Ran-GDP [53]. In the cytoplasm, the concentration of active Ran-GTP is kept very low due to its hydrolysis to inactive Ran-GDP by the Ran-GAP, whose subcellular localization is restricted to the cytoplasm [54,55]. However, the concentration of Ran-GTP in the nucleus is kept very high due to the presence of the Ran-GEF, which primarily localizes to the nucleus [56-58]. Therefore, after an import complex has entered the nucleus, the high-affinity binding of Ran-GTP to the karyopherin disrupts the interaction between the importin and its substrate [59]. The karyopherin then dissociates from its cargo, allowing

the cargo to perform its nuclear function while the Ran-GTP-bound karyopherin is then exported back to the cytoplasm [60]. In the cytoplasm, Ran-GTP is hydrolyzed to Ran-GDP, which disrupts the interaction between Ran and the karyopherin, thereby freeing the karyopherin to bind and transport other nuclear cargo [61]. The hydrolysis of Ran-GTP to Ran-GDP in the cytoplasm completes the transport cycle.

Although there are several more karyopherins in higher organisms than in yeast, the process of nuclear localization is highly conserved across eukaryotes [62]. In fact, a number of karyopherins have been identified based upon sequence conservation [30,49,63-65]. It is hypothesized that the conserved regions within the group of karyopherins are important for interacting with Ran-GTP, components of the nuclear pore complex, and/or transport substrates, suggesting that the mechanism of nuclear transport is highly conserved [66]. For homologous proteins, although precise conservation of a nuclear targeting sequence is not required for conservation of protein function, the sequence motifs used to target proteins to the nucleus are very similar across eukaryotes [67,68]. The specificity of the interaction of a karyopherin with a particular cargo protein also appears to be well-conserved. For example, transportin—karyopherin β2 (Kapβ2) in vertebrates, which is homologous to Kap104p in budding yeast—has been shown to be responsible for the nuclear import of numerous mRNA binding proteins [28,49]. Kap104p binds Nab2p through the recognition of a PY-NLS within Nab2p and the structure of human Kapβ2 bound to the PY-NLS of yeast Nab2p has recently been determined [69-71].

The nuclear import of a number of proteins uniquely depends on a specific karyopherin. Thus, in the absence of its importin, a cargo protein remains confined to the

cytoplasm [72]. However, despite the specificity of the interaction between a karyopherin and its substrate, certain redundancies exist: in the absence of the function of a particular karyopherin, some cargoes are still imported into the nucleus, presumably through alternative karyopherins [48,73-75]. For example, the human nuclear RNA export factor 1 (NXF1) protein, whose homologue in yeast is Mec67p, was shown to be a substrate for Kapβ2 by several groups [76-80]. However, upon treatment of HeLa cells with the Kapβ2-specific inhibitor, M9M, NXF1 was still found to localize to the nucleus, with subsequent studies identifying it as cargo for a number of nuclear import proteins [81]. Under such circumstances, it remains unclear whether two karyopherins bind the cargo protein competitively or cooperatively. Do they recognize the same NLS motif within a particular cargo protein? Is the nuclear phenotype simply compensatory with nuclear transport by the second karyopherin permissible only because of the absence of the first one? Although, these redundancies suggest that backup mechanisms have evolved to ensure nuclear import in critical cellular pathways, further investigation into how such redundancies are coordinated is warranted.

Nuclear Localization and Cellular Function

The information included above reveal that the cell has taken great lengths to regulate traffic into (and out of) the nucleus. This suggests that the process of nuclear localization is critical for normal cellular function. These data also indicate that the dysregulation of nuclear localization can cause considerable deleterious effects for the cell. In fact, there are many examples of the manner in which the process of nuclear localization contributes to cellular function.

Restriction of the subcellular location of the Ran-GAP and Ran-GEF to the cytoplasm and nucleus, respectively, promotes the nuclear transport cycle [53]. In the Wnt/β-catenin signaling pathway, in the absence of the binding of Wnt ligand to the Frizzled receptor, β-catenin is bound by several cytoplasmic proteins that preclude its nuclear localization and allow for targeting to the proteasome for degradation [82]. However, binding of Wnt to Frizzled releases the negative regulation of β-catenin, allowing for its nuclear import to promote the upregulation of genes involved in cell migration and the downregulation of genes involved in cell adhesion. The binding of nucleocytoplasmic shuttling proteins to mRNAs in the nucleus promotes their nuclear export [76,83,84]. After entry into the cytoplasm, dissociation of these proteins from their respective mRNAs allows for return of the proteins to the nucleus and release of the RNAs into the cytoplasm for further processing and/or translation. In budding yeast, because the nuclear envelope does not break down during mitosis, one mechanism through which the re-replication of DNA is prevented is through the regulated nuclear export of replication initiation factors during S phase [85].

While cells use nuclear localization to regulate many endogenous processes, viruses exploit the host nuclear transport machinery, often producing cytopathic effects. Many viral proteins contain one or more NLSs that are recognized by host karyopherins to gain entry into the host cell nucleus. Once in the nucleus, these proteins can promote integration of the viral genome into the genomic DNA of the host. This allows for the virus to hijack host DNA transcription and/or replication machinery to produce more viral particles. Oftentimes, such viral infection inhibits key functions in the cell and ultimately results in host cell death (reviewed in [86]).

One well-studied example of such a virus is the monkey polyomavirus SV40. Initially isolated from the kidney cells of rhesus monkeys, this virus was observed to cause cytopathic effects and vacuole formation [87]. Additionally, subcutaneous injection of the virus into mice and hamsters induced tumor formation [88-91]. The Salk and Sabin poliovirus vaccines administered from 1955 to 1963 in the United States, parts of the Soviet Union, and numerous other countries worldwide were contaminated with active SV40 virions. Consequently, a large amount of research has been executed to determine whether SV40 infection can transform human cells [92-97]. Investigation of the mechanism of action of SV40 infection in its normal host revealed that one of the early viral genes that encodes the large Tumor antigen protein (T_{Ag}) has a predominant role in viral infection [98].

After translation in the cytoplasm, T_{Ag} localizes to the nucleus where it recruits the DNA polymerase α-primase to replicate the viral genome and modulates the host transcription machinery to promote the production of virion particles [99-101]. T_{Ag} deregulates the cell cycle in host cells by interacting with the retinoblastoma family of proteins to abrogate their function [102-104]. It also prevents apoptosis through its interaction with the tumor suppressor p53, thereby allowing for host cell transformation [105-107]. In 1984 the T_{Ag}NLS—the first ever NLS identified—was characterized by Kalderon and colleagues [10]. Subsequent investigations into how T_{Ag} executes its varied functions in the host cell revealed nuclear localization of T_{Ag} as a major determinant of viral pathogenicity [108,109]. In fact, mechanisms that preclude the nuclear import of this viral protein—either through direct mutation of the T_{Ag}NLS or a frameshift mutation that most likely results in the formation of cytoplasmic aggregates of the protein—

abrogate the cytopathic effects of the virus by inhibiting viral replication and cellular transformation [9].

Modulation of the nuclear localization of endogenous proteins can also produce deleterious effects for an organism. Loss of nuclear localization of essential nuclear yeast proteins can result in cell death [110]. Spinal and bulbar muscular atrophy, or Kennedy's disease, results from polyglutamine expansion within androgen receptors [111]. When the testosterone ligand binds the androgen receptor, the receptor normally translocates to the nucleus. Polyglutamine-expanded androgen receptors retain the ability to localize to the nucleus upon binding by testosterone [112]. However, the presence of the expanded repeats precludes nuclear export, thus promoting nuclear accumulation of the mutant receptor and toxicity [113]. One hallmark of Alzheimer's disease is the presence of intracellular tangles consisting of abnormally hyperphosphorylated tau protein in the cytoplasm [114-116]. Protein phosphatase-2A (PP2A) functions to dephosphorylate tau [117] and the SET protein is an inhibitor of PP2A [118,119]. In Alzheimer's disease brains, phosphorylation of serine 9 located near an N-terminal classical NLS within SET disrupts SET nuclear localization [120]. This cytoplasmic SET inhibits PP2A function, thus promoting tau hyperphosphorylation and the formation of the toxic fibrillary tangles.

These data demonstrate that tight control of nuclear traffic is crucial for cell survival. Not only does nuclear localization impact how the cell functions, abrogation of nuclear transport can also impair the function of individual tissues (i.e. the brain, as mentioned above). The observation that aberrant nuclear localization contributes to human disease reveals the impact of this cellular process at the organismal level, with the

potential to reduce life expectancy and worsen the quality of life of humans affected with such conditions.

Biogenesis and Trafficking of Multi-subunit Complexes

Because proteins that participate in RNP complexes must be imported to the nucleus after translation in the cytoplasm, their nuclear transport is likely to be extremely important for the biogenesis of cellular ribonucleoproteins. This is supported by the fact that many RNPs are assembled in the nucleus and/or have nuclear functions. The ribosome and the spliceosome exemplify ribonucleoproteins that rely on nuclear localization for their biogenesis. A discussion of the regulation of the assembly and localization of the components of the ribosome and the uridine-rich small nuclear RNPs that comprise the spliceosome are included below.

Ribosome Biogenesis

The assembly and trafficking of many multi-subunit complexes often rely on tight regulation of the subcellular localization of the individual components that comprise such complexes. The ribosome exemplifies this type of complex with ribosome biogenesis requiring the extremely rapid, high fidelity assembly of a host of ribosomal proteins (r-proteins) with more than 5000 nt of rRNA. This process makes use of the coordinated efforts of more than 70 small nucleolar RNAs (snoRNA) and at least 200 different non-r-protein cofactors for manufacturing mature ribosomes [121]. Though much of the data regarding this essential process has come from studies in budding yeast, the general

mechanisms regulating ribosome fabrication in the cell are highly conserved across eukaryotes [122].

Ribosome manufacturing is coupled to cell growth such that the rate of ribosome production in logarithmically growing yeast is higher than in yeast in stationary phase. Ultimately, this results in the presence of many more ribosomes in actively growing cultures than can be found in stationary yeast [123,124]. The biogenesis of ribosomes begins in the nucleolus—the major subcompartment in the nucleus. The nucleolus is organized around the rDNA repeats and serves as the ribosome manufacturing center of the cell [2]. After transcription of rDNA by RNA polymerase I to make the 35S primary precursor rRNA (pre-rRNA) transcript (RNA polymerase III transcribes the 5S pre-rRNA), a series of endo- and exonucleolytic processing reactions result in the formation of 20S and $27SA_3$ pre-rRNAs that are packaged into 43S and 66S precursor ribosomal ribonocleoprotein (pre-rRNP) particles, respectively [125,126]. The 43S pre-rRNP is then exported to the cytoplasm where further processing of the RNA subunit to become the mature 18S rRNA occurs, thus creating the 40S subunit of the ribosome [127]. However, the 66S pre-rRNP undergoes additional processing steps in the nucleolus before being trafficked into the nucleoplasm. There, two redundant pathways are responsible for further processing of this pre-rRNP prior to its export to the cytoplasm [122]. Cytoplasmic localization of the 66S pre-rRNP ultimately results in the production of the mature 5.8S and 25S rRNAs—constituents of the 60S subunit of the ribosome [122]. In the cytoplasm, the 40S and 60S ribosomal subunits interact to form the mature ribosome, enabling the translation of mRNA into protein [2].

Ribosome biogenesis illustrates how subcellular localization in eukaryotes is used to regulate the production of a fundamental piece of cellular machinery. After translation in the cytoplasm, a great number of r-proteins and assembly factors must localize to the nucleus. Association of these proteins with pre-rRNAs in the nucleolus stabilizes well-folded pre-rRNAs, modulates incorrectly folded pre-rRNAs to promote correct folding, and alters pre-rRNA structure to allow for binding of other r-proteins [128-132]. Maturation of pre-rRNPs in the nucleolus and the nucleoplasm occurs by way of rRNA processing and is marked by the differential association of various r-proteins and assembly factors with pre-rRNAs [133,134]. Association of these rRNA-protein complexes with a number of other proteins, as well as components of the nuclear pore complex, facilitates active nuclear export of the pre-rRNP to the cytoplasm. There, the association with particular cytoplasmic proteins causes the formation of mature ribosomal subunits and allows for protein translation [135-137]. Overall, this process serves to isolate the cellular transcription machinery from the translation apparatus. It provides the cell with the freedom to make proteins without concern for how the production of certain proteins (i.e. nucleases, helicases, acetyl- and methyltransferases, etc.) could negatively affect the integrity of the genetic information in the cell.

U snRNP Biogenesis

The biogenesis of the Uridine-rich small nuclear ribonucleoproteins (U snRNP) that comprise the spliceosome is another well-characterized example of how the cell modulates the subcellular localization of a number of different constituents to produce a multi-subunit complex. The spliceosome is a large 40S cellular machine—made up of

proteins and RNA—that processes precursor mRNAs (pre-mRNA) into mRNA by catalyzing the removal of noncoding intronic sequences [2]. In addition, alternative splicing of coding sequences allows the generation of multiple proteins from a single gene, thereby increasing the complexity of the proteome [138]. Though alternative splicing is mainly found in higher eukaryotes [139,140], the general dynamics of splicing are well-conserved from yeast to metazoans [141]. The spliceosome minimally contains 5 U snRNPs, U1, U2, U4, U5, and U6—named based upon the U snRNA component of the snRNP—that interact with a number of other proteins to mediate splicing [142,143]. The individual components of these U snRNPs differ, but the biogenesis of each requires similar assembly and processing steps in the cell [144,145].

In metazoans, upon U snRNA transcription by RNA polymerase II (or RNA polymerase III in the case of the U6 snRNA [146]) in the nucleus, a 7-methylguanosine (mG) cap is added to the 5′ end of each transcript [147]. This process serves to target the U snRNAs for active nuclear export [148-150]. Once in the cytoplasm, the U snRNAs can associate with one of two different groups of proteins—the seven Sm core proteins or U1A, U170K, U2B′′ and U2A that are specific for certain U snRNA subclasses [145]. Of note, the Sm proteins are sequestered in 4 partially assembled, snRNA-free complexes in the cytoplasm [144,151]. To form the heteroheptameric Sm core complex, these 4 subcomplexes are hypothesized to assemble in a step-wise fashion with a U snRNA by interacting with the conserved Sm-binding site found in the U snRNA [152]. Binding of the Sm D3,B/B′ subcomplex forms the complete U snRNP molecule [153,154].

After maturation in the cytoplasm, the U snRNP must somehow be localized to the nucleus to perform its function in the cell. In yeast and humans, conserved basic

residues in the C-terminal extensions of the SmB and SmD1 proteins have been shown modulate nuclear localization of the Sm core complex. This finding leads to the hypothesis that assembly of these proteins around the designated binding site in a U snRNA creates a protrusion that contains a basic patch that functions in nuclear localization [155,156]. Thus, binding of the Sm core complex to a U snRNA can aid in nuclear localization of the snRNP. Alternatively, binding of the Gemin complex, which contains the survivor motor neuron (SMN) protein [157], promotes U snRNP assembly and SMN helps to mediate the interaction of the U snRNP with importin β to facilitate nuclear import [158-161]. In addition, assembly of the U snRNP results in hypermethylation of the 5′ mG cap to make a 2,2,7-trimethyl-guanosine (m_3G) cap that, through the binding of other proteins, also aids in nuclear localization [149,162]. Therefore, the cytoplasmically-matured U snRNP contains a bipartite nuclear localization mechanism formed by the presence of the m_3G cap structure and association with the Sm core complex or the SMN protein.

Once in the nucleus, the U snRNP undergoes considerable intranuclear shuttling prior to assembly into a spliceosome. First, the U snRNP is trafficked into Cajal bodies, presumably by way of the interaction of the SMN protein with the Cajal body protein coilin p80 [163-166]. Next, the U snRNP quickly migrates through the nucleolus where further maturation steps are hypothesized to occur before subsequent redelivery to Cajal bodies [167-169]. After this accumulation of the U snRNPs in Cajal bodies, the nuclearly-matured U snRNPs are trafficked to interchromatin granule clusters (IGC) for storage and/or assembly into spliceosomes [170-174]. Notably, these mature U snRNPs

possess the ability to migrate freely between IGCs and Cajal bodies—a process that is regulated by the phosphorylation state of these splicing factors [175].

Although U snRNP biogenesis has been fairly well-characterized in higher eukaryotes, specific details regarding the assembly and trafficking of these ribonucleoprotein complexes is less well-understood in yeast [143]. However, available data suggest that though some key differences exist, the general mechanisms controlling the biogenesis of the components of the splicing machinery may be conserved [176,177]. In budding yeast, the U snRNAs are RNA polymerase II (or RNA polymerase III) transcripts that acquire an mG cap after transcription [178-180]. While this cap structure targets metazoan U snRNAs to the cytoplasm, it remains unclear whether yeast U snRNAs necessarily undergo nucleocytoplasmic shuttling [143]. In the case of the U5 snRNA in yeast, it is exported to the cytoplasm after transcription through the interaction of the Crm1p nuclear export protein with the mG cap [181,182]. In the cytoplasm, the U5 snRNA undergoes additional processing before associating with the Sm proteins to form the U5 snRNP precursor that is subsequently imported into the nucleus [183,184]. This process presumably occurs due to the interaction of the Sm proteins with the yeast homolog of importin β as no SMN equivalent has been identified in yeast. Once in the nucleus, the U5 snRNP is subjected to additional phosphorylation-dependent processing that ultimately results in the reorganization and/or restructuring of the proteins that comprise the ribonucleoprotein before assembly with the spliceosome [182,184]. These data present the first observation of a cytoplasmic phase for U snRNP biogenesis in yeast and suggest—because Sm protein association is a requirement for U snRNP biogenesis and because the Sm proteins localize to the cytoplasm until they participate in the

heptameric ring structure that binds U snRNAs—that nucleocytoplasmic shuttling of U snRNAs is also important for the biogenesis of U snRNPs in yeast.

In the absence of Tgs1p, a methyltransferase that is conserved from yeast to mammals, U snRNAs are not m_3G-capped [180]. Thus, this enzyme is responsible for methylating the mG-capped U snRNAs to form the more mature m_3G-capped structures. Immunofluorescence analysis of Tgs1p has revealed that it localizes to the nucleolus [176,180]. In particular, in a quarter of cells grown on solid media, Tgs1p localizes to the nucleolar body [176]. The nucleolar body is a subcompartment of the nucleolus. It is considered to be the yeast Cajal body due to its intimate relationship with the nucleolus, the lack of proteins and/or RNAs associated with ribosome biogenesis within the nucleolar body, and the presence or enrichment of snoRNAs within this region of the nucleolus [185]. Although, in higher eukaryotes, acquisition of the m_3G cap occurs in the cytoplasm and serves as a nuclear-targeting mechanism for U snRNP precursors [149,162], these data suggest that, in yeast, U snRNA precursors receive an m_3G cap after association with the Sm proteins and reimport into the nucleus. These data also suggest that transit through the nucleolus and, strictly speaking, the yeast Cajal body for 25% of cells under certain growth conditions are important steps in the biogenesis of yeast U snRNPs. This localization phenotype has also been shown to be important for vertebrate U snRNP biogenesis.

Telomerase

Telomerase is another type of ribonucleoprotein complex whose function is modulated by the subcellular distribution of its components. Telomerase is a specialized

reverse transcriptase responsible for replicating telomeres, the ends of linear chromosomes [2]. Telomeres are GT-rich, non-protein-coding DNA sequences with associated proteins that aid in the maintenance of genome stability by capping chromosome ends and preventing their recognition as DNA double-strand breaks [186]. Telomeres shorten due to what is termed the end-replication problem (**Figure 1**): after DNA synthesis, in an effort to regenerate the required 3′ overhang at the chromosome end, 5′ end resection of the newly replicated, blunt-ended daughter molecule created by leading strand synthesis results in a net loss of DNA sequence [187,188]. Telomeres act as a buffer zone for this effect by hindering the immediate loss of coding sequences. Nevertheless, as cells divide, in the absence of telomerase, telomeres continually shorten until the shortest telomere triggers cell-cycle arrest [189]. This creates a limit to the number of mitotic divisions a cell can undergo before telomeres are lost and gross chromosomal rearrangements occur, an outcome often leading to cell death [190].

Telomere elongation by telomerase is the preferred mechanism for telomere replication in most eukaryotes [191]. In an effort to circumvent the deleterious effects that could result from aberrant telomere addition throughout the cell cycle, telomerase activity is normally restricted to late S phase and G2/M phases of the cell cycle [192]. The individual components of telomerase vary widely across eukaryotic species. However, the typical telomerase holoenzyme minimally contains an RNA moiety associated with a reverse trancriptase—forming the catalytic core of the enzyme—and a number of other essential regulatory proteins [193]. The telomerase RNA contains a specialized sequence of nucleotides used to template the repetitive telomeric sequence added to the ends of chromosomes [194]. Telomerase can function using two different

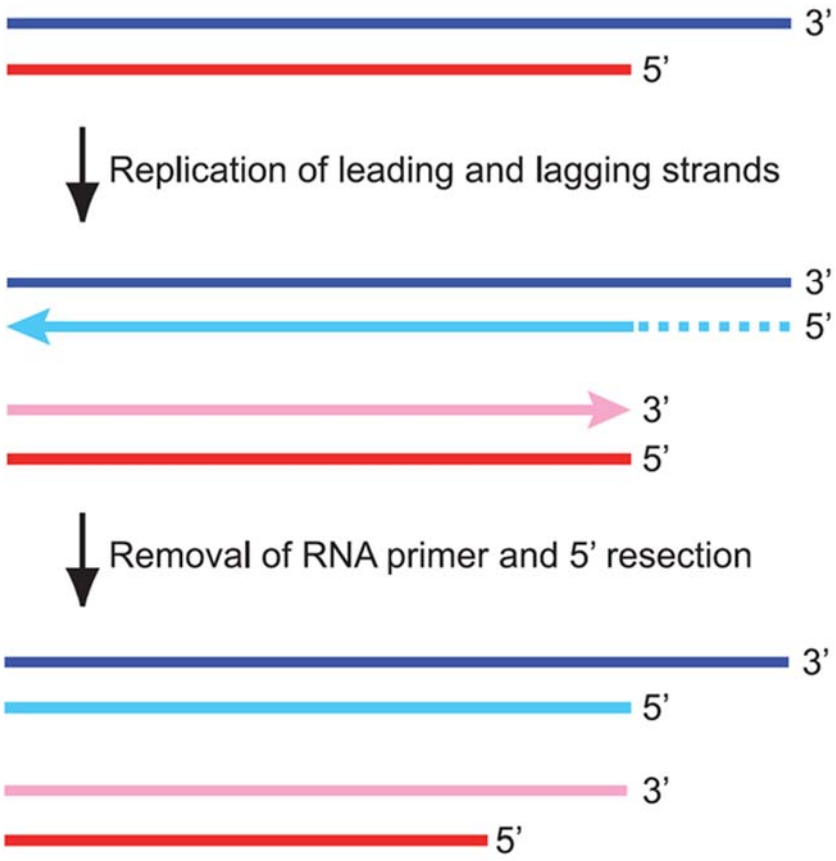

Figure 1. Diagram of the end replication problem.

After DNA replication, two DNA daughter molecules, each comprised of a parental DNA strand (blue and red) and a newly replicate strand of DNA (pink and aqua). Removal of the RNA primer after lagging strand replication (hashed aqua) regenerates the 5´ overhang on that DNA daughter molecule. However, the product of leading strand synthesis is a blunt-ended DNA molecule. Therefore, resection of the 5´ strand of this DNA daughter molecule occurs to generate the required 3´ overhang, ultimately resulting in the net loss of DNA sequence. Figure adapted from [188].

modes of activity, nucleotide addition processivity (NAP) and repeat addition processitivity (RAP) [195]. In NAP, association of telomerase with a DNA substrate occurs just long enough to allow for the addition of only a few nucleotides before telomerase dissociates [196]. The length of one telomeric repeat defines the maximum number of nucleotides added to a DNA substrate using NAP. However, RAP occurs when a single telomerase binds to a DNA substrate and adds multiple telomeric repeats by translocating along the growing DNA molecule, requiring realignment of the RNA template with the DNA end for each round of addition [197].

Human Telomerase

In human cells, in addition to the telomerase RNA component (hTR) and the telomerase reverse transcriptase (hTERT), the telomerase holoenzyme contains a number of other proteins involved in modulating enzyme stability, assembly, and/or recruitment to the telomere. These proteins include Est1A, TCAB1, dyskerin, Nop10, Nhp2, and Gar1 [198,199] (**Figure 2**). Est1A has been shown to be involved in regulating the abundance of telomeric repeat-containing RNA (TERRA), a large non-coding RNA transcribed from telomeric DNA [200]. Depletion of Est1A results in stochastic telomere loss while Est1A overexpression leads to telomere uncapping and, consequently, telomere fusions [200]. Est1A is also involved in nonsense-mediated mRNA decay in the cytoplasm, which is hypothesized by some to be the major role of Est1A in the cell [201]. The Cajal body protein, TCAB1, promotes telomerase delivery to telomeres by modulating the trafficking of telomerase to Cajal bodies (a process described in greater detail below) [202,203].

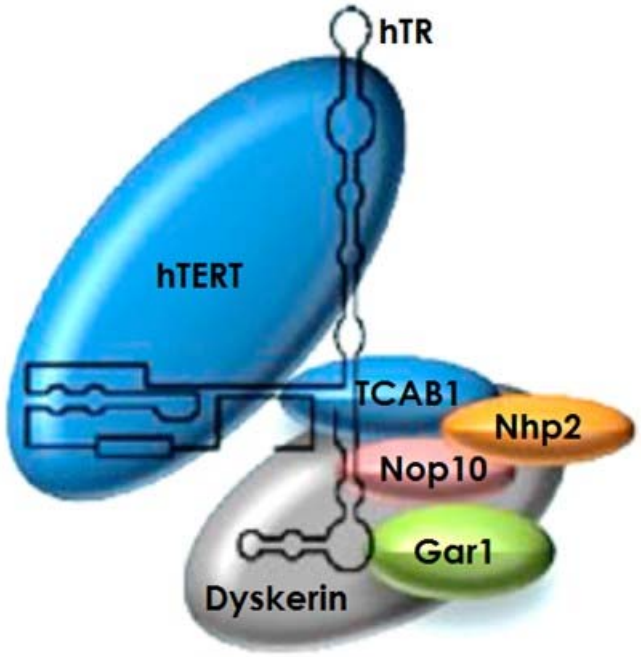

Figure 2. Diagram of human telomerase.

Human telomerase minimally contains the indicated proteins associated with the telomerase RNA, hTR. hTERT is the reverse transcriptase. Together, hTERT and hTR form the catalytic core of the enzyme as they are sufficient for *in vitro* telomerase activity. Dyskerin, Nop10, Nhp2, and Gar1 form a heteroteteramic complex that is required for correct processing of hTR. TCAB1 is involved in recruitment of telomerase to telomeres by way of Cajal bodies. EST1A is also a component of human telomerase. However, the details of its interaction with components of the telomerase holoenzyme and its functional role in telomerase remain unclear. Figure modified from [204].

Dyskerin, Nop10, Nhp2, and Gar1 participate in a chaperoning subcomplex that associates with hTR to modulate its stability as well as the stability of the telomerase holoenzyme [193,205]. Dyskerin, a pseudouridine synthase encoded by the dyskeratosis congenita 1 (DKC1) gene, is a well-conserved nucleolar protein that binds to H/ACA motifs in snoRNAs to promote small nucleolar RNP (snoRNP) assembly [12]. The association of dyskerin with H/ACA containing snoRNAs is important for 18S rRNA production and thus ribosome biogenesis in the cell [206]. However, binding of dyskerin to the H/ACA motif in hTR allows for proper subnuclear trafficking and processing of the RNA, thus promoting stabilization of hTR interaction with hTERT [207].

Dyskerin, Nop10, and Nhp2 form a heterotrimer that associates with hTR [205,208]. This association has been hypothesized to occur cotranscriptionally as is the case for the association of these chaperones with other H/ACA RNAs in the cell [193,209]. Nop10 and Nhp2 directly interact while dyskerin binds both proteins and likely mediates their interaction with hTR [205,208]. Depletion of dyskerin, Nop10, or Nhp2 in telomerase expressing cells destabilizes hTR, ultimately resulting in telomerase deficiency [210]. Thus, the association of these proteins with hTR is essential for optimal telomerase expression and activity in the cell. After transcription, hTR associates with a number of other factors involved in its maturation before binding of Gar1 to hTR-bound dyskerin [193], which appears to be the signal for a mature hTR in the cell. Although Gar1 depletion does not impact hTR stability (most likely due to its relatively late association with the RNA), Gar1 is hypothesized to participate in hTR intranuclear trafficking by enhancing the nucleolar localization of hTR [211]. Further studies to elucidate the exact functional role of Gar1 in the telomerase holoenzyme are warranted.

Trafficking

Not much is known about the intracellular trafficking of human telomerase—a process that, of necessity, is tightly regulated due to and/or providing for the cell cycle restriction of telomerase activity. Certainly, after translation in the cytoplasm, the protein components of the enzyme must localize to the nucleus to execute their function(s) in the cell. However, the mechanisms controlling this process are not well understood. Experiments to directly determine whether hTR transits through the cytoplasm as part of its maturation are lacking. However, the observation that injection of *in vitro*-transcribed hTR into Xenopus oocytes results in cytoplasmic accumulation of the RNA indicates that hTR is inefficiently transported from the cytoplasm to the nucleus in vertebrates [11]. These experiments suggest that it is unlikely that hTR is routed to the cytoplasm during its maturation.

Recently, Chung and colleagues characterized the nuclear localization of hTERT [212]. Their work identifies two patches of basic residues (7 residues in total) within the N-terminal 300 aa of hTERT that are conserved among vertebrates and function as a bipartite NLS. They show that along with the NLS, Akt kinase phosphorylation of serine 227, which lies between the basic clusters comprising the bipartite NLS, is required for hTERT nuclear translocation. Alanine mutations at serine 227 and the residues comprising the NLS resulted in failure of hTERT to localize to the nucleus and the inability of hTERT to immortalize human foreskin fibroblast cells [212]. These findings implicate the nuclear localization of hTERT as an important determinant of telomerase function.

Additionally, modulation of the nuclear localization of telomere-binding proteins has been shown to affect telomerase recruitment and/or access to the telomere in many organisms. In fact, the Songyang group has demonstrated that the subcellular localization of one component of telomeric chromatin in humans—a specialized hexameric complex that specifically associates with telomeric repeats—influences telomere maintenance through its regulation of the nuclear localization of another component of telomeric chromatin [213]. TPP1, POT1, and TIN2 are telomere-binding proteins that form a DNA-end binding subcomplex at chromosomal termini [186]. The Songyang group found that in the nucleus, the interaction of POT1 with TPP1 away from the telomere targets POT1 to the cytoplasm [213]. Abrogation of the nuclear export of this complex resulted in telomere uncapping and telomere elongation, indicating a functional role for the nuclear export of these proteins in telomere homeostasis [213]. In the cytoplasm, POT1-TPP1 associates with TIN2, which then directs nuclear localization of the heterotrimeric complex [213]. Although the exact purpose of this nucleocytoplasmic shuttling remains unclear, these data indicate that the intracellular trafficking of telomere-associated proteins is important for telomere maintenance in human cells.

Instead of focusing on the nucleocytoplasmic trafficking of telomerase, considerably more research has concentrated on the intranuclear shuttling of the enzyme in human cells. Initial studies of the subnuclear localization of hTR and hTERT revealed that during G1 (and G2) phases of the cell cycle, hTR localizes to Cajal bodies while hTERT is confined to distinct foci in the nucleoplasm [214]. During early S phase, hTERT relocalizes to nucleoli while hTR-containing Cajal bodies can be found associated with the nucleolar periphery [214]. During mid S phase, however, just before

the time at which telomerase acts, hTR and hTERT colocalize within Cajal bodies [13,214], an interaction thought to mediate telomerase localization to telomeres.

Additional investigations concerning the Cajal body localization of telomerase components has added to the understanding of telomerase biogenesis in human cells. TCAB1, a Cajal body-associated RNA chaperone, binds the CAB-box motif in hTR and directs telomerase delivery to Cajal bodies [202,203,215-217]. While mutation of the CAB-box in hTR does not impact telomerase *in vitro* activity, humans that possess the CAB-box mutation or expression of the CAB-box mutant cultured cells reduces telomerase association with telomeres and causes telomere shortening [3]. Similarly, depletion of TCAB1 in human cells leads to extensive telomere shortening [3]. Although prior studies in mice and frogs have indicated that localization of telomerase to Cajal bodies is dispensable for telomerase function in these organisms [218,219], the studies mentioned above provide evidence that in human cells, telomerase interaction with Cajal bodies impacts enzyme function.

Of late, the Chung group has published the most detailed investigations into the intranuclear biogenesis of telomerase in an effort to synthesize how the regulation of telomerase assembly and activity are coordinated with its cell cycle regulation in human cells. Using immunogold transmission electron microscopy combined with fluorescence microscopy and co-immunoprecipitation approaches in HeLa cells, they observed that hTERT (and not dyskerin) exhibits differential localization to Cajal bodies in the cell cycle [220]. In G1 phase, hTERT primarily localized to the dense fibrillar and granular subcompartments of the nucleolus and, to a lesser extent, Cajal bodies. However, in mid/late S phase, hTERT localized to DNA and Cajal bodies as well as the dense fibrillar

and granular components of the nucleolus [220]. Using an *in vitro* primer extension assay to monitor telomerase activity in extracts from subdomains within the nucleus, they observed that catalytically active telomerase can be found in the nucleolus. However this nucleolar telomerase is less competent for primer extension than the enzyme activity found in nucleoplasmic extracts and this primer-extension activity does not depend on cell cycle position [220]. Ectopic expression of hTERT in telomerase deficient cells resulted in nucleolar accumulation of hTERT that did not interact with TCAB1 or localize to Cajal bodies [220]. These results indicate that while hTERT can localize to the nucleolus in the absence of hTR, interaction with the RNA subunit is required for hTERT delivery to Cajal bodies.

This work also showed that dyskerin localizes to Cajal bodies and the dense fibrillar compartment of the nucleolus in a manner that does not depend on its association with telomerase. As expected, depletion of dyskerin destabilized hTR, causing a reduction in telomerase activity [220]. Also in the absence of dyskerin, the association of active telomerase with TCAB1 was reduced, resulting in reduced localization of hTERT to Cajal bodies. The authors also showed that TCAB1 localized to the interface between the dense fibrillar and granular components of the nucleolus and colocalized to Cajal bodies with hTERT. While TCAB1 depletion did not affect telomerase activity, reduced TCAB1 resulted in nucleolar retention of active telomerase by precluding the localization of hTERT and dyskerin to Cajal bodies [220].

In an elegant set of experiments using co-immunoprecipitation to monitor the association between telomerase assembly and activity in the cell cycle, these researchers showed that in G1 phase, telomerase components did not assemble. Furthermore, *in vitro*

telomerase activity was virtually undetectable in their immunoprecipitates [220]. Although expression of hTR or dyskerin did not appear to be regulated in the cell cycle, hTERT expression peaked during S phase. Thus, as cells entered early S phase, hTR was found assembled with hTERT and dyskerin primarily in the nucleolus. However, this assembled telomerase was only slightly competent for *in vitro* primer extension. Also during early S phase, assembled telomerase consisting of hTR, hTERT, and dyskerin associated with TCAB1, but this telomerase was only marginally more competent for primer extension than that found in the nucleolus [220]. In mid/late S phase, although some nucleolar assembled telomerase was present, the bulk of telomerase associated with TCAB1 outside of the nucleolus. While the activity associated with nucleolar telomerase was essentially undetectable, TCAB1-associated telomerase activity peaked, reaching an overall maximum value in the cell cycle [220]. Finally, in late S/G2/M phase, telomerase primarily associated with TCAB1 with no assembled telomerase detectable in the nucleolus. Telomerase activity from these immunoprecipitates was also very high for TCAB1-bound telomerase with no detectable activity found in the nucleolus [220].

Taken together, these data lead to the following model of human telomerase biogenesis: after transcription and some processing in the nucleoplasm, hTR localizes to the dense fibrillar component of the nucleolus where it associates with dyskerin (and presumably Nop10, Nhp2, and Gar1) through its H/ACA motif to form the hTR-dyskerin RNP [220]. As the cell traverses into S phase, hTERT trafficking to nucleoli allows for assembly of the telomerase RNP in the dense fibrillar nucleolar subcompartment. This process produces a catalytically active telomerase that is confined to the nucleolus in early/mid S phase through the interaction of hTERT with nucleolin [220]. As the cell

proceeds to mid/late S phase, TCAB1 association with the nucleolus permits its binding to the CAB-box motif in hTR to deliver the telomerase RNP to Cajal bodies [220]. This step is followed by Cajal body-dependent transport of telomerase to telomeres [220]. Telomerase is then recruited to the end of chromosome by an interaction between the telomere-binding protein TPP1 and hTERT, thus allowing for telomere elongation [220].

Telomerase Trafficking and Disease

Telomerase regulation is very important for human disease. Telomerase is expressed in germ cells and stem cells (although relatively less telomerase is expressed in stem cells than germ cells) however, telomerase is not normally expressed in somatic cells [221]. Because telomerase modulates the replicative potential of cells by elongating telomeres, telomerase dysfunction has been implicated in several cellular aging-related syndromes due to telomerase deficiency in the stem cell population [222]. Furthermore, telomerase gain-of-function, typically resulting from the upregulation of hTERT expression in human somatic cells, has been incriminated in the cancer phenotype [223]. In fact, telomerase activity is reactivated in approximately 90% of human tumor cell lines and is implicated in the immortal growth of such cells [224]. However, telomerase-related disease is not limited to those involving direct modulation of the catalytic activity of the enzyme [225]. Instead, there are a number of disease states caused by errors in telomerase biogenesis [3,226].

Dyskeratosis congenita (DC) is an early-onset syndrome of telomerase dysfunction that affects multiple cellular systems, especially those involving highly replicative tissues in humans [226]. Hallmarks of DC include bone marrow failure,

pulmonary fibrosis, and increased cancer risk [227]. Many DC patients present with abnormal skin pigmentation, nail dystrophy, and oral leukoplakia. The rarest form of DC (Hoyeraal-Hreidarrson syndrome) is also characterized by growth retardation, cerebellar hypoplasia, and impaired mental development [228,229]. DC can arise from mutations in a number of genes related to telomere homeostasis. These include mutations in hTR and hTERT that directly impact the catalytic activity of telomerase as well as mutations in TIN2, a component of telomeric heterchromatin [227]. In addition, many DC-related mutations do not affect the catalytic activity of telomerase, including mutations in genes encoding dyskerin and TCAB1 [3,230,231].

An X-linked form of DC results from point mutations in the DKC1 gene that perturb dyskerin association with hTR, leading to a decrease in hTR expression levels and decreased assembly of hTR into active telomerase RNP [230]. Compound heterozygous mutations in TCAB1 cause an autosomal recessive form of DC. In these DC patients, the mutated TCAB1 protein exhibits reduced expression and aberrant subcellular localization. This prevents TCAB1 association with hTR, precludes delivery of hTR to Cajal bodies, and promotes nucleolar accumulation of active telomerase [3]. Mutations in the genes encoding Nhp2 or Nop10 cause rare autosomal recessive forms of DC [210,211,232]. Although the pathology associated with these forms of DC is likely due to destabilization of hTR—as is the case with the dyskerin mutants described above—further investigations are required to elucidate the exact mechanism yielding the disease phenotype.

Idiopathic pulmonary fibrosis (IPF) is an adult-onset condition related to telomerase dysfunction that increases in prevalence with advanced age [233]. Loss of

pulmonary epithelium and progressive scarring of lung tissue causes the development of hypoxia, chronic cough, and shortness of breath in IPF patients [234]. Average patient survival after diagnosis with IPF is 3 years [235]. Although the exact cause of the disease is not well-understood, characterization of mutations in telomerase-associated genes found in patients with familial IPF have begun to shed light on the manifestation of this disease [236,237].

A point mutation at valine 144 in the telomerase essential N-terminal domain of hTERT was determined to associate with IPF [236,238]. While this V144M mutation has no detectable effect on telomerase catalytic activity, cells expressing the mutant protein exhibited a disruption in hTERT recruitment to telomeres resulting from arrest of telomerase trafficking in Cajal bodies [238,239]. A similar phenotype was observed with the expression of the P33S hTERT [238]. However, further characterization is required to determine the mechanism by which this mutant manifests disease. Most recently, a point mutation in the DKC1 gene has been implicated in Familial Interstitial Pneumonia, the inherited form of IPF [240]. An A to G transition at nucleotide 1213 of DKC1 encoded a T405A mutation that correlated with reduced levels of hTR [241], suggesting that this mutation impairs telomerase function by destabilizing hTR.

Liver cirrhosis and aplastic anemia are two additional telomerase-deficiency related disease states. Individuals with aplastic anemia possess hypocellularity of bone marrow and reduced peripheral blood counts, often requiring bone marrow transplantation for survival [242]. Liver tissue fibrosis and scar tissue production are hallmarks of cirrhotic livers [243]. Telomere shortening related to mutations in hTR and hTERT that compromise the catalytic activity of the enzyme have been observed in

patients with these conditions [244-247]. As techniques for elucidating the mechanism of various mutations affecting telomerase function become more prevalent, it will be interesting to see whether telomerase trafficking errors also contribute to these diseases.

Saccharomyces cerevisiae Telomerase

The advances in human telomerase research are in large part founded upon seminal studies of telomeres and telomerase in microorganisms. For example, in the mid-to-late 1980s, Carol Greider and Elizabeth Blackburn set out to isolate the terminal transferase activity that had, at that time, been proposed to elongate telomeres [248]. They took advantage of macronuclear development in the ciliate *Tetrahymena thermophila*—a time at which germline chromosomes are fragmented into ~200 pieces that each require telomeres at both ends followed by DNA replication to a final ploidy of approximately 45C. These researchers reasoned that the activity they were seeking would necessarily be present at relatively high levels as compared to cells undergoing vegetative growth [249,250]. Therefore, using a biochemical approach, they were able to isolate telomerase, eventually characterizing it as a ribonucleoprotein complex that minimally requires an RNA, protein component(s), and a G/T-rich DNA substrate for activity [250,251].

Identification of Components

Studies in budding yeast have also greatly contributed to our understanding of telomeres and telomerase. Prior to the isolation of telomerase in ciliate extracts, studies in

yeast led to several important findings from the Szostak group. They provided for the initial characterization of telomere structure, revealing that ciliate telomeric sequence could be recognized as telomeres in yeast and that short telomeric "seed" sequences on a linearized plasmid could be elongated to allow for stable plasmid maintenance [252,253]. Furthermore, in 1989 Lundblad and Szostak published a genetic screen in which they attempted to identify mutants defective for telomere elongation with the ultimate goal of elucidating the mechanism of telomere replication in yeast [254].

Prior to the publication of this work, two primary hypotheses to explain the properties of telomere elongation observed in yeast had been proposed: (1) the existence of a sequence-specific terminal transferase-like enzyme with a non-template directed activity [253] and (2) the presence of a recombination mediator capable of controlling the addition of repetitive sequences to short telomeres [255,256]. In the absence of existing evidence to definitively support or refute the contribution of either of these proposed mechanisms to telomere replication, Lundblad and Szostak set out to use genetic analysis to identify the enzymatic activities responsible for telomere elongation. They chose a genetic approach because it would allow for the identification of factors contributing to telomere replication without having to make assumptions about how these factors might function—a potential limitation associated with the use of a biochemical approach [254].

To begin, these researchers constructed a single-copy circular plasmid containing yeast *ARS* and *CEN* sequences, the *LEU2* gene as a selectable marker, and the *URA3* gene placed between inverted *Tetrahymena* telomeric repeats, hypothesizing that the telomere seeds exposed by plasmid breakage within *URA3* would need to be extended to produce functional telomeres that could support stable maintenance of the plasmid [254].

Yeast that had been transformed with this plasmid were then mutagenized with ethyl-methyl sulfonate (EMS). Seven thousand EMS-treated single colonies were inoculated into liquid media in 96-well microtiter dishes and the liquid cultures were spotted onto 5-fluoro-orotic acid (5-FOA) synthetic complete media lacking leucine. Cells expressing *URA3* are sensitive to 5-FOA[257]. Thus, selection for 5-FOA resistance allowed for the isolation of colonies that had maintained the plasmid and lost *URA3* function due to the acquisition of an EMS-derived or spontaneous, inactivating mutation in *URA3* or, most desirably, plasmid breakage within *URA3*. They assessed the growth of each spotted culture relative to the growth of wild-type EMS-treated cells to screen for mutants with potential alterations in any of several characteristics of telomere function including: (1) those with alterations in the frequency of plasmid linearization, (2) those with a defect in lengthening the "telomeres" of the plasmid, and (3) those with a defect in maintaining the end-structure of the telomere [254]. Subsequently, they assayed mutants with defects in the plasmid linearization assay for telomere shortening and senescence, leading to the isolation of one mutant that displayed decreased frequencies of 5-FOA resistant colonies as compared to wild-type cells, progressive telomere shortening, and senescence. These characteristics embodied what they termed the Ever Shorter Telomere (EST) phenotype, which led to the discovery of *EST1* [254].

Complementation analysis was conducted to verify that the *est1-1* mutant obtained from their screen did not have a mutation in any genes that had previously been shown to exhibit defects in telomere length maintenance. To accomplish this, the haploid *est1-1* mutants were crossed to haploid *tel1* or *tel2* strains—mutants that had previously been shown undergo telomere shortening [258]—and the telomere lengths of these

diploids were assayed over several generations. Because the telomere length and growth phenotypes of these diploid cells were wild-type, the *est1* mutation was thought to occur in a gene different from *TEL1* or *TEL2* [254]. To further support this conclusion, linkage analysis was used to determine the segregation pattern of *est1* and *tel1* or *tel2* alleles. This was achieved by sporulating the *est1-1*/*EST1*$^+$ *tel1*/*TEL1*$^+$ or *est1-1*/*EST1*$^+$ *tel2*/*TEL2*$^+$ diploid strains to determine the phenotypes of the tetrads produced. Eight wild-type spores were obtained from nine tetrads assayed in these experiments, indicating that the mutant alleles assort independently and therefore cannot be alleles of the same gene [254].

To clone *EST1*, plasmids from a genomic yeast library were transformed into the *est1-1* mutant and assayed for the ability to complement the EST phenotype [254]. To verify that the cloned gene was indeed *EST1* and to ensure that the telomere length and senescence phenotypes exhibited by the *est1-1* allele were the null phenotypes of the *EST1* gene, the cloned *EST1* fragment was used to introduce deletions in the chromosomal copy of *EST1*. Plasmids expressing the *est1*Δ mutant were shown to be unable to complement the phenotype conferred by the *est1-1* allele and displayed the same phenotypes as the *est1-1* mutant when assayed for telomere length, temperature sensitivity, and senescence [254]. Additionally, genomic DNA was isolated from an *est1*Δ/*EST1*$^+$ diploid yeast strain and used for agarose gel-electrophoresis and Southern blotting to demonstrate that both alleles of *EST1* were present and of different sizes in this strain. Upon sporulation of the diploid, there was 2:2 segregation of each allele of *EST1* with shorter telomeres segregating with the *est1*Δ spores [254]. Taken together,

these experiments demonstrated that Lundblad and Szostak had identified and cloned the *EST1* gene.

Despite the fact that *EST1* was isolated in this screen, there were a number of potential limitations in the experimental methodology used that could allow for obtaining false positives or false negatives, thereby hindering the overall power of the screen. Growth of the mutagenized strains on the selective media could result from a *mutation* in *URA3* instead of plasmid breakage, from the lack of selection strength in their 5-FOA media—a problem that, as mentioned in the text of the journal article, prohibited the use of replica-plating to obtain mutant candidates [254]—or from recombination of *LEU2* into the genome. False negatives, mutations in genes that result in a more rapid loss of the linearized plasmid, could also occur, leading to a no-growth phenotype on selective media.

Because the researchers sought to obtain mutants with a defect in telomere elongation [254], the timing of the plasmid linearization assay was an important factor for their experiments: if a telomere elongation mutant was obtained, the telomeres of the plasmid would not be maintained, the plasmid would be lost, cells would lose the *LEU2* gene and be unable to grow on the selective media. Therefore, mutant candidates would need to be isolated within a somewhat narrow window of time after mutagenesis and before plasmid loss. Previous studies in yeast identifying *TEL1* and *TEL2* had revealed that ~150 generations of growth are necessary to detect a telomere length phenotype when these genes were mutated [258]. Although we now know that *tel1* and *tel2* mutants do not display an EST phenotype [259,260], based on the published results at the time of the Lundblad and Szostak work, the researchers may have overestimated the number of

population doublings allowed before plasmid loss would occur, potentially resulting in the death of certain mutants that met the criteria for their screen. In addition, although 276 bp of Tetrahymena telomeric sequence—a value very close to the ~300 bp length of wild-type yeast telomeres [261]—flanked *URA3* in their circular plasmid [254], the ciliate telomeric sequence may not be protected very well by yeast telomere binding proteins, resulting in a more rapid rate of telomere sequence loss on the plasmid due to inadequate telomere structure. Similarly, recognition of ciliate telomeric sequence as a telomere may not occur extremely readily in yeast. Therefore, after plasmid breakage within *URA3*, resection may proceed well into the Tetrahymena repeats, thus making the telomeres of the linearized plasmid shorter than expected and further limiting the number of population doublings possible before plasmid loss.

Furthermore, the identification of only one gene involved in telomere elongation in this study was sufficient evidence to indicate that this screen was not saturated. This lack of a saturating screen prompted the Lundblad group to develop a more high-throughput screen to assay for mutants in the enzymatic activity responsible for lengthening telomeres. By this time, biochemical analyses had identified as a ribonucleoprotein, termed telomerase, of which the protein components were unknown [194,250,251]. This new screen was based on an observation made in the original study by Lundblad and Szostak that the frequency of chromosome loss is increased in *est1* strains, an outcome presumed to be a consequence of telomere loss [254]. Therefore, in the second study, Lendvay *et al*. utilized a visual assay for chromosome loss that allowed them to screen through fifty-fold more mutants than Lundblad and Szostak were able to assay in the initial screen [262].

To identify mutants displaying a chromosome instability phenotype, a yeast artificial chromosome (YAC) expressing the *SUP11* tRNA suppressor in a strain that had an ochre mutation at the endogenous *ADE2* locus was utilized [262]. This *SUP11* gene contained a mutation that results in the insertion of a tyrosine residue at stop codons during translation and is therefore able to suppress the ochre mutation in *ADE2* [263,264]. In the adenine biosynthetic pathway, *ade2* mutant cells produce a red purinic precursor that is unable to be converted to adenine, which is not pigmented [265]. Consequently, *ade2* mutants are red and cells that are wild-type for *ADE2* or that express this *SUP11* gene on the YAC are white. Therefore, expression of this artificial chromosome allowed for visual detection—by an increase in red sectors on agar plates with limiting adenine—of mutagenized strains that were more likely to lose the YAC as compared to wild-type strains. To uncover potential mutants, individual mutagenized colonies were subjected to multiple rounds of growth to allow for telomere shortening before final plating to permit color development [262]. Mutants obtained from this initial screening protocol were then subjected to the plasmid linearization, telomere length, and senescence assays used in the first study to identify four complementation groups that each represented mutations in genes affecting some aspect of telomerase function [262].

Two years prior to the publication of this screen, the Gottschling group published a screen for genes that, when overexpressed, suppressed telomere silencing [266]. In their screen, the telomerase component 1 (*TLC1*) gene was isolated and determined to be the RNA component of yeast telomerase. Therefore, to examine whether the complementation groups obtained from the Lundblad screen included mutations in genes previously determined to be involved in telomere replication, representative haploid

mutants from each complementation group were crossed to haploid *est1*Δ or *tlc1*Δ strains [262]. For three out of the four complementation groups, the telomere length and growth phenotypes of each diploid were wild-type, supporting the notion that three new genes had been identified [262]. However, when mutants from the remaining complementation group were crossed to the *est1*Δ strain, complementation was not observed, indicating that this complementation group represented the *EST1* gene. Linkage analysis was also performed on these strains in the same manner as that carried out in the previous screen [254,262]. Results of these experiments showed that the mutants analyzed displayed a Mendelian pattern of inheritance and more conclusively demonstrated that new genes had been identified.

Epistasis analysis was used to determine whether the newly identified genes participated in a single or multiple pathways contributing to telomere elongation. The double mutant spores resulting from crosses between a *rad52*Δ strain and either EST mutant or a *tlc1*Δ strain exhibited a more severe senescence phenotype and survivor formation, which results from a recombination-based, telomerase-independent mode of telomere maintenance [262]. However, crosses between an *est1*Δ or *tlc1*Δ strain and the newly identified mutants formed diploid strains whose double mutant spores showed no exacerbation of the telomere length or senescence phenotype. This indicated that *TLC1*, *EST1*, *EST2*, *EST3*, and *EST4* all function together in a pathway different from the recombination-based pathway of which *RAD52* is a participant [262,267]. Subsequent analysis of *EST4* revealed that it corresponds to the *CDC13* gene—which encodes a single-stranded DNA end-binding protein with important roles in telomere end protection

and telomerase recruitment [268,269]—identified by the Hartwell group more than a decade before the publication of the Lundblad screen [270].

The use of the YAC and the chromosome loss assay in the Lundblad screen was fortuitous in that the number of potential limitations that could arise from the use of this experimental paradigm were reduced as compared to the original screen. Reversion mutations at *ADE2* or *SUP11* were the most likely means by which false negatives or false positives, respectively, could be obtained from this screen. The protocol utilized in the second screen also allowed for examination of many more mutant colonies. This, ultimately resulted in the isolation of the gene identified in the first screen, the isolation of a previously identified gene involved in chromosome end protection, as well as two new genes involved in telomere maintenance [262]. To date, along with *TLC1* RNA, three of the genes identified in the Lundblad screen are still considered to comprise the telomerase holoenzyme in budding yeast [271]. Thus, in *Saccharomyces cerevisiae*, telomerase minimally contains four components, which include three EST proteins and the *TLC1* RNA. The catalytic reverse transcriptase (Est2p) and *TLC1* RNA are sufficient to provide the *in vitro* activity of the enzyme [272,273], while Est1p and Est3p are hypothesized to serve regulatory functions during complex assembly and/or activation (**Figure 3**).

Est1p Function

Since its isolation, Est1p has been shown to serve many roles in telomere maintenance as part of telomerase and/or through its interaction with the telomere. In telomerase, Est1p binds a specific stem-loop structure on *TLC1* RNA [274-277]. Est1p is necessary and sufficient for the optimal recruitment of Est3p to telomerase [16]. While

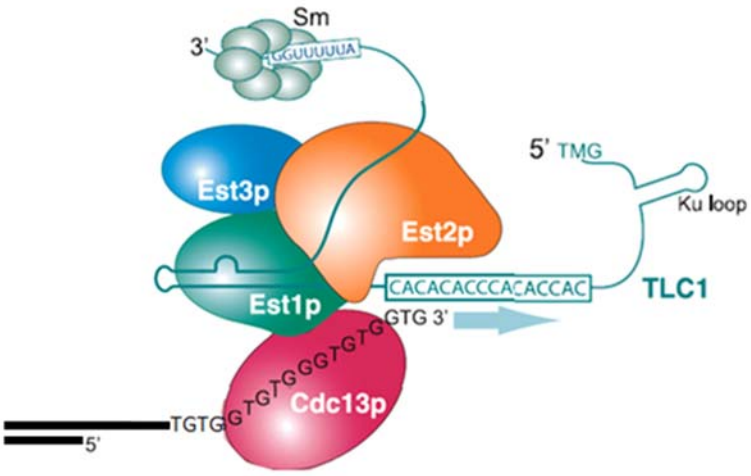

Figure 3. Diagram of *S. cereviasiae* telomerase.

In budding yeast, the telomerase holoenzyme minimally contains the *TLC1* RNA along with three EST proteins. Est2 is the reverse transcriptase and, along with *TLC1* RNA, forms the catalytic core of the enzyme. Est1p and Est3p are a regulatory components. Est1p functions in telomerase recruitment to the telomere through its interaction with the single stranded DNA end-binding protein, Cdc13p. Est1p and Est3p are both hypothesized to contribute to telomerase activation at the telomere.

TLC1 RNA also binds the Sm proteins, an interaction that is essential for its correct maturation in the cell. The interaction of *TLC1* RNA with the double-stranded DNA end-binding yKu70/80p heterodimer is hypothesized to be important for nuclear retention of the RNA. Figure modified from [186].

Est3p has been shown to interact with the N-terminal domain of Est2p [278], a direct interaction between Est1p and Est3p has also been observed [279]. There are conflicting reports regarding the association of Est1p with Est2p. The Lundblad group has shown that Est1p is unable to co-immunoprecipitate with Est2p in a *tlc1Δ* strain and that RNase treatment dissociates Est1p and Est2p, suggesting that Est1p interaction with Est2p is indirect and mediated by *TLC1* RNA [280]. However, the Freeman lab has identified an RNA-independent interaction between Est1p and Est2p *in vitro* [281]. Thus, further investigation into the interaction between these protein components of telomerase is warranted. At the telomere, Est1p, but not Est2p, directly interacts with the single-stranded telomeric DNA binding protein, Cdc13p [269,282]. Expression of a Cdc13-Est2 fusion protein in an *est1*Δ strain results in stable telomere maintenance, bypassing the need for Est1p at the telomere [269]. This result suggests that Est1p recruits telomerase to the telomere through its interaction with Cdc13p.

Est1p is conserved. In fact, it is the budding yeast ortholog of the Est1 and Est1A proteins found in fission yeast and humans, respectively [283,284]. However, while the yeast Est1 proteins contribute to telomerase recruitment to the telomere [269,285], such a role has not been identified for human Est1A.

In addition to the interactions Est1p makes and/or mediates in the telomerase holoenzyme, there is also evidence to support an activating function for Est1p.
As mentioned above, although telomeres are maintained at a short, but stable length in an *est1*Δ strain expressing the Cdc13-Est2 fusion protein, telomere lengthening up to ~800bp—a length more than two-fold greater than the 300 ± 50bp average length of wild-type telomeres—occurs when Cdc13-Est2p is expressed in an *EST1* strain [269].

These data indicate that the presence of Est1p stimulates telomere overelongation even when the recruitment function of Est1p is bypassed, suggesting that Est1p may promote the activation of telomere-bound telomerase *in vivo*. Furthermore, the Freeman lab has shown that recombinant Est1p enhances the *in vitro* DNA extension activity of telomerase up to 14-fold when added to telomerase extracts isolated from an *est1Δ* strain [281].

Est1p is a cell-cycle regulated component of telomerase. Our lab has demonstrated that Est1p is degraded in the G1 phase of the cell cycle in a manner that depends on the proteasome [16,286]. Chromatin immunoprecipitation experiments have shown that although Est2p can associate with telomeric DNA via the interaction of *TLC1* with the DNA-end binding yKu70/80p heterodimer during G1 phase [287,288], Est1p is absent from the telomere at this time [289]. Instead, Est1p association with the telomere peaks in late S phase, the time at which telomerase elongates telomeres [8,289,290]. Since Est1p telomere association varies in the cell cycle in a manner corresponding to the timing of telomerase activity, these data suggest that Est1p levels modulate telomerase activity in a cell cycle dependent fashion, altogether identifying Est1p as an important determinant of telomerase assembly and activity in the cell.

Telomerase Trafficking in Budding Yeast

In contrast to the human system, in which a considerable amount of work has focused on telomerase trafficking, little is known about the biogenesis of telomerase in budding yeast. By definition, telomerase is a small, nuclear ribonucleoprotein. Therefore, it has been hypothesized that telomerase assembles in a manner analogous to a more conventional snRNP. In support of this idea, in *S. cerevisiae*, *TLC1* RNA possesses a

binding site for the Sm proteins and the association between *TLC1* RNA and the heteroseptameric Sm complex is required for the *in vivo* activity of telomerase [14]. This finding is significant because it outlined key differences between the trafficking of vertebrate and yeast telomerase: 1) use of the H/ACA motif to promote maturation of the vertebrate telomerase RNA in the nucleolus along with the unlikelihood of hTR transit through the cytoplasm highlights vertebrate telomerase as a snoRNP and 2) Sm association with *TLC1* RNA and the requirement for a m_3G cap structure for correct processing of the RNA [14] suggests that *TLC1* RNA must transit through the cytoplasm and that telomerase biogenesis in yeast is similar to that of the U snRNP components of the splicing machinery.

As a result of these findings, data concerning telomerase biogenesis in yeast has focused almost exclusively on *TLC1* RNA. Using fluorescence *in situ* hybridization to detect endogenous *TLC1* RNA, the Chartrand group has published the most in-depth investigations into telomerase trafficking in yeast. Their experiments have confirmed routing of *TLC1* RNA to the cytoplasm and identified the karyopherins required for *TLC1* RNA intracellular transport [291]. More specifically, their work demonstrated that *TLC1* RNA undergoes nucleocytoplasmic shuttling in which, after transcription and a number of processing steps in the nucleus, *TLC1* RNA is exported to the cytoplasm by the exportin Crm1p [291] . After presumably further processing and assembly with proteins in the cytoplasm, *TLC1* RNA is then imported to the nucleus by the β importins Mtr10p and Kap122p [291]. Whether this nuclear import occurs by way of direct protein-RNA interactions between *TLC1* and the karyopherins remains unclear. Because *TLC1* RNA possesses binding sites for both Est1p and Est2p [292], a model for yeast telomerase

biogenesis was developed from this body of work (**Figure 4**). Similar to the nuclear import of cytoplasmically matured U snRNPs, this model suggested that binding of the EST and Sm proteins to *TLC1* RNA in the cytoplasm results in a bipartite nuclear localization mechanism for *TLC1* RNA [15], thus presenting the yeast telomerase RNA as a scaffold that mediates telomerase assembly in the cytoplasm before transport of the holoenzyme to the nucleus.

Although this model appears valid, one important caveat lies in the fact that the transport of the protein components of telomerase was not specifically examined. The authors assayed the effect of deleting individual components of telomerase on *TLC1* RNA subcellular localization and found that *TLC1* RNA localized to the cytoplasm in the absence of either of the EST proteins [291]. This phenotype was also observed in an *yku70*Δ strain [291]. However, the methodology used in this work precluded definitive examination of whether it is the nuclear import *or* the nuclear retention of *TLC1* RNA that is perturbed in these deletion strains.

Furthermore, the model for telomerase biogenesis resulting from these initial studies did not take the cell cycle regulation of telomerase into account and failed to synthesize current data regarding the telomere association of telomerase components. Most recently, elegant studies from this group using live-cell imaging techniques to monitor *TLC1* RNA localization dynamics in the cell cycle revealed a transient association of *TLC1* RNA with the telomere in G1 and G2 phases of the cell cycle [293]. This fleeting interaction becomes a persistent focus of *TLC1* RNA at telomeres as the cell traverses through mid/late S phase [293]. This telomere association of *TLC1* in late S phase is greatly reduced in cells harboring the *cdc13-2* mutation, which disrupts the

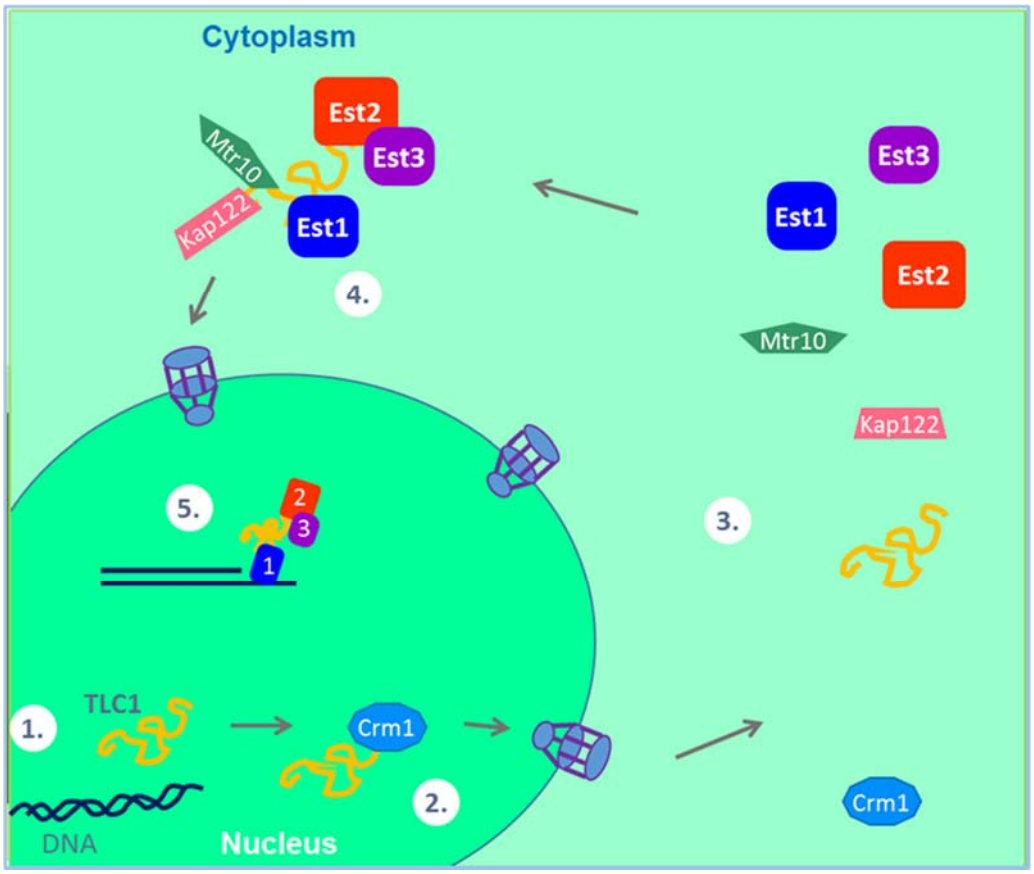

Figure 4. Previous model for telomerase biogenesis in yeast.

Current data about telomerase biogenesis has come from studies focusing on the trafficking of *TLC1* RNA. These data indicate that: (1) after transcription, *TLC1* undergoes several processing steps in the nucleus before (2) associating with the Crm1p nuclear export protein and being exported to the cytoplasm. (3) Once in the cytoplasm, *TLC1* presumably undergoes a number of other processing and assembly steps before (4) associating with the β importins Kap122p and Mtr10 (and presumably the other components of telomerase), which facilitate its import into the nucleus, (5) to allow for the recruitment of telomerase to telomeres for elongation.

Despite what is known about the nucleocytoplasmic trafficking of *TLC1* RNA, the trafficking of the protein components of telomerase has not explicitly been examined. Figure adapted from [15].

Cdc13-Est1 interaction [282]. However, once again, this work did not examine the localization of the protein components of telomerase.

Understandably, low protein abundance has hampered studies of the subcellular localization of telomerase protein components, making it unclear when or how the telomerase complex is imported into the nucleus. The ability of other telomerase components to associate with telomeric DNA when Est1p levels are very low (during G1 phase) [16,290] suggests that Est1p may localize to telomeres independent of its interaction with other telomerase components. Furthermore, nuclear localization of a fusion between Est1p and the Green Fluorescent Protein (GFP) is retained when the fusion protein is expressed in great excess to the other components of telomerase [294]. These data support the idea that Est1p possesses a mechanism for nuclear import that is independent of its interactions with other components of telomerase and suggest that the regulation of Est1p nuclear import may contribute to telomerase biogenesis and function. Therefore, my research has focused on characterizing Est1p nuclear localization. As the only known telomerase component whose abundance is regulated in the cell cycle, Est1p is a particularly attractive target for my efforts to obtain a more integrative model for telomerase biogenesis in yeast.

CHAPTER II

NORMAL TELOMERE LENGTH MAINTENANCE IN YEAST REQUIRES NUCLEAR IMPORT OF THE EVER SHORTER TELOMERES 1 (EST1) PROTEIN VIA THE IMPORTIN ALPHA PATHWAY[1]

Introduction

Telomeres, the heterochromatic, G/T-rich regions of DNA located at the ends of linear chromosomes, are dynamic structures, undergoing multiple rounds of attrition and elongation over the lifetime of many eukaryotic cells. Because telomeres provide an essential capping function that protects DNA ends and aids in the maintenance of genomic stability, most eukaryotes use the enzyme telomerase to elongate telomeres [295].

Telomerase is a ribonucleoprotein complex in which the RNA subunit interacts with a specialized reverse transcriptase to synthesize telomeric DNA. In the yeast *Saccharomyces cerevisiae*, telomerase minimally consists of the *TLC1* RNA, which contains the template for nucleotide addition, and three Ever Shorter Telomere (EST) proteins [254,262,266,296]. Est2p is the reverse transcriptase that, together with *TLC1* RNA, is necessary and sufficient for enzyme activity *in vitro* [272,273]. Est1p and Est3p are essential regulatory components that stimulate the *in vitro* activity of telomerase and

[1]This chapter is adapted from Hawkins C and Friedman KL. (2014) Normal telomere length maintenance in yeast requires nuclear import of the Ever Shorter Telomeres 1 (EST1) protein via the importin alpha pathway. Eukaryot Cell [Epub ahead of print 2014 Jun 6].

have been implicated in the recruitment and/or activation of telomerase at the telomere [273,278,281,296].

Interactions between the subunits of telomerase and between telomerase and the telomere are complex. Est1p interacts with the single-stranded, telomeric DNA binding protein, Cdc13p [268,282]. Ectopic expression of a Cdc13-Est2 fusion protein bypasses the requirement for *EST1*, suggesting that Est1p recruits telomerase to the telomere through the interaction with Cdc13p [269]. *TLC1* RNA possesses distinct binding sites for Est1p and Est2p, suggesting that the interaction between Est1p and Est2p is RNA-mediated *in vivo* [275,276,280,297]. However, an RNA-independent interaction between Est1p and Est2p has been observed [281]. In live cells, persistent foci of *TLC1* RNA are detected at telomeres during S phase—a phenotype greatly reduced in cells harboring the *cdc13-2* mutation in which telomere synthesis is perturbed [293]. During G1 phase, Est2p is detected at telomeres by chromatin immunoprecipitation in a manner that depends on the interaction of *TLC1* RNA with the DNA-end binding yKu70/80p heterodimer [289,290,298,299]. However, imaging of *TLC1* dynamics during G1 phase in live cells suggests that the interactions of *TLC1* with the telomere are transient and qualitatively different from those observed during S phase [293].

In contrast to Est2p and Est3p, Est1 protein levels are low in G1 phase due to proteasome-mediated degradation [16,286]. Low levels of Est3p are detected at telomeres during G1 phase [279], presumably through the interaction of Est3p with Est2p [278], but the association of Est3p with telomeres increases in S phase concurrent with rising Est1p expression and with the ability of telomerase to elongate telomeres [8,279,290,298]. Est1p is necessary and sufficient to stimulate the recruitment of Est3p to telomerase [16],

consistent with the hypothesis that assembly of Est1p with telomerase allows optimal recruitment of Est3p to the complex.

Though much attention has focused on the dynamic associations of telomerase components with the telomere, less is known about where and when the components of telomerase assemble. By fluorescence *in situ* hybridization, endogenous *TLC1* RNA shuttles between the nucleus and the cytoplasm with nuclear import depending on the β importins Mtr10p and Kap122p [291,300]. Furthermore, deletion of any one of the EST proteins or yKu70 perturbs *TLC1* RNA nuclear localization and/or retention [291]. Despite what is known about *TLC1* RNA nucleocytoplasmic shuttling, direct studies of the subcellular localization of telomerase protein components have been hampered by low protein abundance [279,301,302]. The ability of other telomerase components to associate with telomeric DNA during G1 phase (when Est1p levels are low) suggests that Est1p may localize independently to telomeres. Indeed, overexpressed Est1p localizes to the nucleus, even when present in great excess to other telomerase components [274,294]. These data support the idea that Est1p possesses a mechanism for nuclear import that is independent of its interactions with other components of telomerase and suggest that the regulation of Est1p nuclear import may contribute to telomerase biogenesis and function.

Experimental Procedures

Yeast Strains

Standard protocols for manipulation of yeast were carried out as described [303]. Strains and corresponding references are listed in **Table 1**; plasmids and corresponding references are listed in **Table 2**. The hygromycin resistance gene (*HPHMX4*) was PCR-amplified from pBS4 using primers containing sequences found immediately upstream and downstream of the *BAR1* open reading frame (ORF) [304] and the resulting product was transformed into yeast strain K1534 to generate YKF450. *EcoR*V linearization of YIplac204/TKC-dsRED-HDEL allowed for one-step integration of the construct into the *TRP1* locus of YKF450 to create YKF900. PCR-amplification of the kanamycin resistance gene from pFA6a-KANMX6 using primers containing sequences found immediately upstream and downstream of the *EST1* ORF generated a fragment that was transformed into YKF450 to produce YKF901. YKF902 was constructed in a similar manner using sequences flanking *KAP123*. YKF903 was generated by PCR amplification of the *kap122::KANMX4* locus from BY4741 *kap122::KANMX4* followed by transformation of the PCR product into the *mtr10-7* strain. Sequences of PCR primers used in this study are available upon request.

Plasmids

To generate pCH100, pPS809 (originally designed to insert ORFs at the C-terminus of GFP) was altered to allow fusion at the N-terminus of GFP. Briefly, the multiple cloning site (MCS) at the C-terminus of GFP was replaced with a STOP codon. A DNA fragment

Table 1. Yeast strains used in this study.

Strain Name	Genotype	Source
K1534	*MAT***a** *ade2-1 trp1-1 can1-100 leu2-3,113 his3-11,15 ura3 ssd1 bar1::HISG*	M.A. Hoyt [305]
YKF450	K1534 *bar1:: HPHMX4*	This Study
YKF900	YKF450 *dsRED-HDEL*	This Study
YKF901	YKF450 *est1::KANMX6*	This Study
YKF902	YKF450 *kap123::KANMX6*	This Study
mtr10-7	*Mat*α *mtr10::HIS3 ade2 leu2 trp1 ura3 his3 pRS314 mtr10-7*	E. Hurt [306]
YKF903	*mtr10-7 kap122::KANMX4*	This Study
BY4741	*MAT***a** *his3Δ1 leu2Δ0 lys2Δ0 ura3Δ0*	Open Biosystems
	BY4741 *kap122::KANMX4*	Open Biosystems
	BY4741 *kap108::KANMX4*	Open Biosystems
	BY4741 *kap114::KANMX4*	Open Biosystems
	BY4741 *kap120::KANMX4*	Open Biosystems
	BY4741 *los1::KANMX4*	Open Biosystems
	BY4741 *msn5::KANMX4*	Open Biosystems
ACY1563	*MAT***a** *ura3-1 leu2-3 trp1-1 his3-11 can1-100 srp1-54*	A. Corbett [307]
PSY1199	*MAT*α *ade2Δ::hisG ade8Δ100::KAN^R ura3Δ leu2Δ1 his3Δ200 nmd5Δ::HIS3*	P. Silver [308]
PSY688	*MAT***a** *srp1-31 ura3 leu2 trp1 his3 ade2*	P. Silver [309]
PSY1103	*MAT***a** *ura3-52 leu2Δ1 trp1Δ63 rsl1-4*	P. Silver [308]
PSY580 *pse1-1*	*MAT***a** *ura3–52 leu2Δ1 trp1Δ63 pse1-1*	P. Silver [310]

containing the MCS, *GAL1* promoter, and the first 171 base pairs (bp) of the GFP ORF was generated by Overlap Extension PCR [311] and cloned into the *Age*I/*Msc*I sites of the redesigned pPS809 vector. GFP was replaced by enhanced GFP (S65T variant; EGFP) through PCR amplification from pAC1069 and insertion into the *Hin*dIII/*Not*I sites of the redesigned pPS809 plasmid. To generate pCH200 (2GFP), EGFP was PCR-amplified from pCH100 and inserted into the *Hin*dIII site of pCH100.

The *EST1* open reading frame was PCR amplified from pRS416-EST1 and inserted into the *Sph*I/*Not*I sites of pCH100 to generate pCH101. To fuse different regions of *EST1* with *2GFP*, pRS416-EST1 was used as template to amplify regions of *EST1* for cloning into the *Spe*I/*Sph*I sites of pCH200. *EST1* mutants were created by site-directed mutagenesis within the N-terminal 600bp or the central 900bp of *EST1* and cloned as *Bam*HI/*PflM*I or *BspE*I fragments, respectively, into pRS416-EST1. The resultant mutant vectors were used as template to amplify specific regions of *EST1* for cloning in frame into the *Bam*HI/*PflM*I or *BspE*I sites of pCH100 or the *Spe*I/*Sph*I sites of pCH200.

The T_{Ag}NLS [10] (including residues GSP<u>KKKRK</u>VEASEFGS; positively charged amino acids contributing to nuclear localization are underlined) was cloned into pRS416-EST1, pCH100, and pCH200 by annealing two oligonucleotides and inserting the resulting fragment into the *Bam*HI site of each vector. The Nab2NLS [49] containing residues 198-252 based on full-length Nab2p was amplified from pAC719 and the 175bp fragment was cloned into the *Bam*HI/*Spe*I site of pCH101 to generate pCH112. To generate pCH015, a *Spe*I/*Not*I fragment from pCH101 was inserted into the multiple cloning site of pRS416. Next, a *Sac*I fragment containing the *EST1* terminator from

Table 2. Plasmids used in this study.

Plasmid Name	Description	Source
pBS4	CFP-HPHMX4 *Amp^R*	Yeast Resource Center
pKF600	*P_{GAL1}-HA_3-EST1 LEU2 2μ Amp^R*	[286]
	YIplac204/ TKC-dsRED-HDEL TRP1 Amp^R	B. Glick [312]
pFA6a-KANMX6	*pFA6a (P_{T7}KANMX6 Amp^R)*	[313]
pRS416	*URA3 CEN Amp^R*	[314]
pRS416-EST1	*pRS416 P_{EST1} EST1*	[286]
pCH001	*pRS416 P_{EST1} est1(K113A)*	This Study
pCH002	*pRS416 P_{EST1} est1(K122A, K123A)*	This Study
pCH003	*pRS416 P_{EST1} est1-mut1*	This Study
pCH004	*pRS416 P_{EST1} est1-mut2*	This Study
pCH005	*pRS416 P_{EST1} est1-mut3*	This Study
pCH006	*pRS416 P_{EST1} est1-mut4*	This Study
pCH007	*pRS416 P_{EST1} est1-mut5*	This Study
pCH008	*pRS416 P_{EST1} est1-mut2,3*	This Study
pCH009	*pRS416 P_{EST1} est1-mut1,2,3*	This Study
pCH010	*pRS416 P_{EST1} T_{Ag}NLS-EST1*	This Study
pCH011	*pRS416 P_{EST1} T_{Ag}NLS-est1-mut1*	This Study
pCH012	*pRS416 P_{EST1} T_{Ag}NLS-est1-mut2*	This Study
pCH013	*pRS416 P_{EST1} T_{Ag}NLS-est1-mut3*	This Study
pCH014	*pRS416 P_{EST1} T_{Ag}NLS-est1-mut1,2,3*	This Study
pCH015	*pRS416 P_{EST1} EST1-GFP*	This Study
pPS809	*P_{GAL1} GFP 2μ URA3 Amp^R*	P. Silver
pAC1069	*P_{MET25} GFP_2 URA3 CEN AMP*	A. Corbett [315]
pCH100	*P_{GAL1} GFP 2μ URA3 Amp^R*	This Study
pCH101	*pCH100 EST1-GFP*	This Study
pCH102	*pCH100 est1-mut1-GFP*	This Study
pCH103	*pCH100 est1-mut2-GFP*	This Study
pCH104	*pCH100 est1-mut3-GFP*	This Study
pCH105	*pCH100 est1-mut1,2,3-GFP*	This Study
pCH106	*P_{GAL1} T_{Ag}NLS-GFP 2μ URA3 Amp^R*	This Study
pCH107	*pCH100 T_{Ag}NLS-EST1-GFP*	This Study
pCH108	*pCH100 T_{Ag}NLS-est1-mut1-GFP*	This Study
pCH109	*pCH100 T_{Ag}NLS-est1-mut2-GFP*	This Study
pCH110	*pCH100 T_{Ag}NLS-est1-mut3-GFP*	This Study
pCH111	*pCH100 T_{Ag}NLS-est1-mut1,2,3-GFP*	This Study
pCH112	*pCH100 Nab2NLS-EST1-GFP*	This Study
pCH200	*P_{GAL1} 2GFP 2μ URA3 Amp^R*	This Study
pCH201	*pCH200 T_{Ag}NLS-2GFP*	This Study
pCH202	*pCH200 EST1(NT200)-2GFP*	This Study
pCH203	*pCH200 est1(K113A)NT200-2GFP*	This Study

pCH204	*pCH200 est1(K122A, K123A)NT200-2GFP*	This Study
pCH205	*pCH200 est1-mut1(NT200)-2GFP*	This Study
pCH206	*pCH200 EST1(Mid300)-2GFP*	This Study
pCH207	*pCH200 est1-mut2(Mid300)-2GFP*	This Study
pCH208	*pCH200 est1-mut3(Mid300)-2GFP*	This Study
pCH209	*pCH200 est1-mut2,3(Mid300)-2GFP*	This Study
pCH210	*pCH200 EST1(Cterm200)-2GFP*	This Study
pCH211	*pCH200 EST1(CT500)-2GFP*	This Study
pCH212	*pCH200 EST1(199-350)-2GFP*	This Study
pCH213	*pCH200 est1-mut2(199-350)-2GFP*	This Study
pCH214	*pCH200 EST1(351-499)-2GFP*	This Study
pCH215	*pCH200 est1-mut3(351-499)-2GFP*	This Study
pCH216	*pCH200 est1-mut4(351-499)-2GFP*	This Study
pCH217	*pCH200 est1-mut5(351-499)-2GFP*	This Study
pCH218	*pCH200 EST1(351-435)-2GFP*	This Study
pCH219	*pCH200 EST1(436-499)-2GFP*	This Study
pHK537	P_{HRB1} *Hrb1-GFP CEN URA3* Amp^R	H. Krebber [316]
pAC719	P_{NAB2} *NAB2-GFP 2*μ *URA3* Amp^R	A. Corbett [317]
pMH1326	P_{GAL1} *RNR4-GFP CEN URA3* Amp^R	M. Huang [318]
pRS413	*HIS3 CEN* Amp^R	[314]
pCH016	*pRS413* P_{EST1} *EST1*	This Study
pCH017	*pRS413* P_{SRP1} *SRP1*	This Study
pCH018	*pRS413* P_{EST1} *Nab2NLS-EST1*	This Study
pCH019	*pRS313 TLC1 CEN HIS3* Amp^R	This Study
pCH020	*pRS423 TLC1 2*μ *HIS3* Amp^R	This Study

pKF600 was inserted at the 3' end of the *EST1* ORF and a *Pvu*II/*PflM*I fragment from pRS416-EST1 containing the *EST1* promoter as well as the first 717bp of *EST1* coding sequence was inserted.

To generate pCH016, a *Pvu*II fragment from pRS416-EST1 was cloned into pRS413. After PCR amplification of *SRP1* from genomic DNA isolated from strain YKF450, the 2434bp PCR product—containing 506bp and 302bp of *SRP1* promoter and terminator sequence, respectively—was cloned into the *Xho*I/*Bam*HI sites of pRS413 to generate pCH017. A *BamH*I/*PflM*I fragment from pCH112 was cloned into pCH016 to generate pCH018.

Fluorescence Microscopy

Direct fluorescence microscopy was used to examine the localization of GFP fusion proteins as well as dsRED-HDEL in YKF450-derived strains. Cells expressing GFP-fusion proteins under control of the *GAL1* promoter were grown overnight to mid-log phase in synthetic complete media lacking uracil and containing 2% raffinose. Galactose was added to a final concentration of 2% and cells were incubated at 30°C for 1 hour. Cells expressing GFP fusion proteins driven by a native promoter were grown similarly without the addition of galactose. Hoechst 33342 was added to a final concentration of 1 μg/ml and cells were incubated 15 min at 30°C. Cells were washed once and resuspended in the appropriate expression media (described above). Cells were imaged using a Zeiss Axio Observer inverted microscope (40X Oil Immersion objective, 1.3 numerical aperture) with FITC, TexasRED, and DAPI (Semrock Brightline FITC-3540B-ZHE-ZERO, TXRED-4040B-ZHE-ZERO, and DAPI-1160A-ZHE-ZERO, respectively) filters

and a Photometrics Cool Snap EZ CCD camera. Images were acquired using Slidebook 4.2 software, making use of the zoom + feature located under the Scope tab of the Focus Controls window to obtain an additional 2X magnification of the captured images. Images were collected and scaled using ImageJ software [319] and Adobe Photoshop CS5 software was used for image processing.

At least 100 GFP-expressing cells for each GFP-fusion protein examined were quantified and binned as having a Nuclear only (N) phenotype, in which the fluorescent signal was localized exclusively in the nucleus, a Cytoplasmic only (C) phenotype, in which the fluorescence was localized primarily to the cytoplasm with no evidence of nuclear enrichment, or as Intermediate (I), in which GFP fluorescence was both nuclear and cytoplasmic. N, I, and C are mutually exclusive designations. Cells were also categorized non-exclusively as having a Vacuolar phenotype (V) in which GFP fluorescence was observed in the vacuole.

Strains containing temperature-sensitive alleles of importin mutants were grown to mid-log phase in appropriate selective media at the permissive temperature (18°C or 25°C) and galactose was added to the appropriate cultures to induce plasmid expression. A 3 ml aliquot was kept at the permissive temperature while the remainder of the culture was shifted to the restrictive temperature (37°C). Cells were incubated 5 hours before 30 min fixation by the addition of formaldehyde to a 3.7% final concentration and 15 min Hoechst-staining as described above. Cells were washed twice with 0.1M potassium phosphate, pH 6.5 and resuspended in 1X phosphate buffered saline prior to imaging. Because of the high level of cytoplasmic fluorescence associated with expression of

Rnr4-GFPp from pMH1326, strains harboring this construct were incubated for only 2.5 hours at the permissive temperature before fixation.

Telomere Length Analysis by Southern Blot

A YKF901 strain containing the complementing plasmid pRS416-EST1 was grown overnight in rich liquid media and subsequently plated on solid media containing 5-Flourorotic acid (5-FOA; Gold Biotechnology) to select for loss of the complementing plasmid. A single YKF901 colony that grew on 5-FOA was inoculated into rich media and transformed with variants of pRS416 or pCH101. ACY1563 was transformed with pRS413 or pRS423 derived constructs. Transformants were restreaked for ~100 generations on solid selective media with 2% glucose, raffinose, or galactose as the carbon source where appropriate. YKF901 strains were grown at 30°C and ACY1563 strains were grown at 25°C or 35°C. Liquid cultures were grown to saturation in selective media at the appropriate temperature, genomic DNA was isolated from each strain by glass bead lysis [320], digested with *Pst*I, and separated in a 1.2% agarose gel. The DNA was blotted to a Hybond N+ membrane (GE Healthcare), crosslinked to the membrane, and probed at 65°C using a yeast radiolabeled telomeric probe as previously described [321].

Southern blot images were quantified using Image J software. A line drawn down the middle of each lane was used to derive a plot of signal intensity at each lane position. Telomere restriction fragment (TRF) length was defined as the point of highest signal intensity within the predominant smear of Y' telomeres and was converted to base pairs by comparison with a radio-labeled molecular weight ladder. In cases where a second

smear of higher molecular weight was observed on the gel the higher molecular weight smear was not included in the quantification. The derivation of this additional smear is unclear, but could represent partial digestion. To account for slight differences in migration across the gel, where possible, samples were flanked by molecular weight marker lanes placed no more than 6 lanes apart. Marker bands of less than or equal to 4kb were utilized for quantification. In cases where the flanking markers did not migrate identically, the lengths of intervening samples were corrected using the slope of a line connecting marker bands of the same molecular weight. Based on sequenced telomeres available in the *Saccharomyces* genome database (www.yeastgenome.org), the terminal *Pst*I restriction site on Y' element-containing telomeres lies an average of 540bp from the $TG_{1\text{-}3}$ repeats of the yeast telomere. Therefore, telomere lengths were determined by subtracting 540bp from each TRF length. Statistical analysis of the Southern blot data (ANOVA with Tukey's post hoc test or Student's T test) was performed using JMP software.

Fusion of the T_{Ag}NLS to wild-type *EST1* slightly increased telomere length compared to strains complemented with untagged *EST1* alone. To account for this increase, the average difference in telomere length between the *EST1* and *T_{Ag}NLS-EST1* complemented strains was subtracted from the telomere length of strains harboring T_{Ag}NLS fusions with *est1-mut1(FL)*, *est1-mut2(FL)*, or *est1-mut3(FL)* prior to statistical analysis.

Telomere Length Analysis by Ligation-Mediated PCR

After ACY1563 was transformed with pRS413- or pRS423-derived constructs, transformants were restreaked for ~150 generations at 25°C or 35°C on solid selective media. Liquid cultures were grown to saturation in selective media at the appropriate temperature. Genomic DNA was isolated from each strain by glass bead lysis [320] and prepared for ligation-mediated telomere PCR as described [322]. In brief, after RNase-treatment, genomic DNA was blunted with T4 DNA polymerase (New England BioLabs) and ligated to a double-stranded oligonucleotide. Y' element-containing telomeres were amplified by PCR using one primer that anneals to the sub-telomeric DNA of at least five yeast telomeres and a second primer that anneals to the ligated, double-stranded oligonucleotide. PCR products were stained with 1X SYBR Green (Life Technologies), resolved on a 2.5% agarose gel, and imaged using a Typhoon Scanner. TRF lengths were analyzed and quantified from the resulting images using Image J as described for the Southern blot analysis above. Because the telomeric primer anneals, on average, 166bp from the $TG_{1\text{-}3}$ repeats, this value was subtracted from the TRF lengths to obtain the average telomere length of each sample.

Western Blotting

The YKF450 strain was transformed with various constructs expressing GFP-fusion proteins as well as untagged control constructs. Transformants were grown to mid-log phase in 15 ml synthetic complete media lacking uracil and containing 2% raffinose. For cells harboring pCH100- or pCH200-derived constructs, galactose was added to a final concentration of 2% and cells were incubated 1 hour at 30°C to induce plasmid

expression. When the cultures reached an OD_{600} of 1.0, cells were harvested by centrifugation at 4°C for 10 min at 6000 rpm from 10 ml of culture and whole cell extract was prepared by trichloroacetic acid precipitation [323]. Extracts were resuspended in 150 µl 0.05N NaOH, immediately frozen and stored at -80°C. Samples were resolved on 10% Bis-Tris NuPAGE gels (Invitrogen) according to the manufacturer's instructions and transferred to Hybond P membrane (GE Healthcare) by wet transfer in NuPAGE transfer buffer (Invitrogen). A 1:3000 dilution of Rabbit anti-GFP (Torrey Pines Biolabs) was used as primary antibody for GFP detection and 1:5000 dilution of mouse monoclonal anti-actin (Abcam) was used as primary antibody for Actin detection. Peroxidase-conjugated goat anti-rabbit (Millipore) and goat anti-mouse (Chemicon) were used as secondary antibodies, respectively. Proteins were detected using ECL plus Western Blotting Detection system (GE Healthcare).

Results

In initial experiments to monitor and characterize the subcellular localization of Est1p, we utilized strains that overexpress a green fluorescent protein (GFP)-tagged variant because the limited abundance of Est1p precludes the use of fluorescence microscopy to examine localization at endogenous levels [279,301,302]. Importantly, as presented below, we proceed to determine the functional relevance of Est1p nuclear localization using untagged protein expressed from the endogenous *EST1* promoter at low copy number.

An Est1-GFP Fusion Protein Localizes to the Nucleus

Est1p localizes to the nucleus when expressed from a galactose-inducible promoter [274,294] suggesting that Est1p possesses an autonomous mechanism for nuclear import. To confirm these results and to identify residues that mediate nuclear localization, an *EST1-GFP* fusion construct under control of the inducible *GAL1* promoter was cloned into a high-copy vector and transformed into cells possessing the dsRED-HDELp fusion [312], a marker for the nuclear envelope. Upon galactose-induction, the Est1-GFP fusion protein (Est1-GFPp) localized within the area outlined by dsRED-HDELp and colocalized with Hoechst 33342 staining (**Figure 5**). Est1-GFPp exhibited diffuse fluorescence throughout the nucleus with a single bright focus within the nuclear envelope but outside of the region staining for DNA. This phenotype is consistent with nucleolar localization, as previously reported [294], since the nucleolus resists staining by Hoechst 33342 [324]. We conclude that the Est1-GFP fusion protein utilized in this study localizes to the nucleus, with a tendency to concentrate in the nucleolar compartment.

To estimate the extent of overproduction of Est1-GFPp, the expression level upon galactose induction was compared to expression of the same protein from the native *EST1* promoter on a centromere vector (Est1-GFPp$_{CEN}$). While Est1-GFPp$_{CEN}$ was undetectable by Western blot (**Figure 6**, lane 2), the overexpressed protein was visible when whole cell extract was diluted up to 81 fold (**Figure 6**, lane 9), placing a lower boundary on the extent of overexpression relative to Est1-GFPp$_{CEN}$. We cannot rule out the possibility that steady state levels of Est1-GFPp$_{CEN}$ are lower than those of endogenous Est1p. However, the ability of Est1-GFPp$_{CEN}$ to support telomere

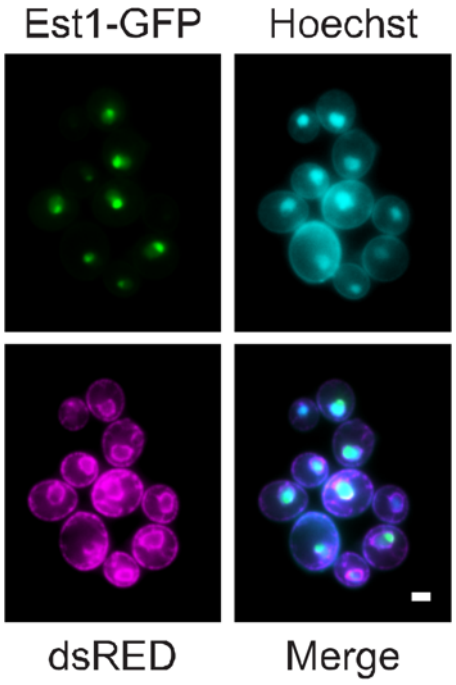

Figure 5. Localization of the overexpressed Est1-GFP fusion protein.

Yeast containing pCH101 (2μ; *EST1-GFP*) were grown in galactose-containing medium and examined by live-cell fluorescence microscopy. Hoechst 33342 (Hoechst) stains DNA and the dsRED-HDEL fusion marks the nuclear envelope. 96% of GFP-fluorescing cells demonstrate exclusive nuclear localization of Est1-GFPp (Merge). n ≥ 100 GFP-expressing cells. Representative images are selected from at least 3 biological replicates. Scale bar = 2μm.

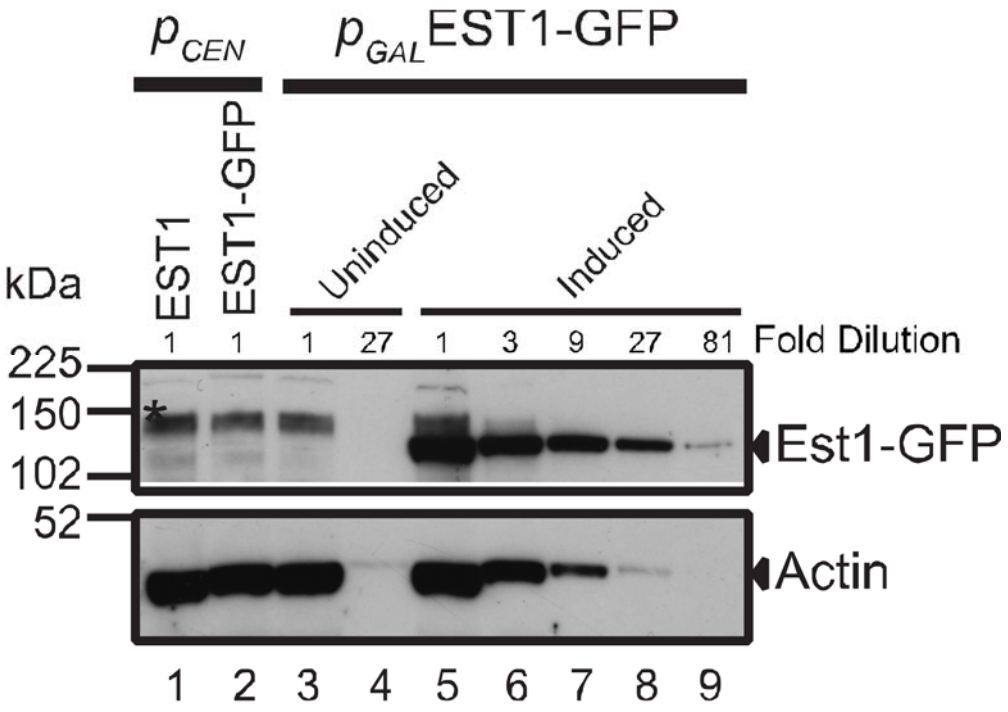

Figure 6. Relative expression levels of the Est1-GFP fusion protein.

Whole cell extracts (WCE) prepared from wild-type cells expressing *EST1* from a centromere vector (pRS416-EST1; lane 1) or *EST1-GFP* from a low-copy (pCH015; lane 2) or high-copy vector (pCH101; lanes 3 thru 9) were separated by gel electrophoresis, Western blotted, and probed with anti-GFP and anti-Actin antibodies. Uninduced samples (lanes 3 and 4) are WCE prepared from cells grown in raffinose; induced samples (lanes 5 thru 9) were grown in galactose. The fold dilutions of each sample of WCE are indicated. (*): nonspecific band.

maintenance (see below) demonstrates that the fusion protein is expressed and at least partially functional. Since there are fewer than 100 molecules of each of the known core components of telomerase in the cell [279,325], we conclude that the galactose-induced Est1-GFPp is expressed in great excess to the levels of endogenous telomerase components.

To test Est1-GFPp function, its ability to complement the deletion of *EST1* was examined. As expected, transformation of an *est1*Δ strain with an empty vector led to senescence followed by the appearance of rare survivors that use a recombination-based mode of telomere maintenance [267,326]. This phenotype is evidenced by amplification of subtelomeric Y′ elements (**Figure 7A**, lanes 1 and 2, see arrows) and the absence of the discrete telomeric signal below 1 kb that is observed in cells transformed with a construct harboring wild-type *EST1* (**Figure 7A,** lanes 3-5). In contrast to the phenotypes observed from cells harboring the empty vector, both low level and over-expression of the Est1-GFP fusion protein in an *est1Δ* strain supported normal growth. Expression of the fusion protein from a centromere plasmid resulted in short, but stable telomere length, while cells overexpressing the fusion protein maintained telomeres at a length comparable to that of cells harboring untagged *EST1* (**Figure 7B**). Thus, the Est1-GFP fusion retains functionality and overexpression is compatible with normal telomere maintenance.

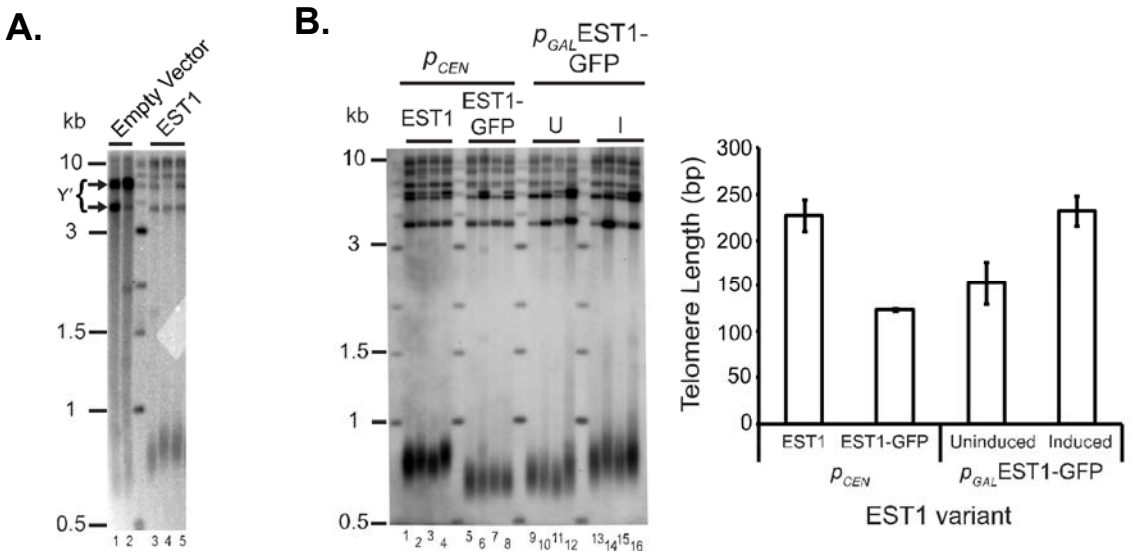

Figure 7. The Est1-GFP fusion protein complements the deletion of *EST1*.

A. Telomere length analysis of *est1Δ* cells containing empty vector (pRS416; lanes 1 and 2) or wild-type *EST1* (pRS416-EST1; lanes 2-5). The indicated constructs were transformed into an *est1*Δ strain following loss of a complementing plasmid and cells were grown for ~100 generations. Marker sizes are indicated in kilobases (kb). Arrows point to bands resulting from amplification of subtelomeric Y′ elements.

B. Telomere length analysis of cells expressing Est1-GFPp from a low- or high-copy number vector. Constructs described in (B) were transformed into an *est1*Δ strain and cells were grown for ~100 generations on solid media containing glucose (lanes 1-12) or galactose (lanes 13-16). Strains were grown to saturation in the appropriate liquid medium, genomic DNA was isolated, and Southern blotted. Four independent colonies were analyzed for each strain. Marker sizes are indicated in kilobases (kb). Quantification of the Southern blot is to the right of the gel. Error bars represent standard deviation.

Three Separable Regions of Est1p Are Able to Mediate Nuclear Localization

To identify sequences capable of supporting nuclear import, Est1p was initially subdivided into three regions of 200-300 residues. To prevent passive import through the nuclear pore [327], each peptide was expressed as a fusion with two tandem GFP monomers (2GFP) under control of the inducible *GAL1* promoter. The localization phenotype(s) observed for at least 100 GFP-expressing cells were quantified and categorized as exhibiting exclusively nuclear *or* cytoplasmic fluorescence (N or C, respectively) or both nuclear *and* cytoplasmic fluorescence (I). We interpret the "I" category as representing a partial phenotype in which nuclear localization can occur, but is incomplete. Proteins that exhibit localization in the "N" and "I" categories, with few or no cells displaying the "C" phenotype, are considered to be capable of nuclear localization while those with 70% or more of the cells in the "C" category are defined as lacking the ability to localize to the nucleus. A few constructs exhibited variable levels of vacuolar fluorescence (V) in addition to nuclear and/or cytoplasmic fluorescence. Because Est1p does not appear to possess a vacuolar targeting sequence and the wild-type Est1-GFP fusion protein was not observed in the vacuole (see **Figure 5**), such localization is likely artifactual.

As expected, 2GFP alone localized primarily to the cytoplasm, while a fusion between the T_{Ag}NLS and 2GFP localized primarily to the nucleus (**Figure 8**). Proteins containing the N-terminal 200 amino acids (aa) (NT200) or the central 300 aa [Mid300; residues 199-499] of Est1p fused to 2GFP showed either complete or partial nuclear localization in most cells, similar to the T_{Ag}NLS-GFP fusion. However, fusion of the C-terminal 200 aa (CT200) of Est1p to 2GFP primarily resulted in cytoplasmic localization

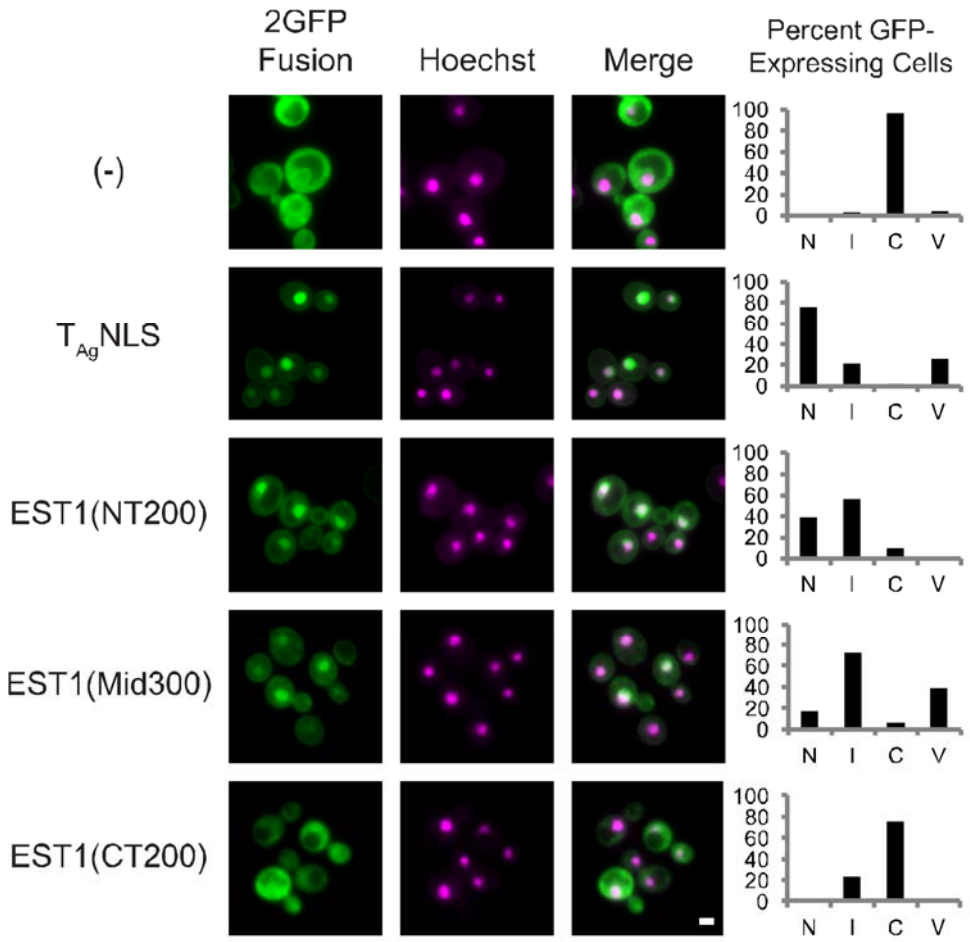

Figure 8. Localization analysis of three regions of Est1p.

Wild-type cells harboring 2GFP fusions of the indicated proteins under control of a galactose-inducible promoter in a high copy vector (from top to bottom: pCH200, pCH201, pCH202, pCH206, pCH210) were grown in galactose-containing medium. Cells were stained with Hoechst 33342 and visualized by live-cell, fluorescence microscopy. Adjacent to each set of images is a graph indicating the localization phenotype observed in the GFP-expressing cells. N = nuclear fluorescence only, I = intermediate (fluorescence in both nucleus and cytoplasm), C = cytoplasmic fluorescence only, and V = vacuolar fluorescence. N, I, and C are mutually exclusive categories, while any cell exhibiting vacuolar staining was counted in the V category regardless of other localization observed. n ≥ 100 GFP-expressing cells for each sample. Representative images are selected from at least 3 biological replicates. Scale bar = 2μm. See Figure 10 for locations of each construct.

(**Figure 8**). To lend additional support to the observation that Est1p possesses at least two separable regions that can direct nuclear localization, a region containing the C-terminal 500 aa (CT500) of Est1p was expressed in the context of the 2GFP fusion protein; this fusion also demonstrated the ability to localize to the nucleus (**Figure 9**). Subdivision of the Mid300 region (aa 199-499) revealed that two shorter regions, 199-350 and 351-499, are each able to direct nuclear localization of 2GFP (**Figure 9**). Finally, the 351-499 region was divided to produce fragments from 351-435 and 436-499. Only the second of these fragments is consistently observed in the nucleus (**Figure 9**). Each fusion protein was expressed and was of the expected molecular weight (**Figure 10**). As summarized in **Figure 11**, we conclude that at least three separable regions within the N-terminal 500 aa of Est1p are able to support nuclear localization of 2GFP.

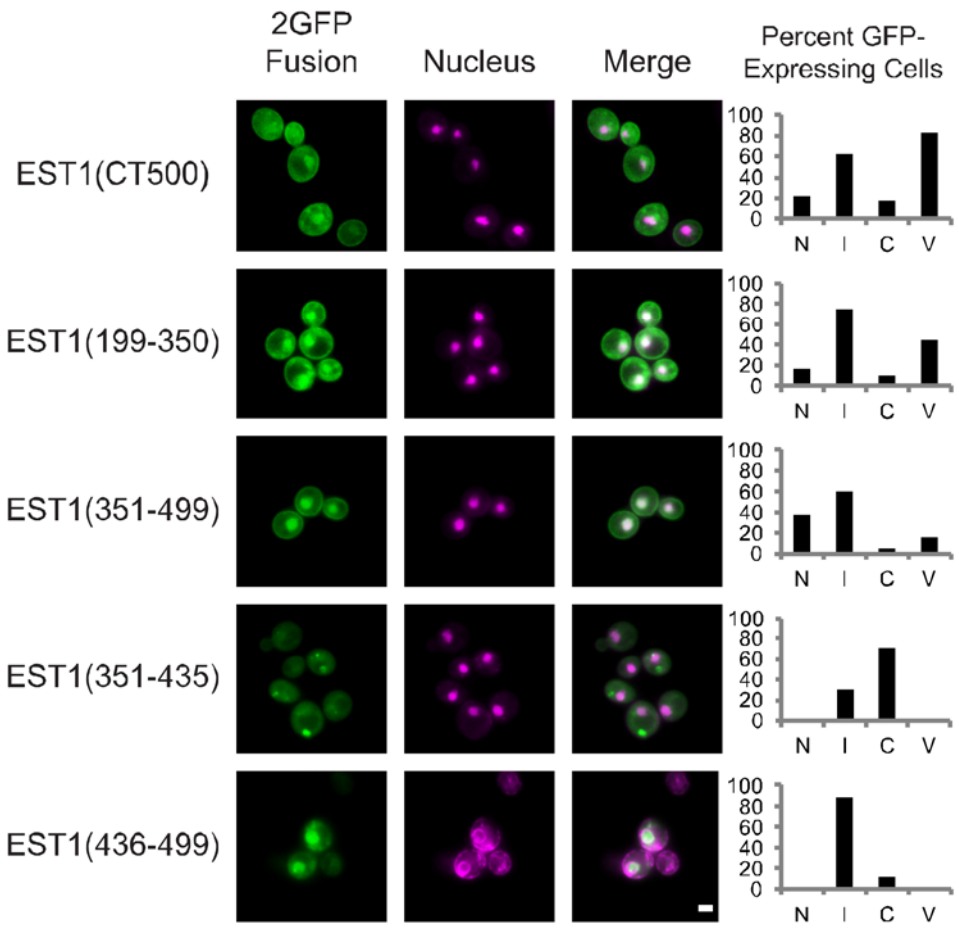

Figure 9. Additional mapping of Est1p sequences sufficient to mediate nuclear localization.

Experiments were conducted as described in (A) on cells containing plasmids (from top to bottom) pCH211, pCH212, pCH214, pCH218, pCH219. In the bottom panel, the location of the nucleus was determined by dsRED-HDELp fluorescence.

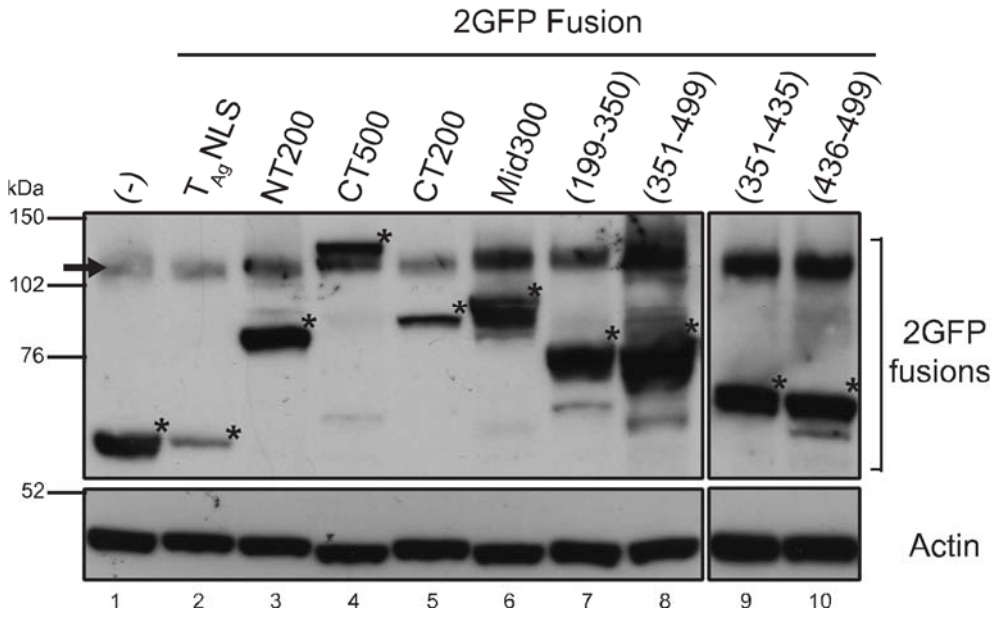

Figure 10. Expression level of Est1-GFP fusion proteins**.**

Whole cell extract was prepared from wild-type yeast cells containing the indicated 2GFP fusion constructs (from left to right: pCH200, pCH201, pCH202, pCH211, pCH210, pCH206, pCH212, pCH214, pCH218, pCH219). Cells were grown to mid-log phase in selective media containing 2% raffinose and protein expression was induced with the addition of galactose for one hour. Samples were separated on an SDS-PAGE gel and Western blotted using anti-GFP and anti-Actin primary antibodies. The 2GFP fusion proteins are marked by an asterisk in each lane. The arrow indicates a nonspecific band. The low expression level of the T_{Ag}NLS-2GFP sample is not reproducible.

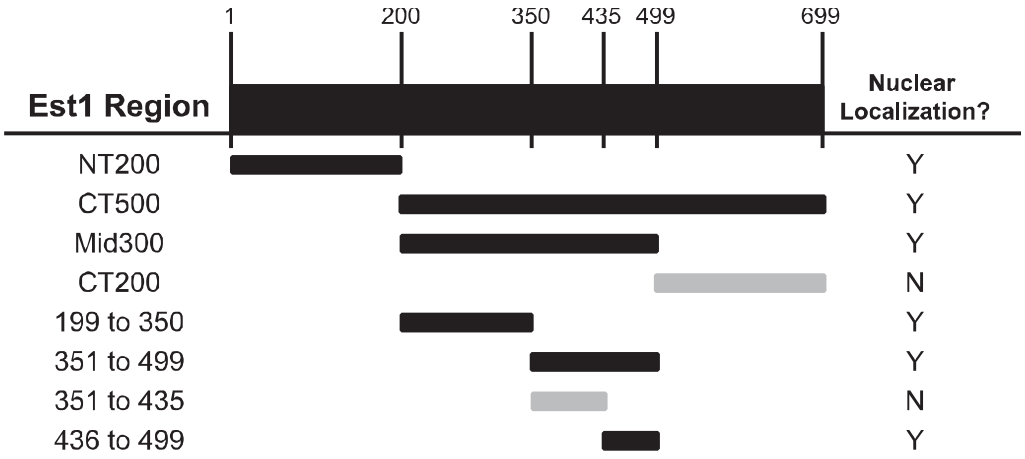

Figure 11. Three separable regions of Est1p support nuclear localization.

Summary of the regions of Est1p sufficient for nuclear localization based on (A) and (B). Black bar = predominantly nuclear distribution. Grey bar = predominantly cytoplasmic distribution.

Est1p Contains Three NLSs that Contribute to Nuclear Localization

To identify specific residues required for nuclear localization, putative NLSs within the three target regions were identified using online NLS prediction programs [PSORT [328,329], PredictNLS [330], and cNLS mapper [331,332]] or through the presence of three or more adjacent basic residues. Positively charged amino acids within each candidate NLS were mutated to alanine and localization was examined in comparison with the appropriate unmutated 2GFP fusion construct. Mutation of lysine 113 or lysines 122 and 123 (positions based on full-length Est1p) in the context of NT200 slightly reduced nuclear localization (compare **Figure 12**, top and middle panels). However, simultaneous mutation of all three lysines (*est1-mut1*) abrogated nuclear localization (**Figure 12**, bottom panel), suggesting that the N-terminal 200 aa of Est1p contains a bipartite NLS, defined as an NLS that contains two required clusters of positively charged amino acids separated by a short linker sequence [39,307].

Alanine mutations of two distinct basic clusters lying within the Mid300 region of Est1p [residues 291 to 293 (*est1-mut2*) and 455 to 458 (*est1-mut3*)] modestly reduced nuclear localization when mutated separately (compare **Figure 13**, top and middle panels). However, simultaneous mutation of these clusters caused loss of Mid300 nuclear localization (**Figure 13**, bottom panel). Expression of *est1-mut2* in the context of residues 199-350 or *est1-mut3* in the context of residues 351-499 severely perturbed nuclear localization of the corresponding 2GFP fusion proteins (**Figure 14**). Mutation of two other basic clusters located between residues 382 and 392 had no effect on localization of the 351-499 fragment (**Figure 15**), consistent with our observation that residues 351-435 do not mediate nuclear localization (**Figures 9** and **10**). We conclude

that each of the three regions of Est1p shown to independently facilitate nuclear localization contains a single cluster of basic residues (defined by *mut1*, *mut2*, and *mut3*) required for localization.

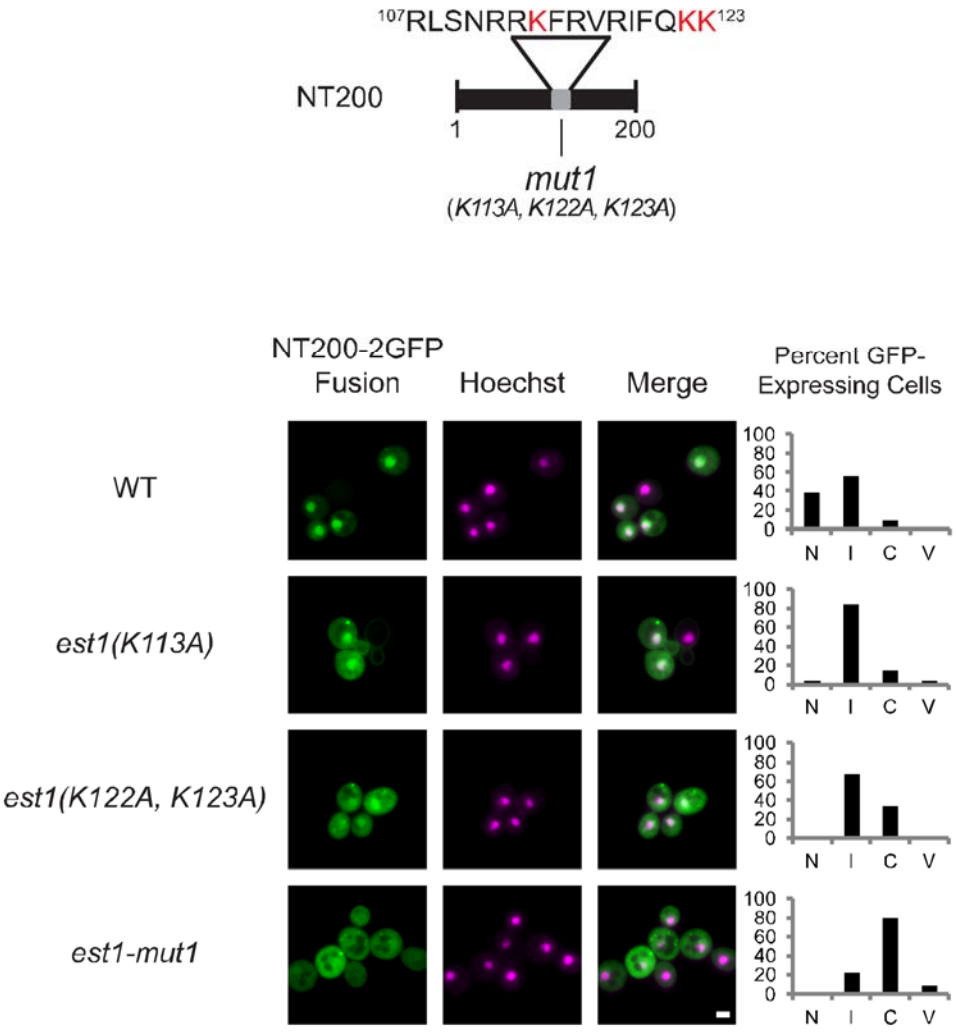

Figure 12. The N-terminal 200 aa of Est1p contains a bipartite NLS.

Live-cell, fluorescence microscopy images were generated and quantified as in Figure 8 on cells containing the indicated fusion constructs. Mutational analysis was conducted in the context of the EST1(NT200)-2GFP fusion with mutated residues shown in red (from top to bottom: pCH202, pCH203, pCH204, pCH205). The *est1-mut1* allele contains mutations K113A, K122A, and K123A. n ≥ 100 GFP-expressing cells for each sample. Scale bar = 2μm. Representative images are selected from at least 3 biological replicates for.

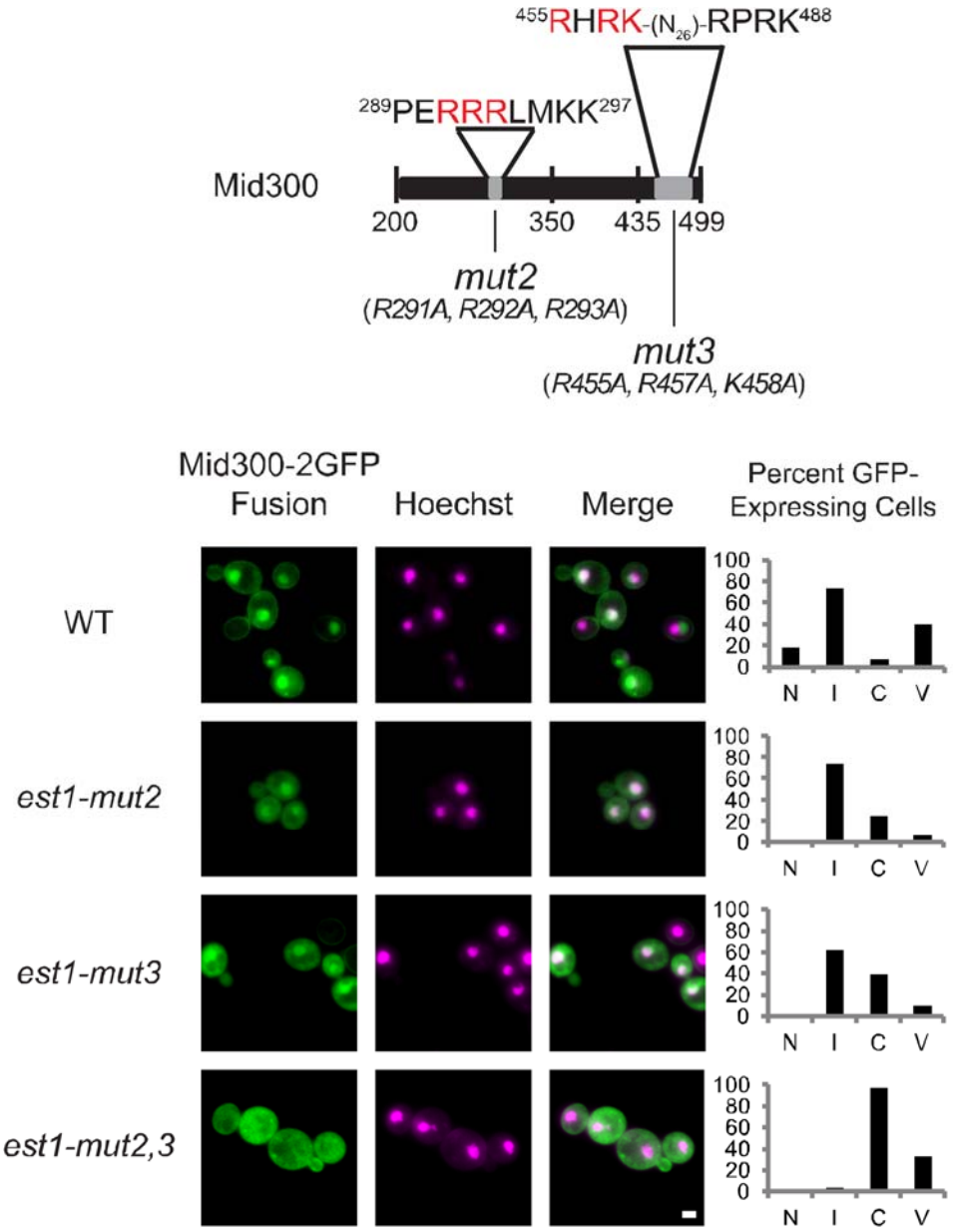

Figure 13. Mutational analysis conducted in the context of the EST1(Mid300)-2GFP fusion identifies 2 NLSs in this region of Est1p (from top to bottom: pCH206, pCH207, pCH208, pCH209). *est1-mut2*: R291A, R292A, R293A; *est1-mut3*: R455A, R457A, K458A.

Live cell fluorescence microscopy was conducted and images were quanified as in Figure 12.

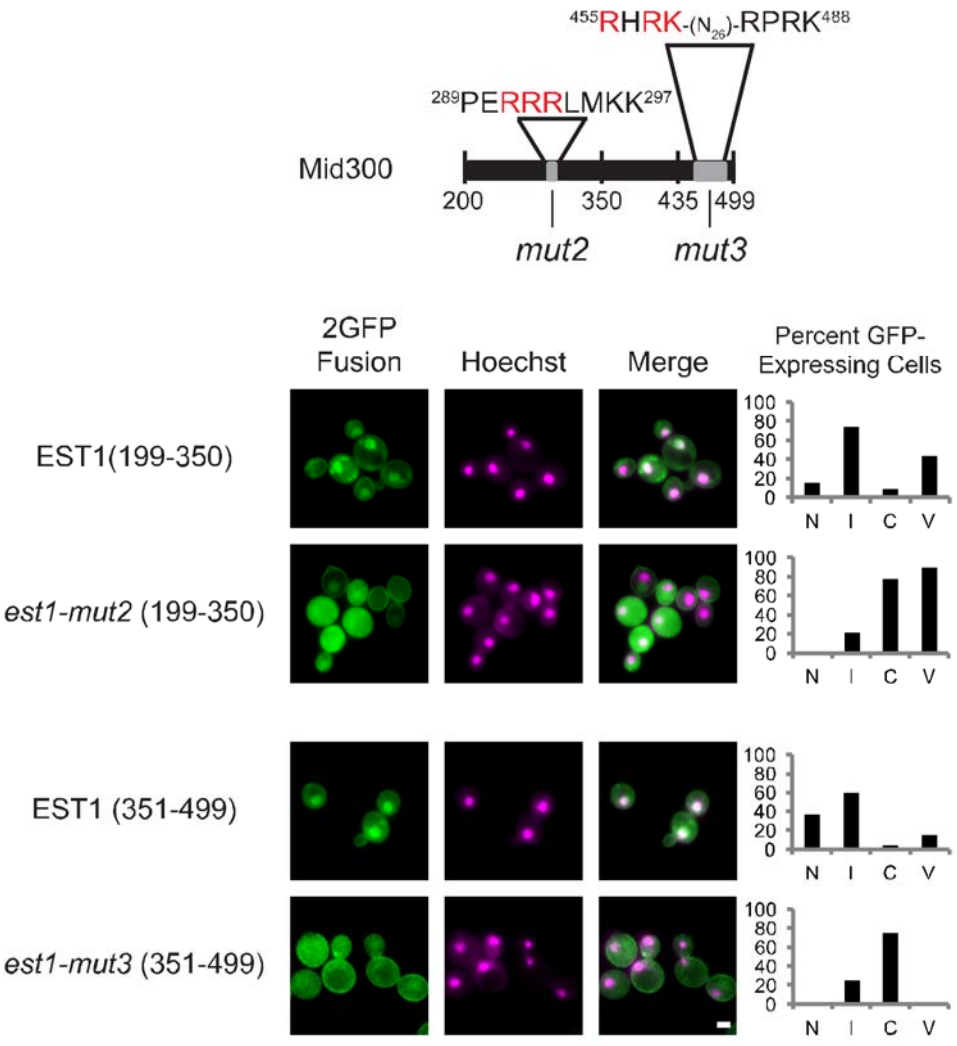

Figure 14. Analysis of cells expressing *mut2* or *mut3* Est1p variants in the context of EST1(199-350)-2GFP or EST1(351-499)-2GFP, respectively (from top to bottom: pCH212, pCH213, pCH214, pCH215).

Live cell fluorescence microscopy was conducted and images were quanified as in Figure 12.

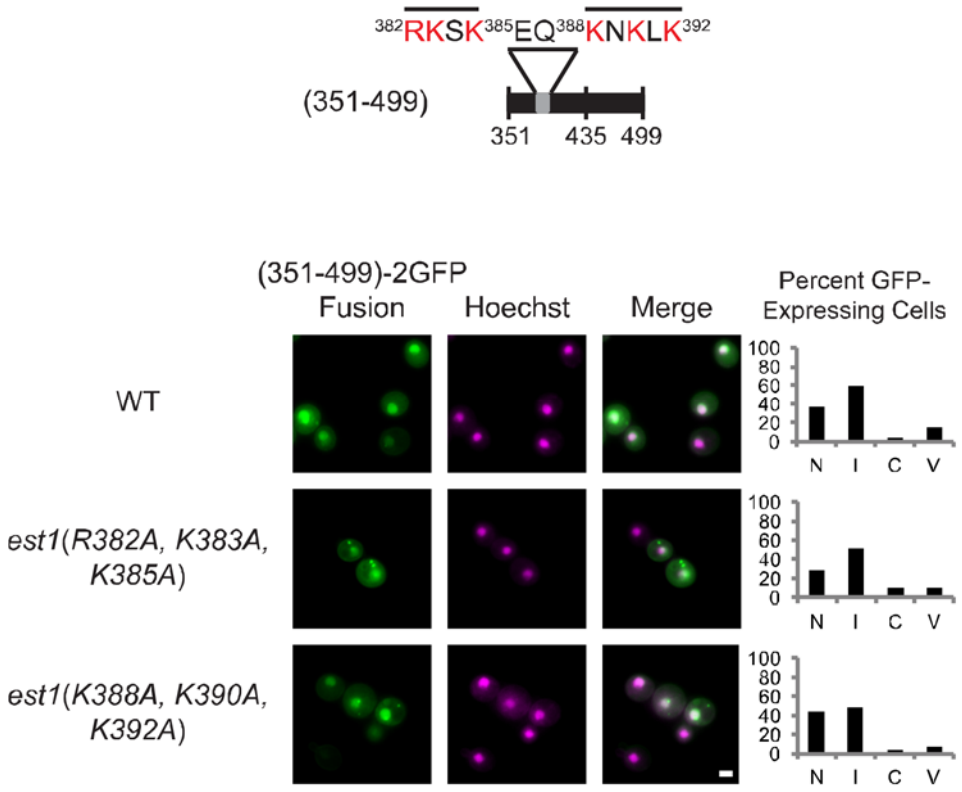

Figure 15. Mutational analysis conducted in the context of the EST1(351-499)-2GFP fusion (from top to bottom: pCH214, pCH216, pCH217).

Live cell fluorescence microscopy was conducted and images were quantified as in Figure 12.

The *est1-mut1*, *est1-mut2*, and *est1-mut3* mutations were simultaneously introduced into the full-length Est1-GFP overexpression plasmid utilized in Figure 5. As predicted, this NLS triple mutant [*est1-mut1,2,3(FL)*] caused cytoplasmic localization (**Figure 16**, middle panel). To determine whether loss of nuclear localization is solely due to loss of NLS function, the T_{Ag}NLS was fused with *est1-mut1,2,3(FL)* in the context of the GFP overexpression plasmid. Although this T_{Ag}NLS-*est1-mut1,2,3(FL)*-GFP fusion protein regains some ability to enter the nucleus, the rescue of mislocalization is incomplete (**Figure 16**, bottom panel).

To investigate redundancy among the three NLSs, the localization phenotypes of the individual *est1-mut1*, *est1-mut2*, and *est1-mut3* alleles were examined in the context of full-length *EST1*. The *est1-mut1* mutation causes a partial reduction in the nuclear localization of Est1p, a phenotype that is completely rescued by fusion with the T_{Ag}NLS (**Figure 17**). This partial phenotype suggests that the first NLS contributes to the nuclear localization of Est1p, but that the two remaining NLSs have some ability to direct nuclear localization in its absence. Similar to *est1-mut1*, the *est1-mut2* and *est1-mut3* mutations partially perturbed nuclear localization of full-length Est1p (**Figure 17**). However, for reasons that are unclear, fusion of the T_{Ag}NLS only modestly suppressed the localization defect (**Figure 17**).

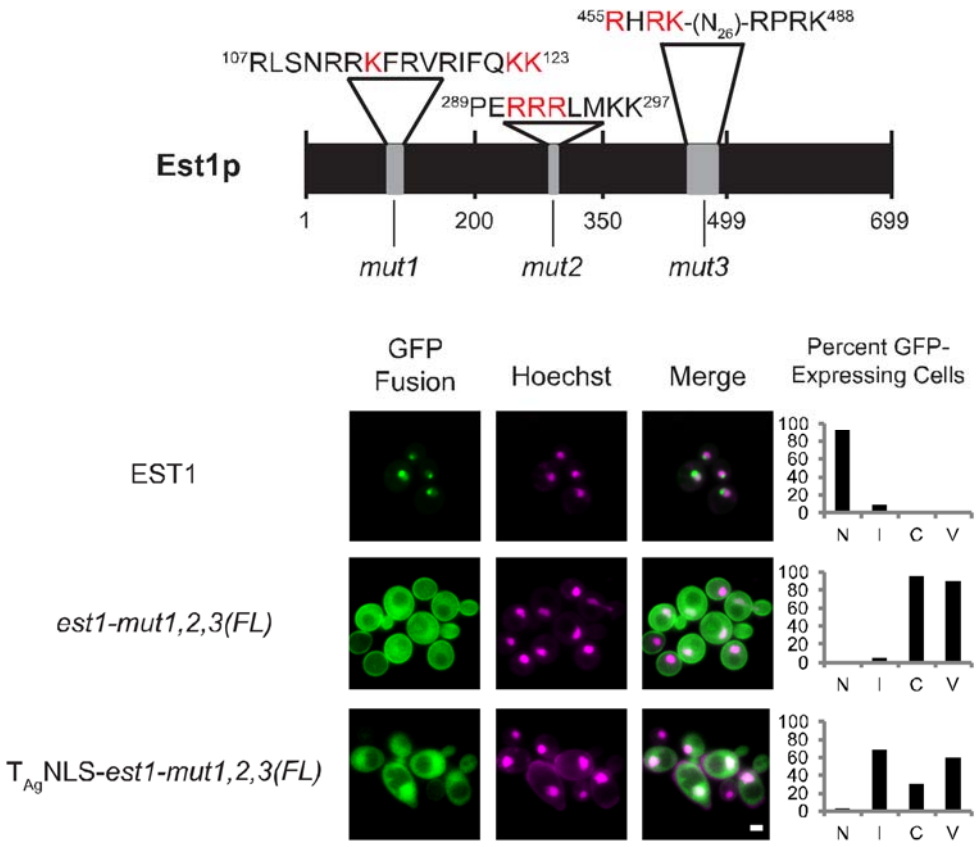

Figure 16. NLS mutations perturb nuclear localization of full length Est1p.

TOP: Diagram illustrating the three NLSs in the context of full-length Est1p. Alanine mutations of the nine residues in red constitute the NLS triple mutant, *est1-mut1,2,3(FL)*.

BOTTOM: Live-cell fluorescence microscopy was conducted on cells harboring full-length, wild-type Est1p, *est1-mut1,2,3(FL)*, and the T_{Ag}NLS-*est1-mut1,2,3(FL)* proteins expressed as fusions with GFP in a high-copy vector (from top to bottom: pCH101, pCH105, pCH111). Representative images are selected from at least 3 biological replicates. Quantification as in Figure 8. Scale bar = 2μm.

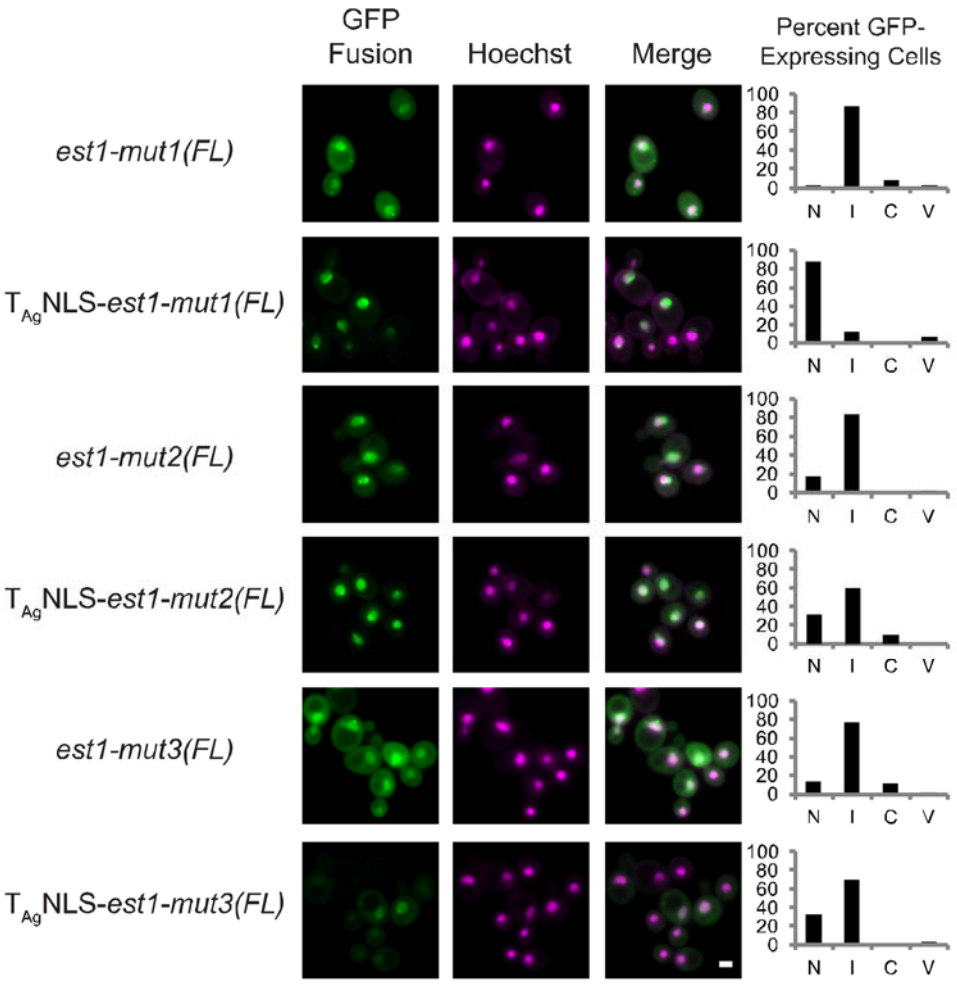

Figure 17. The NLSs in Est1p are partially redundant.

Localization analysis of single NLS mutants in full-length Est1p with and without the T_{Ag}NLS fusion was conducted as in Figure 16. Fluorescence microscopy images of cells expressing *est1-mut1(FL)* or T_{Ag}NLS-*est1-mut1(FL)*, *est1-mut2(FL)* or T_{Ag}NLS-*est2-mut1(FL)*, and *est1-mut3(FL)* or T_{Ag}NLS-*est1-mut3(FL)* as fusions with GFP from a high copy vector (from top to bottom: pCH102, pCH108, pCH103, pCH109, pCH104, and pCH110).

Autonomous Nuclear Localization of Est1p Contributes to Telomere Maintenance

To ascertain whether the NLSs contribute to telomere maintenance *in vivo*, the complementation phenotypes of the individual NLS mutant alleles were examined in the context of full-length, untagged *EST1* expressed from the native *EST1* promoter in a low-copy number vector. When the *est1-mut1(FL)* allele was expressed from a centromere vector in an *est1Δ* strain, telomeres shortened by an average of 63bp compared to cells harboring the *EST1* construct (**Figure 18**). To test whether this decrease in telomere length is due to mislocalization, we fused the T_{Ag}NLS to the N-terminus of wild-type and mutant *EST1*. Addition of T_{Ag}NLS to wild-type *EST1* caused a small, but reproducible increase in telomere length. Importantly, cells expressing the T_{Ag}NLS-*est1-mut1* allele maintained telomeres only 26±11bp shorter than cells expressing the T_{Ag}NLS-*EST1* allele, a decrease in length significantly smaller than the 63±15bp difference observed between the *EST1* and *est1-mut1* strains. The ability of the T_{Ag}NLS to substantially rescue the telomere length defect of the *est1-mut1* allele is consistent with a functional role for the autonomous localization of Est1p during telomerase biogenesis.

Similar to *est1-mut1*, the *est1-mut2* and *est1-mut3* alleles caused telomere length to be maintained at a shorter, but stable length (**Figures 19** and **20**; average decreases of 30±11bp and 90±7bp relative to *EST1*, respectively). However, in neither case did fusion of the T_{Ag}NLS significantly restore telomere length (average decreases of the T_{Ag}NLS-fused mutant alleles relative to T_{Ag}NLS-*EST1* of 33±16bp and 99±12bp, respectively), consistent with the lack of rescue observed for the overexpressed proteins (**Figure 17**).

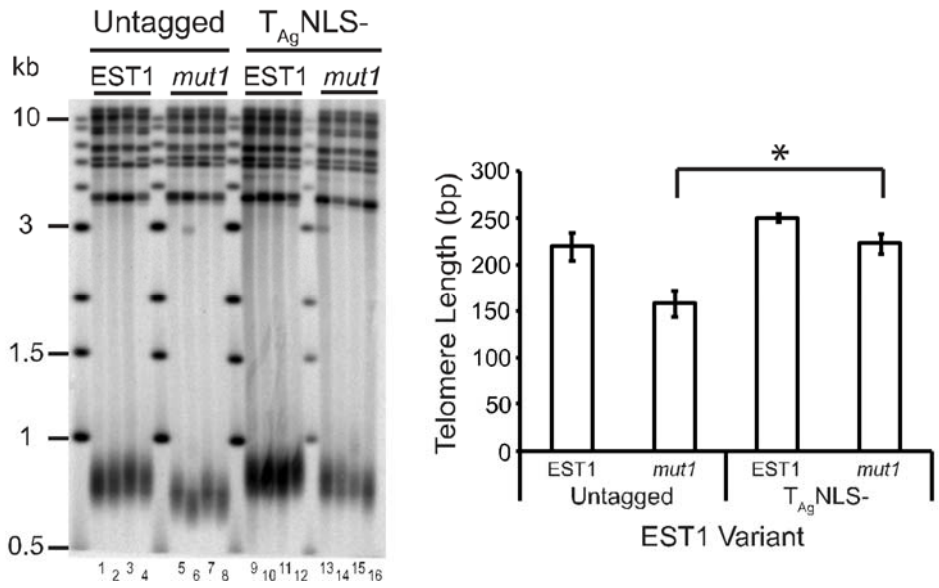

Figure 18. The T$_{Ag}$NLS rescues telomere shortening of the N-terminal NLS mutant.

Untagged and T$_{Ag}$NLS fusions of wild-type *EST1* or *est1NLS* mutants were expressed on a centromere vector under control of the endogenous *EST1* promoter and transformed into an *est1*Δ strain (YKF901). After growth for ~100 generations, genomic DNA was isolated from each strain and Southern blotted (Experimental Procedures). Where appropriate, quantification of the Southern blot is shown to the right of each gel. After correcting for telomere lengthening observed in the *T$_{Ag}$NLS-EST1* strain (see text and Materials and Methods), statistical analysis was performed by one way ANOVA with Tukey's HSD. Marker sizes are indicated in kilobases (kb). Error bars represent standard deviation.

Telomere length analysis of *est1-mut1(FL)*. Four independent colonies were analyzed from each strain (pRS416-EST1, lanes 1-4; pCH003, lanes 5-8; pCH010, lanes 9-12; pCH011, lanes 13-16). (*) = Telomere lengths of cells expressing *est1-mut1(FL)* are significantly shorter than those of the *EST1* or *T$_{Ag}$NLS-est1-mut1(FL)* expressing strains ($p = 0.006$).

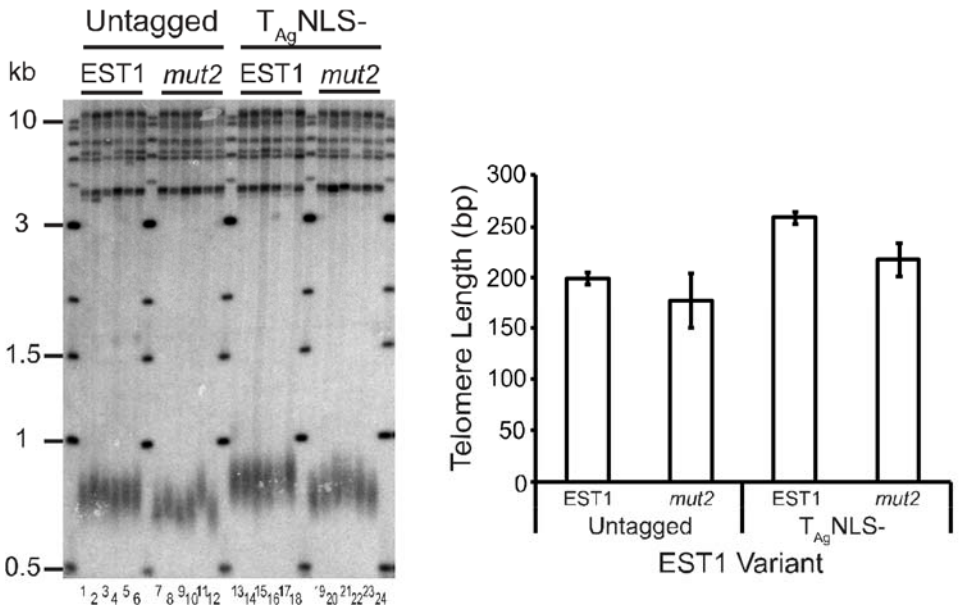

Figure 19. Telomere shortening observed in *est1-mut2(FL)* strain is not rescued by T_{Ag}NLS fusion.

Telomere length analysis of *est1-mut2(FL)* was conducted as in Figure 18. Six independent colonies were analyzed from each strain (pRS416-EST1, lanes 1-6; pCH004, lanes 7-12; pCH010, lanes 13-18; pCH012, lanes 19-24). There is no statistical difference between telomere lengths of cells harboring *est1-mut2(FL)* or *T_{Ag}NLS-est1-mut2(FL)* ($p = 0.21$).

We attempted to test the essential nature of Est1p nuclear localization by expressing an untagged allele containing all three mutations [*est1-mut1,2,3(FL)*] from a centromere vector. This strain maintains very short telomeres and shows evidence of subtelomeric Y' amplification (**Figure 21**), a phenotype observed when telomerase function is lost and rare survivors arise that utilize recombination to maintain viability (see **Figure 7A**) [267,326]. Although fusion of the T_{Ag}NLS with the *est1-mut1,2,3(FL)* variant restored some nuclear localization to the GFP-tagged protein (**Figure 16**), addition of the T_{Ag}NLS to the untagged *est1-mut1,2,3(FL)* low-copy number construct was unable to restore telomere maintenance in an *est1Δ* strain (**Figure 21**). Thus, the telomere length defect of the *est1-mut1,2,3(FL)* allele cannot be solely attributed to a defect in nuclear localization.

Taken together, these data suggest that the three NLS sequences in Est1p contribute in a partially redundant manner to the nuclear localization of Est1p. Rescue of the telomere length defect of the *est1-mut1* allele by addition of the T_{Ag}NLS demonstrates that normal localization of Est1p is important for telomerase function. However, the mutations required to eliminate the function of the other two NLSs (*est1-mut2* and *est1-mut3*) have additional effects that preclude the unambiguous determination of whether the ability of Est1p to mediate its own nuclear localization is essential for telomerase function.

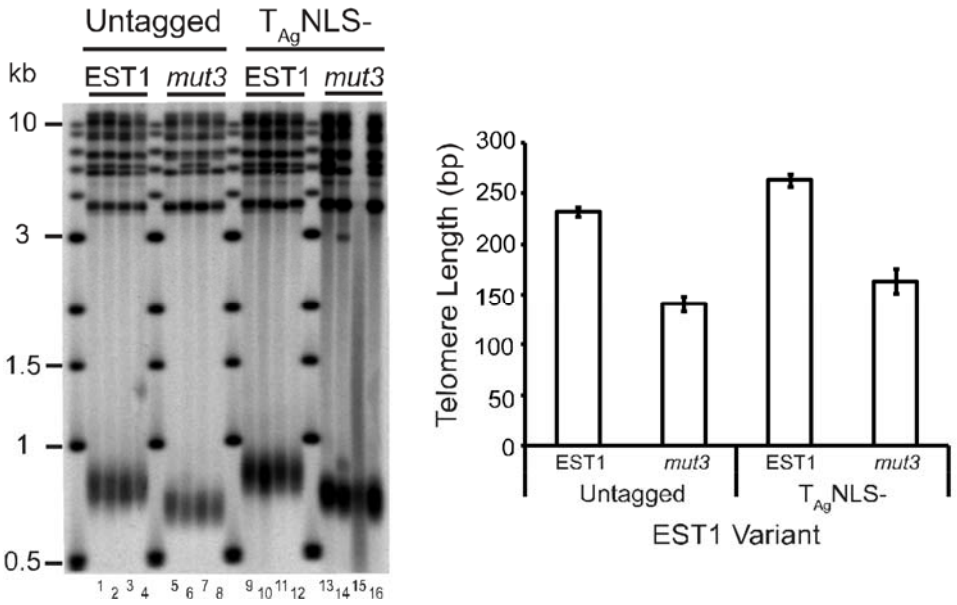

Figure 20. The T_{Ag}NLS does not suppress the telomere shortening of *est1-mut3(FL)*.

Telomere length analysis of *est1-mut3(FL)* was conducted as in Figure 18. Four independent colonies were analyzed from each strain (pRS416-EST1, lanes 1-4; pCH005, lanes 5-8; pCH010, lanes 9-12; pCH013, lanes 13-16). There is no statistical difference between telomere lengths of cells harboring *est1-mut3(FL)* or *T_{Ag}NLS-est1-mut3(FL)* ($p = 0.54$).

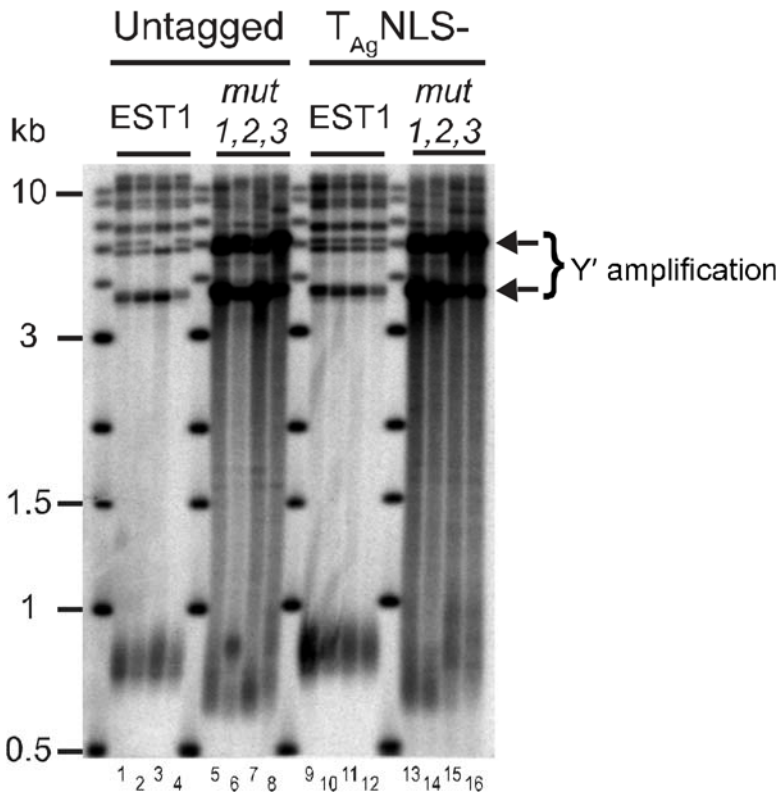

Figure 21. The T_{Ag}NLS does not rescue the telomere length defect of the NLS triple mutant.

Telomere length analysis of *est1-mut1,2,3 (FL)* was conducted as in Figure 18. Four independent colonies were analyzed for each strain (pRS416-EST1, lanes 1-4; pCH009, lanes 5-8; pCH010, lanes 9-12; pCH014, lanes 13-16). Arrows point to Y' amplification indicative of a failure to complement the *est1Δ* phenotype (see Figure 7A). Because the cells are utilizing recombination to maintain telomeres, telomere length is not quantified.

Est1p Does Not Require Kap122p or Mtr10p for Nuclear Import

The β importins Mtr10p and Kap122p have been implicated in the nuclear import of *TLC1* RNA [291,300,333,334]. However, the nucleocytoplasmic shuttling of the protein components of telomerase was not explicitly examined. Since our overexpression analysis suggests that Est1p does not require interaction with the other components of telomerase for nuclear localization, we sought to determine whether Est1p also requires *MTR10* and *KAP122* for nuclear accumulation. A *kap122*Δ strain and a strain harboring a conditional allele of *MTR10*, *mtr10-7*, were transformed with the *EST1-GFP* overexpression construct and with GFP fusions to Nab2p, Rnr4p, or Hrb1p, proteins that depend upon the importins Kap104p, Kap122p, or Mtr10p for nuclear import, respectively [28,306,316,335]. As expected, each of these GFP fusions localized primarily to the nucleus in wild-type yeast cells (**Figure 22**).

Even in the complete absence of Kap122p, Est1-GFPp retained nuclear localization (**Figure 23**). The Rnr4-GFP fusion exhibited partial mislocalization [the previously reported phenotype [335]], while Nab2-GFPp localized to the nucleus as expected (**Figure 23**). At the permissive temperature of 18˚C, all of the GFP constructs showed nuclear localization in *mtr10-7* cells. Upon shift to the restrictive temperature, the Hrb1-GFP fusion protein was redistributed to the cytoplasm as expected, while Est1-GFPp and the other control proteins retained nuclear localization (**Figure 24**). To rule out redundancy, localization was examined in *mtr10-7 kap122*Δ double-mutant cells. Once again, the Est1-GFP and Nab2-GFP fusion proteins remained localized to the nucleus at both temperatures tested while Rnr4-GFPp exhibited a primarily cytoplasmic distribution and Hrb1-GFPp lost nuclear localization after shift to the restrictive

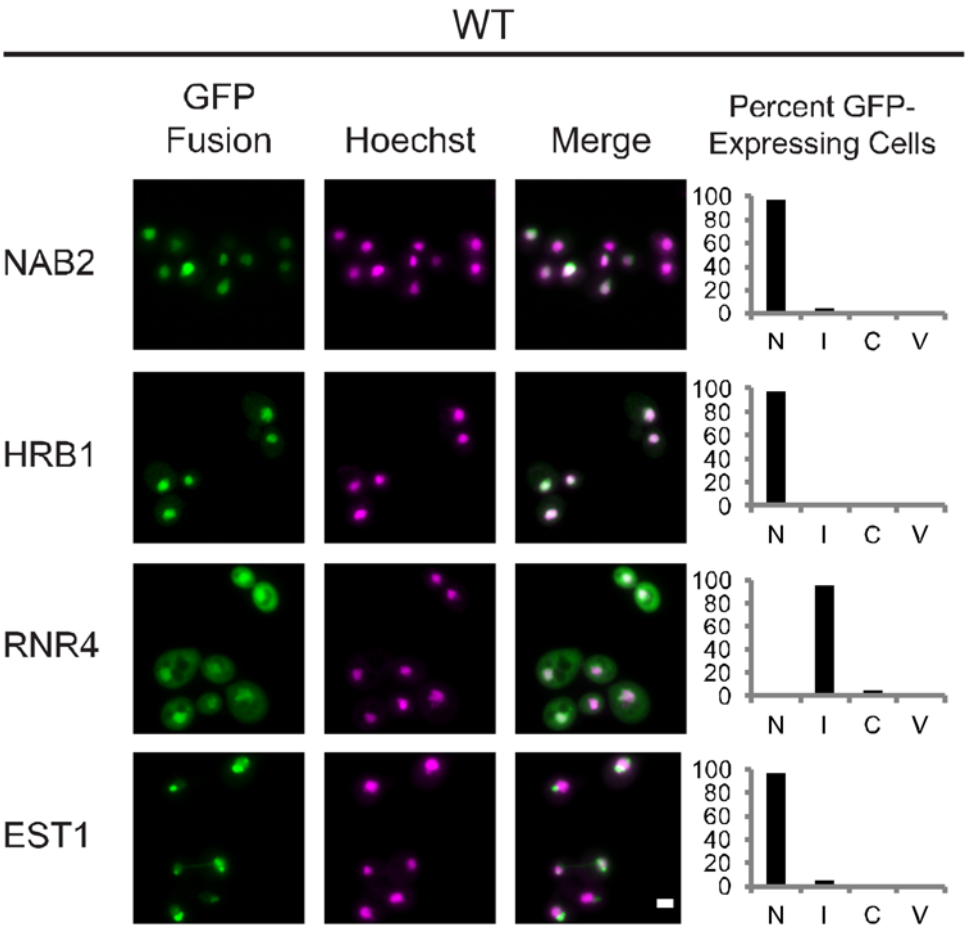

Figure 22. Analysis of protein localization in wild-type cells.

Live-cell fluorescence microscopy of wild-type cells (BY4741) expressing GFP fusions of *NAB2* (pAC719), *HRB1* (pHK537), *RNR4* (pMH1326) or *EST1* (pCH101). *NAB2* and *HRB1* are expressed under control of their native promoters while *RNR4* and *EST1* are expressed under control of galactose-inducible promoters. Quantification in (A-D) was performed as in Figure 8. Representative images are selected from at least 3 biological replicates. Scale bar = 2μm.

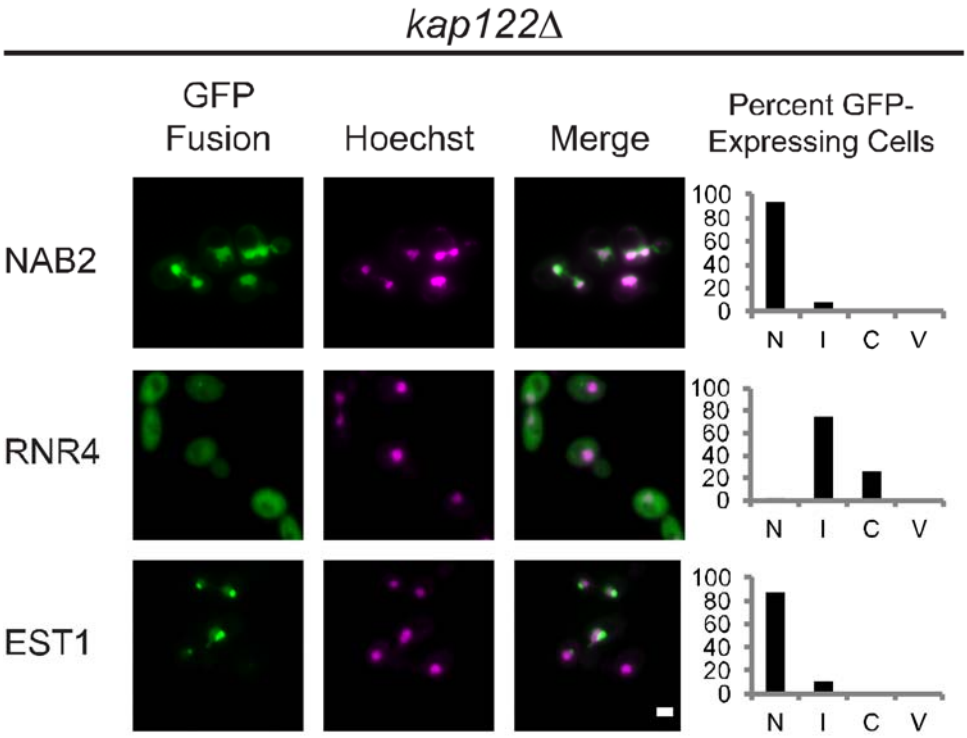

Figure 23. Est1p localizes to the nucleus in the absence of Kap122p function.

Analysis of protein localization in *kap122*Δ cells. Live-cell fluorescence microscopy of a BY4741 *kap122*Δ strain containing the *NAB2*, *RNR4*, and *EST1* vectors was conducted as described in Figure 22.

temperature (**Figure 25**). Since Est1p localization is unaffected by perturbations in both *KAP122* and *MTR10*, these results indicate that under conditions of overexpression, Est1p is imported to the nucleus via a different pathway than *TLC1* RNA.

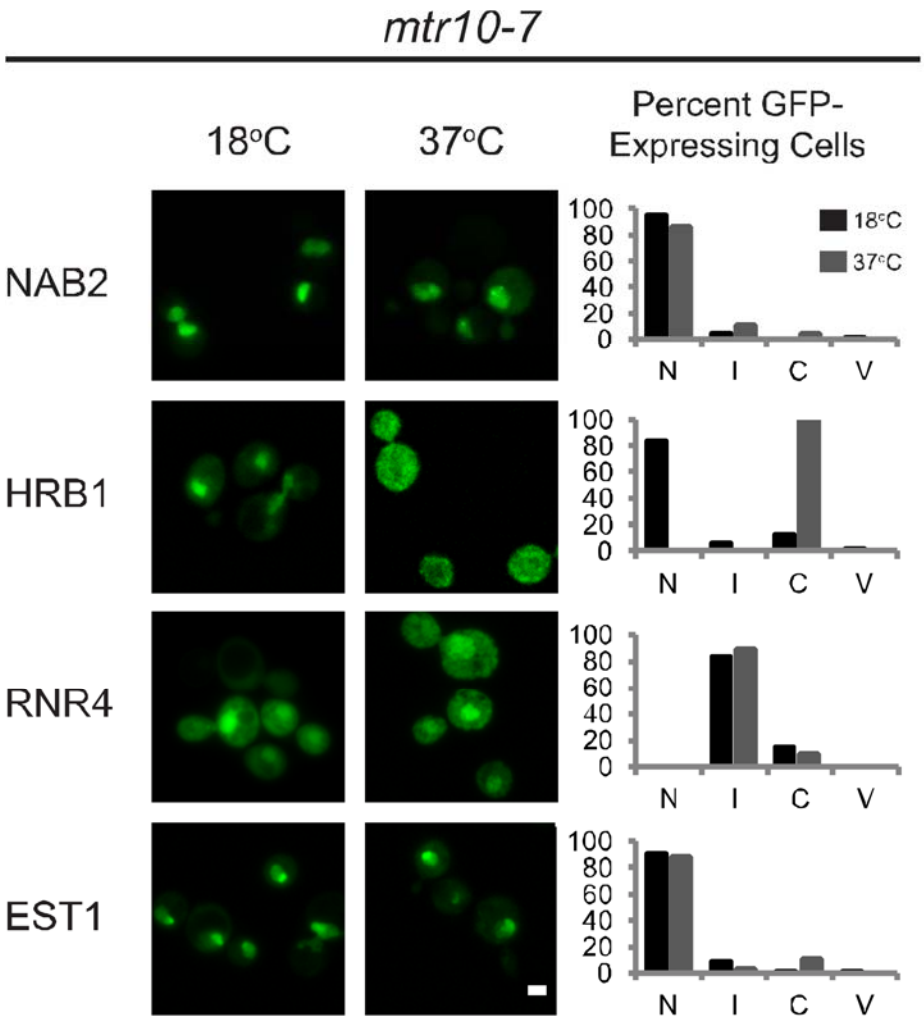

Figure 24. Est1p does not require the function of Mtr10p to for nuclear localization.

Analysis of protein localization in *mtr10-7* cells. Cells containing a temperature-sensitive allele of *MTR10*, *mtr10-7*, were transformed with the indicated GFP fusion constructs [described in (Figure 22)]. Cells were grown to mid-log phase at the permissive temperature of 18˚C in selective media and galactose was added to the cultures containing *RNR4*- or *EST1-GFP* fusion plasmids to induce protein expression. Cultures were split and incubated at 18˚C or 37˚C. Cells were fixed and visualized as described in Materials and Methods. Black: localization at 18˚C; grey: localization at 37˚C.

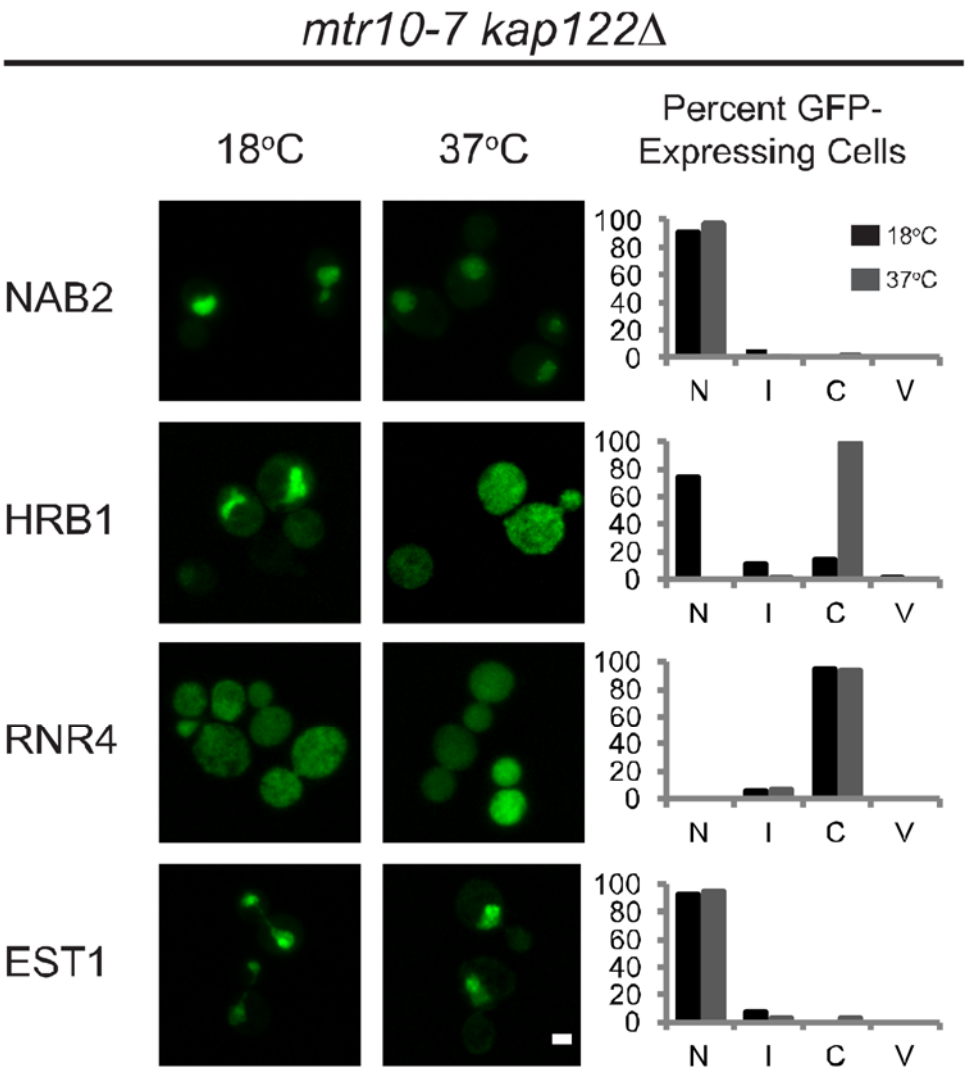

Figure 25. Neither Mtr10p nor Kap122p is required for Est1p nuclear localization.

Analysis of protein localization in *mtr10-7 kap122*Δ cells. The indicated GFP fusion constructs were transformed into an *mtr10-7 kap122Δ* strain and analyzed as in (Figure 24).

Est1p Requires the Classical Nuclear Import Machinery for Import to the Nucleus

The classical nuclear import pathway—defined by binding of the adapter, importin α, to a cargo protein followed by recruitment of importin β to permit active transport through the nuclear pore [38,336,337]—is purported to participate in the transport of ~40% of nuclear proteins [35]. To test whether the classical nuclear import machinery is required for Est1p nuclear import, localization phenotypes of Est1-GFP, Nab2-GFP and T_{Ag}NLS-2GFP fusion proteins were examined in a strain containing a temperature-sensitive allele of the yeast importin α, *srp1-54* [41,338].

At the permissive temperature (25˚C), each GFP fusion protein localized predominantly to the nucleus. As expected, Nab2-GFPp, the nuclear import of which does not require importin α, retained nuclear localization after incubation at the restrictive temperature (**Figure 26**). However, T_{Ag}NLS-2GFPp—known to utilize importin α [331]—and Est1-GFPp relocalized to the cytoplasm upon shift to 37˚C, indicating that Est1p requires importin α for nuclear import (**Figure 26**). To rule out the possibility of a non-specific effect of temperature on Est1-GFPp localization, the Nab2NLS [49,70] was fused to Est1-GFPp and localization was monitored in the *srp1-54* strain. The Nab2NLS-Est1-GFP fusion protein retained nuclear localization at both permissive and non-permissive temperatures (**Figure 26**), indicating that mislocalization of Est1-GFPp at the restrictive temperature is specifically due to reduced importin α function.

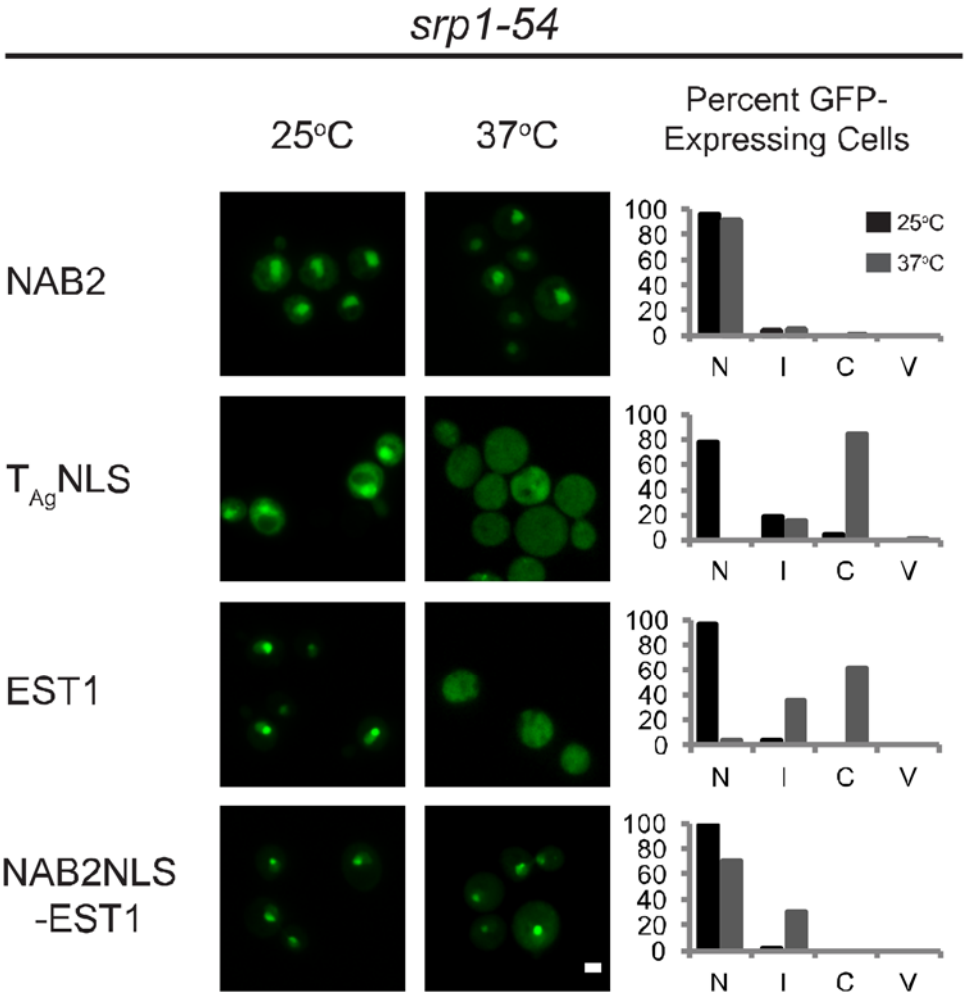

Figure 26. Importin α is required for Est1p nuclear import.

Analysis of protein localization in *srp1-54* cells. A temperature-sensitive *srp1-54* strain (ACY1563) was transformed with the indicated GFP fusion constructs (top to bottom: pAC719, pCH201, pCH101, pCH112). Localization analysis and quantification were performed as described in Figure 24 except that 25°C was the permissive temperature. Representative images are selected from at least 3 biological replicates. Scale bar = 2μm.

To exclude the possibility that other nuclear import proteins function in Est1p localization, the *EST1-GFP* overexpression construct was transformed into a panel of yeast importin mutants. Est1p nuclear import was retained in all strains except those associated with the classical nuclear import machinery, namely *srp1* and *rsl1*, the yeast homolog of importin β (**Figure 27**) [41,339].

Strain Background	%N	%I	%C	%V
WT	96	4	0	0
kap108Δ	94	6	0	0
kap114Δ	92	8	0	0
kap120Δ	76	24	3	3
kap123Δ	81	19	0	0
los1Δ	90	10	0	1
msn5Δ	80	20	0	0
nmd5Δ	87	13	0	0
pse1-1 (25°C)	90	10	0	0
pse1-1 (37°C)	93	5	2	0
rsl1-4 (25°C)	90	10	0	0
rsl1-4 (37°C)	3	32	64	0
srp1-31 (25°C)	32	21	47	0
srp1-31 (37°C)	0	4	96	0
srp1-54 (25°C)	96	4	0	0
srp1-54 (37°C)	4	35	62	0

Figure 27. The classical nuclear import machinery is uniquely required for Est1p import.

Table containing localization data for Est1-GFPp in strains defective for different nuclear import pathways. The *EST1-GFP* overexpression construct was transformed into the indicated mutant strain backgrounds. Live-cell fluorescence microscopy was used to quantify localization as described in Figure 8. Values for the wild-type (BY4741) strain are from the experiment shown in Figure 22, bottom panel. Strains *pse1-1*, *rsl1-4*, and *srp1-31* were analyzed as described in (A) and localization is reported at both permissive and restrictive temperatures. $n \geq 100$ GFP-expressing cells for each sample. Data for *srp1-54* are repeated from Figure 26 for completeness.

Import of Est1p Via the Classical Pathway Contributes to Telomere Length Maintenance

The results presented above indicate that Est1p requires the *SRP1/RSL1* pathway for nuclear import upon overexpression. To address whether this import pathway affects telomere maintenance under endogenous conditions, we examined telomere length in the *srp1-54* strain. At the permissive temperature of 25˚C, telomere length was identical in *srp1-54* cells containing either an empty vector or a complementing *SRP1* gene on a centromere vector. After ~100 generations of growth at the semi-permissive temperature of 35˚C, telomeres shortened in both the complemented and non-complemented strains. However, there was a significantly greater decrease in telomere length in cells transformed with the empty vector relative to those complemented with wild-type *SRP1* (**Figure 28**). Since steady-state telomere length decreases upon growth at elevated temperature in wild-type yeast strains [340], these data suggest that the exaggerated decrease in telomere length that occurs in the non-complementated strain is specifically attributable to decreased *SRP1* function.

Given the importance of the importin α pathway for the nuclear localization of overexpressed Est1-GFPp, we hypothesized that compromised nuclear localization of endogenous Est1p is responsible for the difference in telomere length between the complemented and non-complemented *srp1-54* strains at the semi-permissive temperature. If true, we predicted that expression of a Nab2NLS-EST1 fusion protein, which attains nuclear localization in the *srp1-54* mutant at 37˚C when overexpressed, would be sufficient to rescue the telomere length defect at 35˚C even when expressed at more moderate levels. As shown in **Figure 29**, expression of *Nab2NLS-EST1* from a

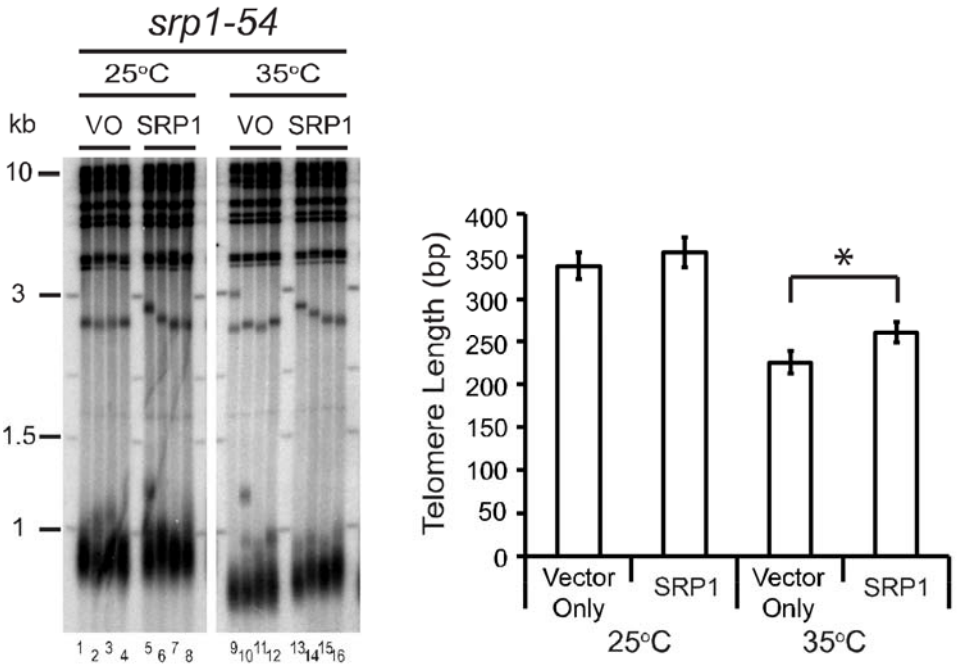

Figure 28. The *srp1* mutant strain undergoes telomere shortening when grown at high temperature.

Four independent colonies were restreaked four times on solid media and grown to saturation in liquid culture for a total of ~100 generations of growth at the indicated temperature. Genomic DNA was isolated and telomeres were detected by Southern blot. Telomere length analysis of strain ACY1563 transformed with an empty vector (VO; pRS413) or a plasmid expressing wild-type *SRP1* (CEN; pCH017) and grown at 25˚C (lanes 1-8) or 35˚C (9-16). At 25˚C, there is no significant difference in the telomere lengths of cells expressing the empty vector versus those expressing *SRP1* ($p = 0.16$ by Student's T-test). However, cells harboring the empty vector have significantly shorter telomeres than those harboring *SRP1* when grown at 35˚C by Student's T-test ($p = 0.0052$).Error bars represent standard deviation. (*) indicates statistically significant increase in telomere length above that of cells expressing the empty vector.

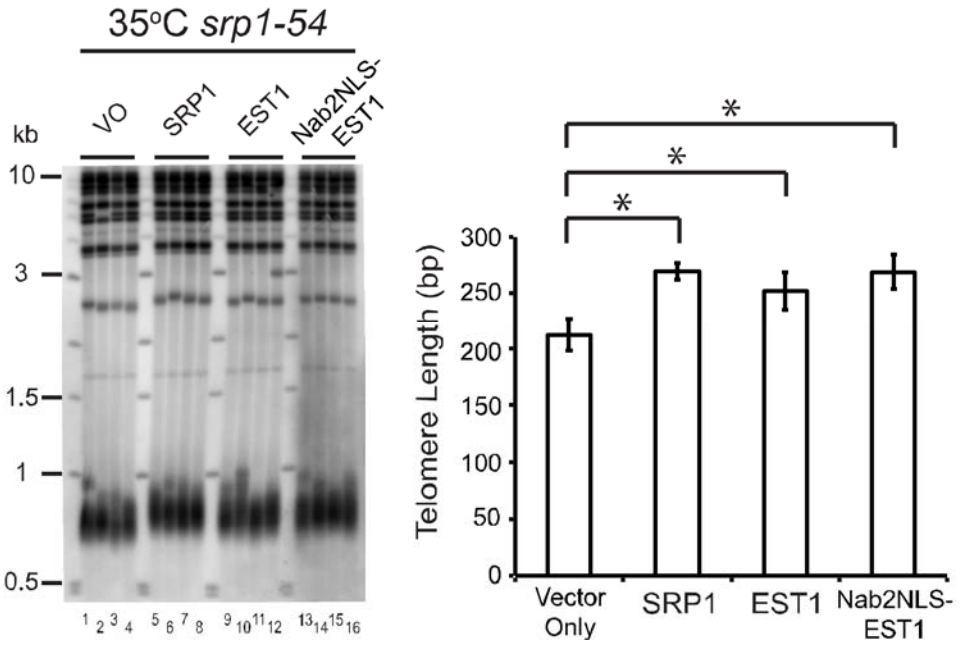

Figure 29. Introduction of *EST1* into *srp1* cells suppresses the telomere length defect observed at high temperature

The *srp1-54* strain (ACY1563) was transformed with an empty vector (VO; pRS413) or with centromere vectors containing *SRP1* (pCH017), *EST1* (pCH016), or *Nab2NLS-EST1* (pCH018), each expressed from the native *SRP1* or *EST1* promoters. Telomere length analysis was conducted as in Figure 28. Cells containing the *SRP1*, *EST1*, or *Nab2NLS-EST1* plasmids have significantly longer telomeres than cells containing the empty vector ($p = 0.0004$, $p = 0.007$, and $p = 0.0004$, respectively, by one way ANOVA with Tukey's HSD).

centromere vector rescued telomere length in the *srp1-54* strain to a similar extent as the *SRP1* complementing plasmid.

Since we are limited to performing these experiments at a semi-permissive temperature, we reasoned that slight overexpression of even wild-type *EST1* may be sufficient to overcome the telomere shortening observed in the *srp1-54* strain at 35˚C. When the *srp1-54* strain containing either the empty vector or low-copy number *EST1* was grown at the semi-permissive temperature, cells expressing additional *EST1* had significantly longer telomeres than those harboring the empty vector (**Figure 29**). The decrease in telomere length attributable to reduced Srp1p function at 35˚C averaged 57±14bp, while expression of an extra copy of *EST1* restored telomere length by an average of 40±16bp as measured by Southern blot (**Figure 29**).

We confirmed this result using a different method to measure the telomere lengths of eight additional colonies of each genotype. Amplification of a subset of Y' telomeres using ligation-mediated PCR to measure the length of the double-stranded telomere sequence confirmed that low-level expression of *EST1* rescues the telomere length defect conferred by the *srp1-54* allele at 35˚C (**Figure 30**). Although the absolute telomere lengths measured by PCR are slightly longer than those measured by Southern blot (perhaps reflecting extrapolation of migration distances between the 500 and 1000bp markers on the Southern blot), the increase in telomere length conferred by *EST1* expression relative to empty vector is indistinguishable in the two assays (40±16bp by Southern blot and 42±16bp by ligation-mediated PCR).

To confirm that this level of *EST1* overexpression does not result in telomere elongation in a wild-type strain, we examined telomere length in *srp1-54* strains

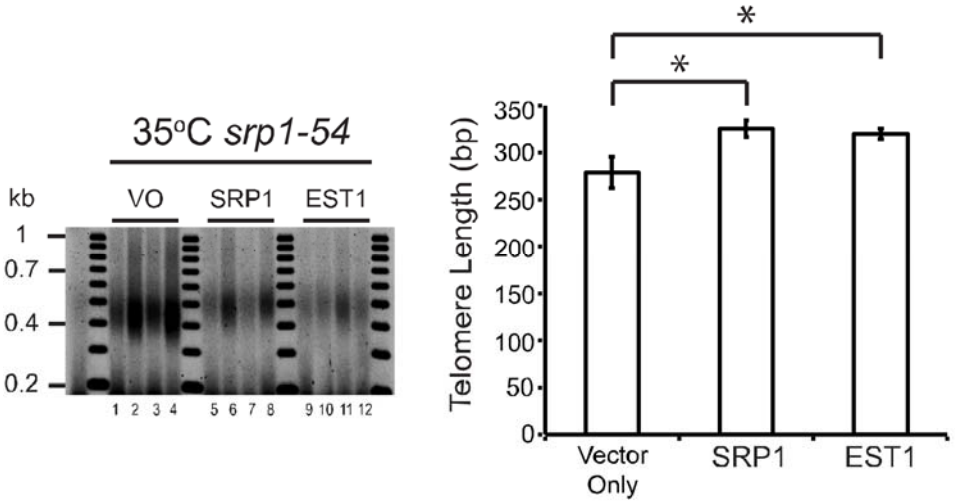

Figure 30. Telomere length analysis of *srp1-54* cells harboring an additional copy of *EST1* at 35˚C by ligation-mediated telomere PCR.

Experiment shown in panel B was repeated by growth of an additional eight colonies of the *srp1-54* strain harboring the empty vector or low copy-number plasmids expressing *SRP1* or *EST1* at 35˚C. Genomic DNA was isolated and telomeres were detected by ligation-mediated telomere PCR using a primer specific to the Y' element (see Materials and Methods). Representative results from four independent colonies of each strain are shown. Telomere length is quantified in the accompanying graph as described in Materials and Methods. Error bars represent standard deviation. Telomeres are significantly longer in strains containing an additional copy of *EST1* or *SRP1* than in cells containing the empty vector ($p < 0.0001$ for each by one way ANOVA with Tukey's HSD; $n = 8$).

complemented by plasmid-borne *SRP1* and additionally expressing either low-copy number *EST1* or an empty vector at the permissive temperature. Under these conditions, an additional copy of *EST1* did not affect telomere length (**Figure 31**). Furthermore, the rescue of telomere length by additional *EST1* expression is specific since it was not observed upon introduction of *TLC1* RNA at low or high expression levels into the *srp1-54* strain (**Figure 32**). We conclude that the telomere attrition observed in the importin α mutant at semipermissive temperature is substantially due to Est1p mislocalization, indicating that the autonomous localization of Est1p to the nucleus via the classical nuclear import pathway contributes to normal telomere length maintenance.

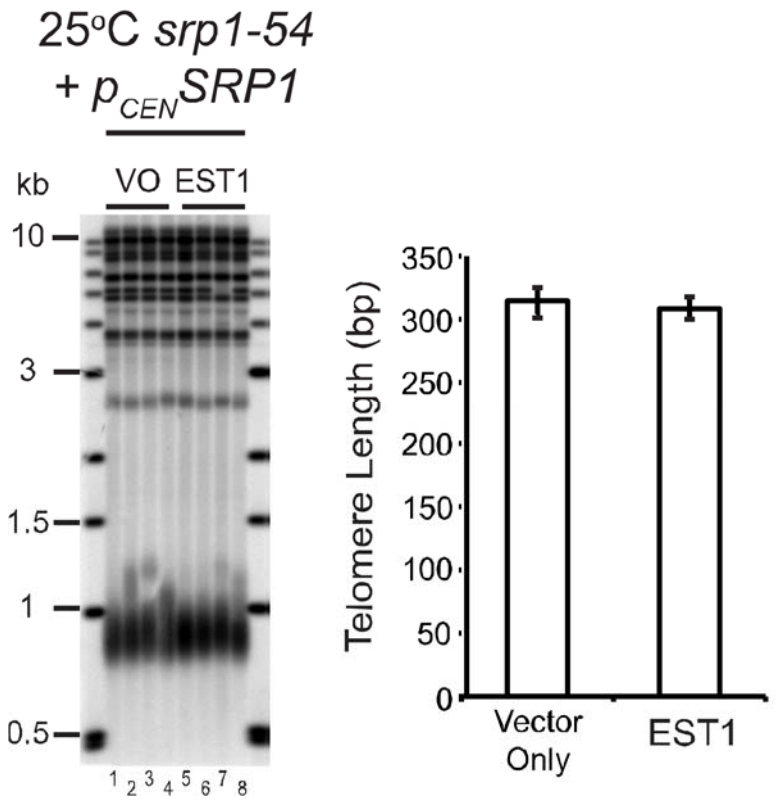

Figure 31. Introduction of *EST1* into *SRP1* cells does not cause telomere elongation.

Telomere length analysis of the *srp1-54* strain (ACY1563) complemented by plasmid-borne wild-type *SRP1* (CEN; pCH017)—denoted $p_{CEN}SRP1$—and containing either an empty vector (VO; pRS416) or *EST1* expressed from a centromere vector (pRS416-EST1) at 25°C was conduct as in Figure 28. Expression of an additional copy of *EST1* does not significantly increase telomere length in the *SRP1* background ($p = 0.5$ by one way ANOVA).

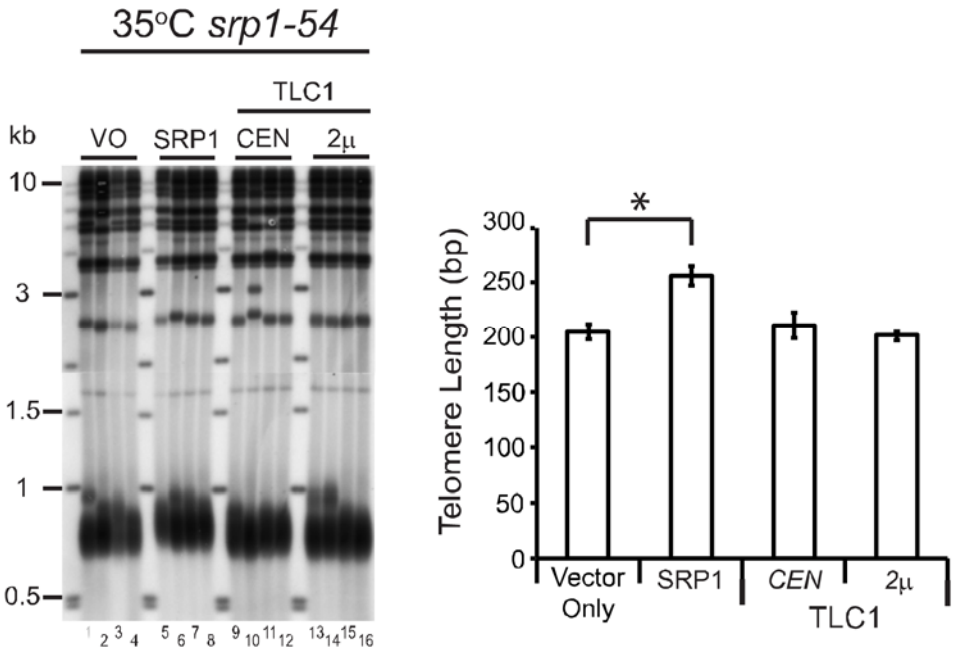

Figure 32. Expression of additional *TLC1* RNA does not suppress the telomere shortening of the *srp1* mutant.

Telomere length analysis of *srp1-54* cells harboring an additional copy of *TLC1* RNA expressed from a low- or high-copy vector. Experiment was conducted as in (B) except that the *srp1-54* strain was transformed with constructs containing *TLC1* expressed from its native promoter in a centromere (pCH019) or high-copy (2μ; pCH020) vector. While expression of *SRP1* complements the telomere length defect of the mutant ($p < 0.0001$ by one way ANOVA with Tukey's HSD), there is no statistical difference between telomere lengths of cells containing the empty vector and those transformed with either *TLC1* construct ($p = 0.8$ for cells harboring pCH018 and $p = 0.9$ for cells harboring pCH019 by one way ANOVA with Tukey's HSD).

Discussion

Here we describe the first in-depth characterization of the mechanism through which a protein component of *S. cerevisiae* telomerase undergoes nuclear localization. While our studies, of necessity, used an overexpression approach to characterize sequences required for Est1p nuclear localization, we established the functional relevance of these sequences by showing that telomere shortening occurs when the *cis*-acting sequences (NLS) or *trans*-acting import machinery (importins α or β) are mutated. Furthermore, this telomere maintenance defect is specific since it can be rescued by conditions predicted to restore nuclear localization of Est1p.

Our overexpression studies demonstrate that Est1p contains three sequences that mediate nuclear localization and that mutation of any one NLS within full-length Est1p only partially affects the exclusive nuclear localization of the protein (**Figures 16** and **17**). Such redundancy is not unprecedented and many yeast proteins that contain multiple NLSs—including ribosomal proteins and a subset of the MCM proteins [341-343]—are part of multiprotein complexes. At endogenous expression levels, we have only been able to unambiguously demonstrate a contribution by the most N-terminal NLS to telomere length maintenance, since mutations in the second and third NLS (*est1-mut2* and *est1-mut3*) affect protein function(s) in addition to localization. Therefore, the N-terminal NLS may contribute disproportionately to Est1p nuclear localization under endogenous conditions.

To determine whether Est1p NLSs contribute to telomerase function, we examined the consequence of mutating these sequences in the context of full-length Est1p expressed at or near normal levels. Consistent with the partial mislocalization of the *est1-*

mut1(FL) protein, expression of the *est1-mut1* allele in an *est1Δ* strain results in short, but stable telomeres. This defect is suppressed by fusion of the mutant protein with the T_{Ag}NLS (**Figure 18**), indicating that the autonomous nuclear localization of Est1p contributes to normal telomerase function.

We were unable to identify a triple NLS mutant allele that is uniquely defective for nuclear import, perhaps reflecting effects of the multiple mutations on Est1p folding and/or function. Thus, although we favor the idea that the NLSs of Est1p are essential for telomere maintenance, we cannot rule out the possibility that additional binding partners partially compensate for the loss of Est1p NLS function when the protein is expressed at endogenous levels.

TLC1 RNA acquires a 2,2,7-tri-methyl guanosine cap as step in its maturation to become a functional component of telomerase and it possesses a binding site for the Sm proteins, thus making telomerase a small nuclear ribonucleoprotein particle (snRNP) [14]. Another class of snRNPs with functions vital to the cell include the uridine-rich snRNPs (UsnRNP) that comprise the spliceosome [143]. Although the mechanisms controlling UsnRNP biogenesis in yeast have yet to be completely elucidated, current data support assembly of these ribonucleoproteins in the cytoplasm prior to nuclear import of the assembled complex [143]. Telomerase biogenesis has been hypothesized to occur in a similar manner, with the most prevalent model asserting that the protein components of the enzyme assemble onto the RNA like beads on a string before shuttling of the complex into the nucleus [15].

Our demonstration that Est1p nuclear translocation via the classical import pathway is important for normal telomere length maintenance (**Figures 28-32**) suggests

that there may be additional complexity to the current model of telomerase biogenesis. *TLC1* nucleocytoplasmic shuttling depends on the nuclear exportin, Crm1p, and the β importins Mtr10p and Kap122p [30,291,300]. In contrast, the nuclear import of overexpressed Est1p is unperturbed in mutants of Kap122p and/or Mtr10p (**Figures 22-25**). Nuclear localization of *TLC1* is unaffected at the restrictive temperature in a *srp1* strain [291], while overexpressed Est1p is excluded from the nucleus under this condition (**Figures 26** and **27**). Finally, overexpression of *TLC1*, but not Est1p, in an *mtr10* strain rescues the telomere length defect of the mutant [300]. In contrast, telomere shortening occurs when trafficking through the classical import pathway is disrupted and this defect is counteracted by expression of excess Est1p, but not *TLC1* RNA (**Figures 28-32**). Together, these data point to independent nuclear localization of *TLC1* RNA and Est1p.

A possible explanation for these findings is that Est1p does not assemble with the telomerase holoenzyme in the cytoplasm, but rather is imported autonomously, associating with telomerase at a later step of biogenesis within the nucleus. This model is consistent with the cell cycle regulated abundance of Est1p and with the ability of *TLC1* to localize to the nucleus during G1 phase when Est1p levels are low [16,289,290,293]. One caveat is that deletions of any of the EST proteins, including Est1p, disrupt the nuclear localization of *TLC1* RNA [291]. However, as previously suggested, it may be the nuclear retention of *TLC1* RNA, rather than its import into the nucleus, that is disrupted when *EST1* is deleted.

The studies described here address only the mechanism of Est1p import and do not clarify the trafficking of the other protein components of telomerase. A GFP fusion with Est2p also localizes to the nucleus when overexpressed [294], suggesting that Est2p

contains an NLS that is capable of facilitating nuclear import. However, further investigations are required to determine whether the localization of Est2p is autonomous. Est3p, with a mass of 20kDa, is theoretically capable of passive diffusion into the nucleus [25]. However, direct interactions of Est3p with both Est1p and Est2p have been observed [278,279], so the free diffusion of Est3p may be limited through its interaction with other telomerase components. Although Est3p associates with the telomere at low levels during G1 phase [279], its interaction with telomerase is stimulated by Est1p [16], suggesting that at least a fraction of Est3p may assemble with telomerase after the import and assembly of Est1p within the nucleus.

CHAPTER III

CONCLUSIONS AND FUTURE DIRECTIONS

The ribonucleoprotein complex telomerase functions to counteract the gradual telomere shortening that dividing cells experience when the conventional DNA replication machinery fails to fully replicate chromosome ends [188]. Telomerase is inactive in somatic cells, but its activity may contribute to the continued proliferation of stem cells [221]. Reactivation of telomerase is observed in ~90% of cancer cell lines and is essential for the immortalization of these cells [224]. Hence, the study of the function and regulation of telomerase has significant implications for our understanding of the mechanisms underlying cellular aging and cancer.

The biogenesis of telomerase exemplifies a significant layer of regulation that the cell uses to restrict enzyme activity in the cell cycle. In fact, in human cells, mutations that uniquely perturb telomerase assembly and/or subnuclear localization can have the same effects as those that reduce the catalytic activity of the enzyme, resulting in a range of aging-related diseases and/or syndromes [3,230,246]. In recent years, characterization of the intranuclear localization dynamics of human telomerase components has produced a fairly comprehensive model of the cell cycle regulation of telomerase biogenesis [220].

Mechanisms of telomerase biogenesis in yeast are also important. Mutations that abrogate telomerase recruitment to telomeres result in an EST phenotype, ultimately leading to cell death [268,269,282]. However the paucity of studies related to this phenomenon causes the model for telomerase biogenesis to remain primarily incomplete.

Therefore in this work we sought to characterize the nuclear localization of a protein component of yeast telomerase to shed more light on how the cell accomplishes the correctly-timed assembly and shuttling of such an enzyme.

Telomerase biogenesis in budding yeast requires the regulated assembly of the *TLC1* RNA with three essential proteins, Est1p, Est2p, and Est3p. Est1p is a critical determinant of telomerase assembly and function: its cell cycle-regulated degradation precludes telomerase assembly in G1 phase of the cell cycle [16,290]; it interacts directly with *TLC1* RNA (and likely with Est2p and Est3p) [275,279,281]; it stimulates the association of Est3p with the telomerase complex [16]; and it recruits telomerase to telomeres through its interaction with a telomere end-binding protein [290]. Therefore, in this study we chose to examine mechanisms of telomerase biogenesis from the standpoint of Est1p nuclear localization, proposing that the subcellular localization of Est1p, as mediated through endogenous NLSs, functions as an additional mechanism for the regulation of telomerase assembly and activity in the cell.

In this study, we used the overexpression of an Est1-GFP fusion protein, which precludes association with other telomerase components due to their limited abundance, to characterize the requirements for Est1p nuclear localization. We have shown that three endogenous sequences are capable of directing nuclear localization of Est1p. Mutation of any single NLS resulted in partial mislocalization of the full-length Est1-GFP fusion. Abrogation of Est1-GFPp nuclear localization was observed only with simultaneous substitutions within each NLS. Thus, the NLSs in Est1p are partially redundant. We found that mutation of the most N-terminal NLS resulted in telomere shortening. Fusion with an exogenous NLS suppressed the nuclear localization and telomere length defects

of the N-terminal NLS mutant. To determine the nuclear import pathway that Est1 utilizes, we monitored the localization of the Est1-GFP fusion protein in a number of importin mutants and found that Est1p requires the classical nuclear import machinery for nuclear import. We also found that low level expression of *EST1* (and not *TLC1* RNA) from the native promoter suppressed the telomere shortening observed at the semipermissive temperature in strain harboring a conditional allele of the yeast homolog of importin α. These data reveal that the autonomous nuclear localization of Est1p through its endogenous NLS(s) is important for telomerase function in the cell.

The presence of multiple NLSs in Est1p may serve to promote nuclear localization if Est1p assembles with an unidentified binding partner, during which time one or more of the NLSs may be concealed. Alternatively, though the multimerization state of telomerase is debated [344], if Est1p possesses the ability to self-assemble, its NLSs that function relatively weakly in the context of a single molecule of Est1p may function more strongly upon protein multimerization. Therefore, Est1p tertiary structure or the quaternary structure resulting from its interaction(s) with other proteins may—by concealing or revealing an NLS—account for the observed differences in NLS function. Another possibility is that the NLSs in Est1p may contribute to different modes of telomerase activity. The regulation of telomerase function during normal telomere replication is intrinsically different from the regulation that occurs during *de novo* telomere addition [345] and the subcellular or subnuclear localization of the entire telomerase complex or a specific component of the enzyme may contribute to this difference.

This work alters the model of yeast telomerase biogenesis (**Figure 33**). Our observations that Est1p and *TLC1* RNA utilize two distinct mechanisms for nuclear import indicate that the previously hypothesized assembly of telomerase protein components with *TLC1* RNA in the cytoplasm prior to nuclear import of the assembled telomerase holoenzyme is likely too simple. Instead, our data suggest that Est1p and *TLC1* RNA, which may or may not be associated with other telomerase proteins, are trafficked into the nucleus independently.

The nucleolus has been shown to play an important role in telomerase biogenesis in human cells [220]. The same also appears to be true for yeast telomerase. The observation that Est1p localizes to the nucleolus when overexpressed [294] suggests that one or more of its NLSs may function as a nucleolar localization sequence, serving to modulate the subnuclear trafficking of Est1p and potentially influencing its association with the other components of telomerase within the nucleus.

Additionally, in the only other publication specifically examining the localization of protein components of yeast telomerase, the Lingner group showed that co-overexpression of Est2-GFPp and *TCL1* RNA caused redistribution of Est2-GFPp from the nucleolus to the nucleoplasm—a phenotype that was not observed when an Est2-GFPp mutant protein that cannot bind *TLC1* RNA was expressed [294]. These results suggest that the interaction of *TLC1* RNA with Est2p modulates the subnuclear localization of Est2p, a phenotype somewhat similar to the effect of hTR on hTERT localization in humans [193,214,220]. Furthermore, overexpression of Est2p in an *est1*Δ or *est3*Δ strain resulted in nucleolar localization of Est2p [294]. While the nuclear localization of endogenous *TLC1* RNA was disrupted in an *est1*Δ or *est3*Δ strain,

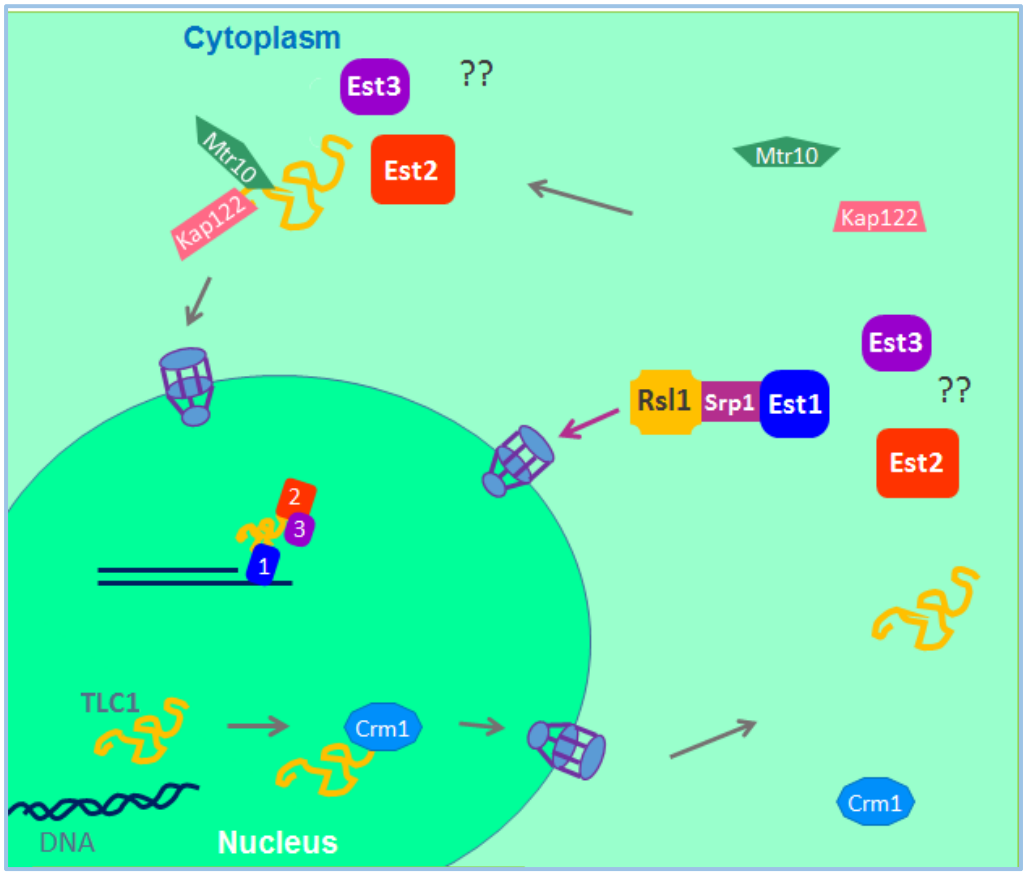

Figure 33. New model of telomerase biogenesis.

The results of my dissertation work add further complexity to the previous model of telomerase biogenesis. After nuclear export of *TLC1* RNA by Crm1p, *TLC1* may or may not associate with the other protein components of telomerase before its nuclear import by Kap122p and Mtr10p. Instead, through endogenous NLSs in the protein, Est1p associates with the components of the classical nuclear import machinery in yeast, Srp1p and Rs11p, to allow for its nuclear import. These findings suggest that at least under some circumstances, Est1p can localize to the nucleus autonomously. The nuclear import of Est2p and Est3p may or may not depend on interaction with *TLC1* or Est1p. Characterization of the nuclear import of these protein components of telomerase is warranted.

overexpression of Est2p under these conditions rescued *TCL1* RNA nuclear localization [294]. These observations suggest a cooperative relationship between Est2p and *TLC1* RNA for (sub)nuclear localization. They also suggest that the interaction between *TLC1* RNA and Est1p or Est3p facilitates nuclear retention of the RNA, providing further support for our data demonstrating independent trafficking of Est1p and *TLC1* RNA into the nucleus.

Future directions for this work involve using more direct approaches to detect the subcellular localization of telomerase components when expressed at endogenous levels. The use of overexpressed protein proved beneficial for our investigations, especially since our functional analysis using proteins expressed at or near endogenous levels corroborated the findings from our overexpression studies. However, the use of overexpressed proteins could cause artifactual results. Our studies only examined the nuclear localization of Est1p. To obtain a more complete model of telomerase biogenesis in yeast, the nuclear localization of Est2p and Est3p should also be characterized. Also, because telomerase is a multi-subunit complex, simultaneous examination of the nuclear localization of each of its components should be performed. Using an overexpression system to conduct these experiments would be difficult and may ultimately prove uninformative. Thus, subcellular fractionation followed by immunoblotting of cytosolic and nuclear or nucleoplasmic and nucleolar extracts should be conducted to monitor localization.

Our experiments do not specifically address the cell cycle regulation of the assembly and trafficking of telomerase components. However, this layer of regulation is important for the model of telomerase biogenesis. Therefore, future experiments should

include using subcellular fractionation to characterize the subcellular localization of telomerase components in a normal cell cycle. Treatment of cells with hydroxyurea or nocadazole will allow for the observation of the subcellular localization of telomerase proteins in S phase and G2/M phase, respectively. An alternative way to monitor the subcellular localization of telomerase components in the cell cycle includes arresting cells in G1 phase (when Est1p levels are essentially undetectable) with α-factor and releasing into the cell cycle by α-factor removal.

One question of interest to us has been whether Est1p nuclear localization modulates the localization of other telomerase components. We were not able to obtain a variant of Est1p that is uniquely deficient for nuclear localization to permit us to answer this question—primarily due to effects on protein function(s) unrelated to nuclear localization caused by mutating all three NLSs in Est1p simultaneously. However, our findings suggest that Est1p nuclear localization does not necessarily impact *TLC1* RNA localization and vice versa. To examine the effect of Est1p mislocalization on the distribution of other telomerase components more directly, fusion of a cytoplasmic targeting sequence to Est1p to shift its steady state localization to the cytoplasm can be used with subcellular fractionation experiments to monitor the localization of other telomerase components. The localization of endogenous *TLC1* RNA can be determined by Northern blotting of nuclear and cytosolic extracts isolated using subcellular fractionation or by using fluorescence *in situ* hybridization with probes specific for *TLC1* RNA. If Est1p nuclear localization is required for *TLC1* RNA nuclear retention, these experiments should be performed in a leptomycin B (LMB)-sensitive yeast strain. LMB is a specific inhibitor of Crm1p [346], thus LMB treatment should essentially trap *TLC1*

RNA in the nucleus. These experiments would need to be carefully timed so that *TLC1* RNA is exported from the nucleus to undergo cytoplasmic maturation, but cannot be re-exported after nuclear import of the mature RNA. In addition, subcellular fractionation can be used to examine which subunit interactions can occur in the absence of Est1p nuclear localization.

In this work, we sought to identify mechanisms that regulate the biogenesis of yeast telomerase by determining whether Est1p contains an NLS that is important for telomerase function at the telomere. We found that Est1p possesses three NLSs that impact telomerase function in the cell by influencing Est1p nuclear localization. Investigation of Est1p nuclear import revealed a previously unreported mechanism for the biogenesis of telomerase in yeast, the independent nuclear import of two telomerase components, Est1p and *TLC1* RNA. These experiments impact our understanding of how telomerase might function as a snRNP and provide evidence for how the cell accomplishes the cell cycle restricted activity of such a complex enzyme.

REFERENCES

1. Heinrich PC, Gross V, Northemann W, Scheurlen M (1978) Structure and function of nuclear ribonucleoprotein complexes. Reviews of Physiology, Biochemistry and Pharmacology, Volume 81: Springer Berlin Heidelberg. pp. 101-134.

2. Alberts B, Johnson A, Lewis J, Raff M, Roberts K, et al. (2007) Molecular Biology of the Cell. New York: Garland Science. 1392 p.

3. Zhong F, Savage SA, Shkreli M, Giri N, Jessop L, et al. (2011) Disruption of telomerase trafficking by TCAB1 mutation causes dyskeratosis congenita. Genes & Development 25: 11-16.

4. Mroczek S, Dziembowski A (2013) U6 RNA biogenesis and disease association. Wiley Interdisciplinary Reviews: RNA 4: 581-592.

5. Coady TH, Lorson CL (2011) SMN in spinal muscular atrophy and snRNP biogenesis. Wiley Interdisciplinary Reviews: RNA 2: 546-564.

6. Huranová M, Hnilicová J, Fleischer B, Cvačková Z, Staněk D (2009) A mutation linked to retinitis pigmentosa in HPRP31 causes protein instability and impairs its interactions with spliceosomal snRNPs. Human Molecular Genetics 18: 2014-2023.

7. Freed EF, Bleichert F, Dutca LM, Baserga SJ (2010) When ribosomes go bad: diseases of ribosome biogenesis. Molecular BioSystems 6: 481-493.

8. Marcand S, Brevet V, Mann C, Gilson E (2000) Cell cycle restriction of telomere elongation. Curr Biol 10: 487-490.

9. Schneider J, Schindewolf C, van Zee K, Fanning E (1988) A mutant SV40 large T antigen interferes with nuclear localization of a heterologous protein. Cell 54: 117-125.

10. Kalderon D, Roberts BL, Richardson WD, Smith AE (1984) A short amino acid sequence able to specify nuclear location. Cell 39: 499-509.

11. Lukowiak AA, Narayanan A, Li ZH, Terns RM, Terns MP (2001) The snoRNA domain of vertebrate telomerase RNA functions to localize the RNA within the nucleus. RNA 7: 1833-1844.

12. Kiss T, Fayet E, Jády BE, Richard P, Weber M (2006) Biogenesis and Intranuclear Trafficking of Human Box C/D and H/ACA RNPs. Cold Spring Harbor Symposia on Quantitative Biology 71: 407-417.

13. Tomlinson RL, Ziegler TD, Supakorndej T, Terns RM, Terns MP (2006) Cell Cycle-regulated Trafficking of Human Telomerase to Telomeres. Mol Biol Cell 17: 955-965.

14. Seto AG, Zaug AJ, Sabel SG, Wolin SL, Cech TR (1999) *Saccharomyces cerevisiae* telomerase is an Sm small nuclear ribonucleoprotein particle. Nature 401: 177-180.

15. Gallardo F, Chartrand P (2008b) Telomerase biogenesis: The long road before getting to the end. RNA Biology 5: 212-215.

16. Osterhage JL, Talley JM, Friedman KL (2006) Proteasome-dependent degradation of Est1p regulates the cell cycle-restricted assembly of telomerase in *Saccharomyces cerevisiae*. Nat Struct Mol Biol 13: 720-728.

17. Hartwell L, Hood L, Goldberg ML, Reynolds A, Silver LM, et al. (2008) Genetics: From Genes to Genomes: McGraw-Hill

18. Gruenbaum Y, Goldman RD, Meyuhas R, Mills E, Margalit A, et al. (2003) The Nuclear Lamina and Its Functions in the Nucleus. International Review of Cytology: Academic Press. pp. 1-62.

19. Olson MOJ (2010) Nucleolus: Structure and Function. eLS: John Wiley & Sons, Ltd.

20. Cooper G (2000) The Cell: A Molecular Approach: Sunderland: Sinauer Associates.

21. Morimoto M, Boerkoel C (2013) The Role of Nuclear Bodies in Gene Expression and Disease. Biology 2: 976-1033.

22. Jackson DA (1997) Chromatin domains and nuclear compartments: establishing sites of gene expression in eukaryotic nuclei. Mol Bio Rep 24: 209-220.

23. Lamond AI, Spector DL (2003) Nuclear speckles: a model for nuclear organelles. Nat Rev Mol Cell Biol 4: 605-612.

24. Wente SR, Rout MP (2010) The Nuclear Pore Complex and Nuclear Transport. Cold Spring Harbor Perspectives in Biology 2.

25. Wang R, Brattain MG (2007) The maximal size of protein to diffuse through the nuclear pore is larger than 60kDa. FEBS Letters 581: 3164-3170.

26. Shulga N, Mosammaparast N, Wozniak R, Goldfarb DS (2000) Yeast Nucleoporins Involved in Passive Nuclear Envelope Permeability. The Journal of Cell Biology 149: 1027-1038.

27. Weis K (2003) Regulating Access to the Genome: Nucleocytoplasmic Transport throughout the Cell Cycle. Cell 112: 441-451.

28. Aitchison JD, Blobel G, Rout MP (1996) Kap104p: a karyopherin involved in the nuclear transport of messenger RNA binding proteins. Science 274: 624-627.

29. Rout MP, Blobel G, Aitchison JD (1997) A Distinct Nuclear Import Pathway Used by Ribosomal Proteins. Cell 89: 715-725.

30. Fornerod M, Ohno M, Yoshida M, Mattaj IW (1997) *CRM1* is an export receptor for leucine-rich nuclear export signals. Cell 90: 1051-1060.

31. Mingot JM, Bohnsack MT, Jäkle U, Görlich D (2004) Exportin 7 defines a novel general nuclear export pathway. EMBO J 23: 3227-3236.

32. Mingot JM, Kostka S, Kraft R, Hartmann E, Görlich D (2001) Importin 13: a novel mediator of nuclear import and export. The EMBO Journal 20: 3685-3694.

33. Gontan C, Güttler T, Engelen E, Demmers J, Fornerod M, et al. (2009) Exportin 4 mediates a novel nuclear import pathway for Sox family transcription factors. The Journal of Cell Biology 185: 27-34.

34. Weis K (1998) Importins and exportins: how to get in and out of the nucleus. Trends in Biochemical Sciences 23: 185-189.

35. Lange A, Mills RE, Lange CJ, Stewart M, Devine SE, et al. (2007) Classical nuclear localization signals: definition, function, and interaction with importin alpha. J Biol Chem 282: 5101-5105.

36. Adam SA, Gerace L (1991) Cytosolic proteins that specifically bind nuclear location signals are receptors for nuclear import. Cell 66: 837-847.

37. Adam EJ, Adam SA (1994) Identification of cytosolic factors required for nuclear location sequence-mediated binding to the nuclear envelope. The Journal of Cell Biology 125: 547-555.

38. Görlich D, Prehn S, Laskey RA, Hartmann E (1994) Isolation of a protein that is essential for the first step of nuclear protein import. Cell 79: 767-778.

39. Dingwall C, Robbins J, Dilworth SM, Roberts B, Richardson WD (1988) The nucleoplasmin nuclear location sequence is larger and more complex than that of SV-40 large T antigen. J Cell Biol 107: 841-849.

40. Enenkel C, Blobel G, Rexach M (1995) Identification of a Yeast Karyopherin Heterodimer That Targets Import Substrate to Mammalian Nuclear Pore Complexes. Journal of Biological Chemistry 270: 16499-16502.

41. Moroianu J, Blobel G, Radu A (1995) Previously identified protein of uncertain function is karyopherin alpha and together with karyopherin beta docks import substrate at nuclear pore complexes. PNAS USA 92: 2008-2011.

42. Moroianu J, Blobel G, Radu A (1996) The binding site of karyopherin alpha for karyopherin beta overlaps with a nuclear localization sequence. Proceedings of the National Academy of Sciences 93: 6572-6576.

43. Richardson WD, Mills AD, Dilworth SM, Laskey RA, Dingwall C (1988) Nuclear protein migration involves two steps: Rapid binding at the nuclear envelope followed by slower translocation through nuclear pores. Cell 52: 655-664.

44. Akey CW, Goldfarb DS (1989) Protein import through the nuclear pore complex is a multistep process. The Journal of Cell Biology 109: 971-982.

45. Ryan KJ, Wente SR (2000) The nuclear pore complex: a protein machine bridging the nucleus and cytoplasm. Current Opinion in Cell Biology 12: 361-371.

46. Lusk CP, Makhnevych T, Wozniak RW (2004) New ways to skin a kap: mechanisms for controlling nuclear transport. Biochemistry and Cell Biology 82: 618-625.

47. Chook YM, Süel KE (2011) Nuclear import by karyopherin-βs: Recognition and inhibition. Biochimica et Biophysica Acta (BBA) - Molecular Cell Research 1813: 1593-1606.

48. Leslie DM, Zhang W, Timney BL, Chait BT, Rout MP, et al. (2004) Characterization of karyopherin cargoes reveals unique mechanisms of Kap121p-mediated nuclear import. Mol Cell Biol 24: 8487-8503.

49. Siomi MC, Fromont M, Rain J-C, Wan L, Wang F, et al. (1998) Functional conservation of the transportin nuclear import pathway in divergent organisms. Mol Cell Biol 18: 4141-4148.

50. Kahle J, Baake M, Doenecke D, Albig W (2005) Subunits of the Heterotrimeric Transcription Factor NF-Y Are Imported into the Nucleus by Distinct Pathways Involving Importin β and Importin 13. Molecular and Cellular Biology 25: 5339-5354.

51. Chen M-H, Ben-Efraim I, Mitrousis G, Walker-Kopp N, Sims PJ, et al. (2005) Phospholipid Scramblase 1 Contains a Nonclassical Nuclear Localization Signal with Unique Binding Site in Importin α. Journal of Biological Chemistry 280: 10599-10606.

52. Van Dusen CM, Yee L, McNally LM, McNally MT (2010) A Glycine-Rich Domain of hnRNP H/F Promotes Nucleocytoplasmic Shuttling and Nuclear Import through an Interaction with Transportin 1. Molecular and Cellular Biology 30: 2552-2562.

53. Steggerda SM, Paschal BM (2002) Regulation of nuclear import and export by the GTPase ran. In: Kwang WJ, editor. International Review of Cytology: Academic Press. pp. 41-91.

54. Hopper AK, Traglia HM, Dunst RW (1990) The yeast RNA1 gene product necessary for RNA processing is located in the cytosol and apparently excluded from the nucleus. The Journal of Cell Biology 111: 309-321.

55. Corbett AH, Koepp DM, Schlenstedt G, Lee MS, Hopper AK, et al. (1995) Rna1p, a Ran/TC4 GTPase activating protein, is required for nuclear import. The Journal of Cell Biology 130: 1017-1026.

56. Ohtsubo M, Okazaki H, Nishimoto T (1989) The RCC1 protein, a regulator for the onset of chromosome condensation locates in the nucleus and binds to DNA. The Journal of Cell Biology 109: 1389-1397.

57. Lee A, Tam R, Belhumeur P, DiPaolo T, Clark MW (1993) Prp20, the Saccharomyces cerevisiae homolog of the regulator of chromosome condensation, RCC1, interacts with double-stranded DNA through a multi-component complex containing GTP-binding proteins. Journal of Cell Science 106: 287-298.

58. Nemergut ME, Macara IG (2000) Nuclear Import of the Ran Exchange Factor, Rcc1, Is Mediated by at Least Two Distinct Mechanisms. The Journal of Cell Biology 149: 835-850.

59. Görlich D, Pante N, Kutay U, Aebi U, Bischoff FR (1996b) Identification of different roles for RanGDP and RanGTP in nuclear protein import. EMBO J 15: 5584-5594.

60. Izaurralde E, Kutay U, von Kobbe C, Mattaj IW, Görlich D (1997) The asymmetric distribution of the constituents of the Ran system is essential for transport into and out of the nucleus. The EMBO Journal 16: 6535-6547.

61. Bischoff FR, Görlich D (1997) RanBP1 is crucial for the release of RanGTP from importin β-related nuclear transport factors. FEBS letters 419: 249-254.

62. O'Reilly AJ, Dacks JB, Field MC (2011) Evolution of the Karyopherin-β Family of Nucleocytoplasmic Transport Factors; Ancient Origins and Continued Specialization. PLoS ONE 6: e19308.

63. Brinkmann U, Brinkmann E, Gallo M, Pastan I (1995) Cloning and characterization of a cellular apoptosis susceptibility gene, the human homologue to the yeast chromosome segregation gene CSE1. Proceedings of the National Academy of Sciences 92: 10427-10431.

64. Köhler M, Ansieau S, Prehn S, Leutz A, Haller H, et al. (1997) Cloning of two novel human importin-α subunits and analysis of the expression pattern of the importin-α protein family. FEBS letters 417: 104-108.

65. Fornerod M, van Deursen J, van Baal S, Reynolds A, Davis D, et al. (1997) The human homologue of yeast CRM1 is in a dynamic subcomplex with

CAN/Nup214 and a novel nuclear pore component Nup88. The EMBO Journal 16: 807-816.

66. Chook Y, Blobel G (2001) Karyopherins and nuclear import. Current Opinion in Structural Biology 11: 703-715.

67. Williams RS, Shohet RV, Stillman B (1997) A human protein related to yeast Cdc6p. Proceedings of the National Academy of Sciences 94: 142-147.

68. Takei Y, Yamamoto K, Tsujimoto G (1999) Identification of the sequence responsible for the nuclear localization of human Cdc6. FEBS Letters 447: 292-296.

69. Truant R, Fridell RA, Benson RE, Bogerd H, Cullen BR (1998) Identification and Functional Characterization of a Novel Nuclear Localization Signal Present in the Yeast Nab2 Poly(A)+ RNA Binding Protein. Molecular and Cellular Biology 18: 1449-1458.

70. Lee DCY, Aitchison JD (1999) Kap104p-mediated nuclear import: nuclear localization signals in mRNA-bindng proteins and the role of Ran and RNA. J Biol Chem 274: 29031-29037.

71. Soniat M, Sampathkumar P, Collett G, Gizzi A, Banu R, et al. (2013) Crystal structure of human Karyopherin β2 bound to the PY-NLS of Saccharomyces cerevisiae Nab2. Journal of Structural and Functional Genomics 14: 31-35.

72. Mallet P-L, Bachand F (2013) A Proline-Tyrosine Nuclear Localization Signal (PY-NLS) Is Required for the Nuclear Import of Fission Yeast PAB2, but Not of Human PABPN1. Traffic 14: 282-294.

73. Pemberton LF, Rosenblum JS, Blobel G (1999) Nuclear Import of the TATA-binding Protein: Mediation by the Karyopherin Kap114p and a Possible Mechanism for Intranuclear Targeting. The Journal of Cell Biology 145: 1407-1417.

74. Mühlhäusser P, Müller E-C, Otto A, Kutay U (2001) Multiple pathways contribute to nuclear import of core histones. EMBO reports 2: 690-696.

75. Nikolaev I, Cochet M-F, Felenbok B (2003) Nuclear Import of Zinc Binuclear Cluster Proteins Proceeds through Multiple, Overlapping Transport Pathways. Eukaryotic Cell 2: 209-221.

76. Segref A, Sharma K, Doye V, Hellwig A, Huber J, et al. (1997) Mex67p, a novel factor for nuclear mRNA export, binds to both poly(A)+ RNA and nuclear pores. 3256-3271 p.

77. Katahira J, Sträßer K, Podtelejnikov A, Mann M, Jung JU, et al. (1999) The Mex67p-mediated nuclear mRNA export pathway is conserved from yeast to human. 2593-2609 p.

78. Truant R, Kang Y, ‖, Cullen BR, ‖ (1999) The Human Tap Nuclear RNA Export Factor Contains a Novel Transportin-dependent Nuclear Localization Signal That Lacks Nuclear Export Signal Function. Journal of Biological Chemistry 274: 32167-32171.

79. Lee BJ, Cansizoglu AE, Süel KE, Louis TH, Zhang Z, et al. (2006) Rules for Nuclear Localization Sequence Recognition by Karyopherinβ2. Cell 126: 543-558.

80. Imasaki T, Shimizu T, Hashimoto H, Hidaka Y, Kose S, et al. (2007) Structural Basis for Substrate Recognition and Dissociation by Human Transportin 1. Molecular Cell 28: 57-67.

81. Zhang ZC, Satterly N, Fontoura BMA, Chook YM (2011) Evolutionary development of redundant nuclear localization signals in the mRNA export factor NXF1. Molecular Biology of the Cell 22: 4657-4668.

82. Clevers H (2006) Wnt/β-Catenin Signaling in Development and Disease. Cell 127: 469-480.

83. Brown JA, Bharathi A, Ghosh A, Whalen W, Fitzgerald E, et al. (1995) A Mutation in the Schizosaccharomyces pombe rae1 Gene Causes Defects in Poly(A)+ RNA Export and in the Cytoskeleton. Journal of Biological Chemistry 270: 7411-7419.

84. Murphy R, Wente SR (1996) An RNA-export mediator with an essential nuclear export signal. Nature 383: 357-360.

85. Dalton S, Whitbread L (1995) Cell cycle-regulated nuclear import and export of Cdc47, a protein essential for initiation of DNA replication in budding yeast. Proceedings of the National Academy of Sciences 92: 2514-2518.

86. Ding Q, Zhao L, Guo H, Zheng A (2010) The nucleocytoplasmic transport of viral proteins. Virologica Sinica 25: 79-85.

87. Sweet BH, Hilleman MR (1960) The vacuolating virus, S.V. 40. Proc Soc Exp Biol Med 105: 402-427.

88. Eddy BE, Borman GS, Berkeley WH, Young RD (1961) Tumors induced in hamsters by injection of rhesus monkey kidney cell extracts. Proc Soc Exp Biol Med 107: 191-197.

89. Eddy BE, Borman GS, Grubbs GE, Young RD (1962) Identification of the oncogenic substance in rhesus monkey kidney cell culture as simian virus 40. Virology 17: 65-75.

90. Girardi AJ, Sweet BH, Slotnick VB, Hilleman MR (1962) Development of tumors in hamsters inoculated in the neonatal period with vacuolating virus, SV-40. Proc Soc Exp Biol Med 109: 649-660.

91. Kirschstein RL, Gerber P (1962) Ependymomas produced after Intracerebral Inoculation of SV40 into New-born Hamsters. Nature 195: 299-300.

92. Shein HM, Enders JF (1962) Transformation induced by Simian Virus 40 in human renal cell cultures, I. Morphology and growth characteristics. ProcNatlAcadSciUSA 48: 1164-1172.

93. Jensen F, Koprowski H, Pontén JA (1963) Rapidtransformation of human fibroblast cultures by simian virus 40. Proceedings of the National Academy of Sciences 50: 343-348.

94. Jensen F, Koprowski H, Pagano JS, Pontén J, Ravdin RG (1964) Autologous and Homologous Implantation of Human Cells Transformed In Vitro by Simian Virus 40. Journal of the National Cancer Institute 32: 917-937.

95. Fraumeni JFJ, Ederer F, Miller RW (1963) An evaluation of the carcinogenicity of simian virus 40 in man. JAMA 185: 713-718.

96. Girardi AJ, Jensen FC, Koprowski H (1965) SV40-induced transformation of human diploid cells: crisis and recovery. JCellCompPhysiol 65: 69-84.

97. Lowe DB, Shearer MH, Jumper CA, Kennedy RC (2007) SV40 association with human malignancies and mechanisms of tumor immunity by large tumor antigen. Cellular and Molecular Life Sciences 64: 803-814.

98. Garcea RL, Imperiale MJ (2003) Simian Virus 40 Infection of Humans. Journal of Virology 77: 5039-5045.

99. Dean FB, Bullock P, Murakami Y, Wobbe CR, Weissbach L, et al. (1987) Simian virus 40 (SV40) DNA replication: SV40 large T antigen unwinds DNA containing the SV40 origin of replication. Proceedings of the National Academy of Sciences 84: 16-20.

100. Smale ST, Tjian R (1986) T-antigen-DNA polymerase alpha complex implicated in simian virus 40 DNA replication. Molecular and Cellular Biology 6: 4077-4087.

101. Stahl H, Dröge P, Knippers R (1986) DNA helicase activity of SV40 large tumor antigen. EMBO J 5: 1939-1944.

102. DeCaprio JA, Ludlow JW, Figge J, Shew J-Y, Huang C-M, et al. (1988) SV40 large tumor antigen forms a specific complex with the product of the retinoblastoma susceptibility gene. Cell 54: 275-283.

103. Dyson N, Bernards R, Friend SH, Gooding LR, Hassell JA, et al. (1990) Large T antigens of many polyomaviruses are able to form complexes with the retinoblastoma protein. Journal of Virology 64: 1353-1356.

104. Hannon GJ, Demetrick D, Beach D (1993) Isolation of the Rb-related p130 through its interaction with CDK2 and cyclins. Genes & Development 7: 2378-2391.

105. Lane DP, Crawford LV (1979) T antigen is bound to a host protein in SV40-transformed cells. Nature 278: 261-263.

106. Linzer DIH, Levine AJ (1979) Characterization of a 54K dalton cellular SV40 tumor antigen present in SV40-transformed cells and uninfected embryonal carcinoma cells. Cell 17: 43-52.

107. McCormick F, Harlow E (1980) Association of a murine 53,000-dalton phosphoprotein with simian virus 40 large-T antigen in transformed cells. Journal of Virology 34: 213-224.

108. Pope JH, Rowe WP (1964) Detection of specific antigen in SV40-transformed cells by immunofluorescence The Journal of Experimental Medicine 120: 121-128.

109. Butel JS, Guentzel MJ, Rapp F (1969) Variants of Defective Simian Papovavirus 40 (PARA) Characterized by Cytoplasmic Localization of Simian Papovavirus 40 Tumor Antigen. Journal of Virology 4: 632-641.

110. Anderson JT, Wilson SM, Datar KV, Swanson MS (1993) NAB2: a yeast nuclear polyadenylated RNA-binding protein essential for cell viability. Molecular and Cellular Biology 13: 2730-2741.

111. Chamberlain NL, Driver ED, Miesfeld RL (1994) The length and location of CAG trinucleotide repeats in the androgen receptor N-terminal domain affect transactivation function. Nucleic Acids Research 22: 3181-3186.

112. Brooks BP, Paulson HL, Merry DE, Salazar-Grueso EF, Brinkmann AO, et al. (1997) Characterization of an Expanded Glutamine Repeat Androgen Receptor in a Neuronal Cell Culture System. Neurobiology of Disease 3: 313-323.

113. Montie HL, Cho MS, Holder L, Liu Y, Tsvetkov AS, et al. (2009) Cytoplasmic retention of polyglutamine-expanded androgen receptor ameliorates disease via autophagy in a mouse model of spinal and bulbar muscular atrophy. Human Molecular Genetics 18: 1937-1950.

114. Grundke-Iqbal I, Iqbal K, Tung YC, Quinlan M, Wisniewski HM, et al. (1986) Abnormal phosphorylation of the microtubule-associated protein tau (tau) in Alzheimer cytoskeletal pathology. Proceedings of the National Academy of Sciences 83: 4913-4917.

115. Iqbal K, Grundke-Iqbal I, Smith AJ, George L, Tung YC, et al. (1989) Identification and localization of a tau peptide to paired helical filaments of Alzheimer disease. Proceedings of the National Academy of Sciences 86: 5646-5650.

116. Lee V, Balin B, Otvos L, Trojanowski J (1991) A68: a major subunit of paired helical filaments and derivatized forms of normal Tau. Science 251: 675-678.

117. Liu F, Grundke-Iqbal I, Iqbal K, Gong C-X (2005) Contributions of protein phosphatases PP1, PP2A, PP2B and PP5 to the regulation of tau phosphorylation. European Journal of Neuroscience 22: 1942-1950.

118. Tanimukai H, Grundke-Iqbal I, Iqbal K (2004) Inhibitors of protein phosphatase-2A: topography and subcellular localization. Molecular Brain Research 126: 146-156.

119. Tanimukai H, Grundke-Iqbal I, Iqbal K (2005) Up-Regulation of Inhibitors of Protein Phosphatase-2A in Alzheimer's Disease. The American journal of pathology 166: 1761-1771.

120. Yu G, Yan T, Feng Y, Liu X, Xia Y, et al. (2013) Ser9 phosphorylation causes cytoplasmic detention of I2PP2A/SET in Alzheimer disease. Neurobiology of aging 34: 1748-1758.

121. Cisterna B, Biggiogera M (2010) Chapter Two - Ribosome Biogenesis: From Structure to Dynamics. In: Kwang WJ, editor. International Review of Cell and Molecular Biology: Academic Press. pp. 67-111.

122. Woolford JL, Baserga SJ (2013) Ribosome Biogenesis in the Yeast Saccharomyces cerevisiae. Genetics 195: 643-681.

123. Kief DR, Warner JR (1981) Coordinate control of syntheses of ribosomal ribonucleic acid and ribosomal proteins during nutritional shift-up in Saccharomyces cerevisiae. Molecular and Cellular Biology 1: 1007-1015.

124. Ju Q, Warner JR (1994) Ribosome synthesis during the growth cycle of Saccharomyces cerevisiae. Yeast 10: 151-157.

125. Geiduschek EP, Tocchini-Valentini GP (1988) Transcription by RNA Polymerase III. Annual Review of Biochemistry 57: 873-914.

126. Venema J, Tollervey D (1999) RIBOSOME SYNTHESIS IN Saccharomyces cerevisiae. Annual Review of Genetics 33: 261-311.

127. Fatica A, Oeffinger M, Dlakić M, Tollervey D (2003) Nob1p Is Required for Cleavage of the 3′ End of 18S rRNA. Molecular and Cellular Biology 23: 1798-1807.

128. Semrad K, Green R, Schroeder R (2004) RNA chaperone activity of large ribosomal subunit proteins from Escherichia coli. RNA 10: 1855-1860.

129. Kovacs D, Rakacs M, Agoston B, Lenkey K, Semrad K, et al. (2009) Janus chaperones: Assistance of both RNA- and protein-folding by ribosomal proteins. FEBS letters 583: 88-92.

130. Woodson SA (2011) RNA Folding Pathways and the Self-Assembly of Ribosomes. Accounts of Chemical Research 44: 1312-1319.

131. Jagannathan I, Culver GM (2004) Ribosomal Protein-dependent Orientation of the 16 S rRNA Environment of S15. Journal of Molecular Biology 335: 1173-1185.

132. Ramaswamy P, Woodson SA (2009) Global Stabilization of rRNA Structure by Ribosomal Proteins S4, S17, and S20. Journal of Molecular Biology 392: 666-677.

133. Fatica A, Cronshaw AD, Dlakić M, Tollervey D (2002) Ssf1p Prevents Premature Processing of an Early Pre-60S Ribosomal Particle. Molecular Cell 9: 341-351.

134. Dez C, Froment C, Noaillac-Depeyre J, Monsarrat B, Caizergues-Ferrer M, et al. (2004) Npa1p, a Component of Very Early Pre-60S Ribosomal Particles, Associates with a Subset of Small Nucleolar RNPs Required for Peptidyl Transferase Center Modification. Molecular and Cellular Biology 24: 6324-6337.

135. Warner JR (1999) The economics of ribosome biosynthesis in yeast. Trends in Biochemical Sciences 24: 437-440.

136. Zemp I, Kutay U (2007) Nuclear export and cytoplasmic maturation of ribosomal subunits. FEBS letters 581: 2783-2793.

137. Panse VG, Johnson AW (2010) Maturation of eukaryotic ribosomes: acquisition of functionality. Trends in Biochemical Sciences 35: 260-266.

138. Kelemen O, Convertini P, Zhang Z, Wen Y, Shen M, et al. (2013) Function of alternative splicing. Gene 514: 1-30.

139. Alekseyenko AV, Kim N, Lee CJ (2007) Global analysis of exon creation versus loss and the role of alternative splicing in 17 vertebrate genomes. RNA 13: 661-670.

140. Artamonova II, Gelfand MS (2007) Comparative Genomics and Evolution of Alternative Splicing: The Pessimists' Science. Chemical Reviews 107: 3407-3430.

141. Belfort M, Shub DA (1990) RNA: Catalysis, Splicing, Evolution. Amsterdam, The Netherlands: Elsevier Science Publishers B.V.

142. Krummel DAP, Nagai K, Oubridge C (2010) Structure of spliceosomal ribonucleoproteins. F1000 Biol Rep.

143. Will CL, Lührmann R (2001) Spliceosomal UsnRNP biogenesis, structure and function. Current Opinion in Cell Biology 13: 290-301.

144. Lührmann R, Kastner B, Bach M (1990) Structure of spliceosomal snRNPs and their role in pre-mRNA splicing. Biochim Biophys Acta 1087: 265-292.

145. Shaw DJ, Eggleton P, Young PJ (2008) Joining the dots: Production, processing and targeting of U snRNP to nuclear bodies. Biochimica et Biophysica Acta (BBA) - Molecular Cell Research 1783: 2137-2144.

146. Hernandez N (2001) Small Nuclear RNA Genes: a Model System to Study Fundamental Mechanisms of Transcription. Journal of Biological Chemistry 276: 26733-26736.

147. Hamm J, Mattaj IW (1990) Monomethylated cap structures facilitate RNA export from the nucleus. Cell 63: 109-118.

148. Hellmuth K, Lau DM, Bischoff FR, Künzler M, Hurt E, et al. (1998) Yeast Los1p Has Properties of an Exportin-Like Nucleocytoplasmic Transport Factor for tRNA. Molecular and Cellular Biology 18: 6374-6386.

149. Huber J, Cronshagen U, Kadokura M, Marshallsay C, Wada T, et al. (1998) Snurportin1, an m3G-cap-specific nuclear import receptor with a novel domain structure. 4114-4126 p.

150. Hood JK, Silver PA (1999) In or out? Regulating nuclear transport. Current Opinion in Cell Biology 11: 241-247.

151. Fisher DE, Conner GE, Reeves WH, Wisniewolski R, Blobel G (1985) Small nuclear ribonucleoprotein particle assembly in vivo: Demonstration of a 6S RNA-free core precursor and posttranslational modification. Cell 42: 751-758.

152. Tardiff DF, Rosbash M (2006) Arrested yeast splicing complexes indicate stepwise snRNP recruitment during in vivo spliceosome assembly. RNA 12: 968-979.

153. Plessel G, Lührmann R, Kastner B (1997) Electron microscopy of assembly intermediates of the snRNP core: morphological similarities between the RNA-free (E.F.G) protein heteromer and the intact snRNP core. Journal of Molecular Biology 265: 87-94.

154. Raker VA, Plessel G, Lührmann R (1996) The snRNP core assembly pathway: identification of stable core protein heteromeric complexes and an snRNP subcore particle *in vitro*. EMBO J 15: 2256-2269.

155. Bordonné R (2000) Functional Characterization of Nuclear Localization Signals in Yeast Sm Proteins. Molecular and Cellular Biology 20: 7943-7954.

156. Girard C, Mouaikel J, Neel H, Bertrand E, Bordonné R (2004) Nuclear localization properties of a conserved protuberance in the Sm core complex. Experimental Cell Research 299: 199-208.

157. Kolb SJ, Battle DJ, Dreyfuss G (2007) Molecular Functions of the SMN Complex. Journal of Child Neurology 22: 990-994.

158. Liu Q, Fischer U, Wang F, Dreyfuss G (1997) The Spinal Muscular Atrophy Disease Gene Product, SMN, and Its Associated Protein SIP1 Are in a Complex with Spliceosomal snRNP Proteins. Cell 90: 1013-1021.

159. Golembe TJ, Yong J, Dreyfuss G (2005) Specific Sequence Features, Recognized by the SMN Complex, Identify snRNAs and Determine Their Fate as snRNPs. Molecular and Cellular Biology 25: 10989-11004.

160. Palacios I, Hetzer M, Adam SA, Mattaj IW (1997) Nuclear import of U snRNPs requires importin β. 6783-6792 p.

161. Freitas N, Cunha C (2009) Mechanisms and signals for the nuclear import of proteins. Curr Genomics 10: 550-557.

162. Narayanan U, Achsel T, Lührmann R, Matera AG (2004) Coupled In Vitro Import of U snRNPs and SMN, the Spinal Muscular Atrophy Protein. Molecular Cell 16: 223-234.

163. Raška I, Andrade LEC, Ochs RL, Chan EKL, Chang C-M, et al. (1991) Immunological and ultrastructural studies of the nuclear coiled body with autoimmune antibodies. Experimental Cell Research 195: 27-37.

164. Fakan S, Leser G, Martin TE (1984) Ultrastructural distribution of nuclear ribonucleoproteins as visualized by immunocytochemistry on thin sections. The Journal of Cell Biology 98: 358-363.

165. Eliceiri GL, Ryerse JS (1984) Detection of intranuclear clusters of Sm antigens with monoclonal anti-Sm antibodies by immunoelectron microscopy. Journal of Cellular Physiology 121: 449-451.

166. Bauer DW, Gall JG (1997) Coiled bodies without coilin. Molecular Biology of the Cell 8: 73-82.

167. Lange TS, Gerbi SA (2000) Transient Nucleolar Localization Of U6 Small Nuclear RNA InXenopus Laevis Oocytes. Molecular Biology of the Cell 11: 2419-2428.

168. Gerbi SA, Lange TS (2002) All Small Nuclear RNAs (snRNAs) of the [U4/U6.U5] Tri-snRNP Localize to Nucleoli; Identification of the Nucleolar Localization Element of U6 snRNA. Molecular Biology of the Cell 13: 3123-3137.

169. Isaac C, Yang Y, Thomas Meier U (1998) Nopp140 Functions as a Molecular Link Between the Nucleolus and the Coiled Bodies. The Journal of Cell Biology 142: 319-329.

170. Sleeman J (2007) A regulatory role for CRM1 in the multi-directional trafficking of splicing snRNPs in the mammalian nucleus. Journal of Cell Science 120: 1540-1550.

171. Pellizzoni L, Kataoka N, Charroux B, Dreyfuss G (1998) A Novel Function for SMN, the Spinal Muscular Atrophy Disease Gene Product, in Pre-mRNA Splicing. Cell 95: 615-624.

172. Sleeman JE, Ajuh P, Lamond AI (2001) snRNP protein expression enhances the formation of Cajal bodies containing p80-coilin and SMN. Journal of Cell Science 114: 4407-4419.

173. Visa N, Puvion-Dutilleul F, Bachellerie JF, Puvion E (1993a) Intranuclear distribution of U1 and U2 snRNAs visualized by high resolution in situ hybridization: revelation of a novel compartment containing U1 but not U2 snRNA in HeLa cells. Eur J Cell Biol 60: 308-321.

174. Visa N, Puvion-Dutilleul F, Harper F, Bachellerie J-P, Puvion E (1993b) Intranuclear Distribution of Poly(A) RNA Determined by Electron Microscope in Situ Hybridization. Experimental Cell Research 208: 19-34.

175. Misteli T, Spector DL (1997) Protein phosphorylation and the nuclear organization of pre-mRNA splicing. Trends in Cell Biology 7: 135-138.

176. Verheggen C, Lafontaine DLJ, Samarsky D, Mouaikel J, Blanchard JM, et al. (2002) Mammalian and yeast U3 snoRNPs are matured in specific and related nuclear compartments. 2736-2745 p.

177. Lygerou Z, Christophides G, Séraphin B (1999) A Novel Genetic Screen for snRNP Assembly Factors in Yeast Identifies a Conserved Protein, Sad1p, Also Required for Pre-mRNA Splicing. Molecular and Cellular Biology 19: 2008-2020.

178. Xue D, Rubinson DA, Pannone BK, Yoo CJ, Wolin SL (2000) U snRNP assembly in yeast involves the La protein. 19: 1650-1660.

179. Yu Y-T, Scharl EC, Smith CM, Steitz JA (1999) The Growing World of Small Nuclear Ribonucleoproteins. In: Gesteland RF, Cech TR, Atkins JF, editors. The RNA World 2nd ed. pp. 487-524.

180. Mouaikel J, Verheggen C, Bertrand E, Tazi J, Bordonné R (2002) Hypermethylation of the Cap Structure of Both Yeast snRNAs and snoRNAs Requires a Conserved Methyltransferase that Is Localized to the Nucleolus. Molecular Cell 9: 891-901.

181. Gottschalk A, Kastner B, Lührmann R, Fabrizio P (2001) The yeast U5 snRNP coisolated with the U1 snRNP has an unexpected protein composition and includes the splicing factor Aar2p. RNA 7: 1554-1565.

182. Boon K-L, Grainger RJ, Ehsani P, Barrass JD, Auchynnikava T, et al. (2007) prp8 mutations that cause human retinitis pigmentosa lead to a U5 snRNP maturation defect in yeas. Nat Struct Mol Biol 14: 1077-1083.

183. Weber G, Cristão VF, de L. Alves F, Santos KF, Holton N, et al. (2011) Mechanism for Aar2p function as a U5 snRNP assembly factor. Genes & Development 25: 1601-1612.

184. Weber G, Cristão VF, Santos KF, Jovin SM, Heroven AC, et al. (2013) Structural basis for dual roles of Aar2p in U5 snRNP assembly. Genes & Development 27: 525-540.

185. Verheggen C, Mouaikel J, Thiry M, Blanchard JM, Tollervey D, et al. (2001) Box C/D small nucleolar RNA trafficking involves small nucleolar RNP proteins, nucleolar factors and a novel nuclear domain. 5480-5490 p.

186. Smogorzewska A, de Lange T (2004) Regulation of telomerase by telomeric proteins. Annual Review of Biochemistry 73: 177-208.

187. Soudet J, Jolivet P, Teixeira Maria T (2014) Elucidation of the DNA End-Replication Problem in Saccharomyces cerevisiae. Molecular Cell 53: 954-964.

188. Osterhage JL, Friedman KL (2009) Chromosome End Maintenance by Telomerase. Journal of Biological Chemistry 284: 16061-16065.

189. Xu Z, Duc KD, Holcman D, Teixeira MT (2013) The Length of the Shortest Telomere as the Major Determinant of the Onset of Replicative Senescence. Genetics 194: 847-857.

190. Counter CM (1996) The roles of telomeres and telomerase in cell life span. MutatResRevGenetToxicol 366: 45-63.

191. Nabetani A, Ishikawa F (2011) Alternative lengthening of telomeres pathway: Recombination-mediated telomere maintenance mechanism in human cells. Journal of Biochemistry 149: 5-14.

192. Buchkovich KJ (1996) Telomeres, telomerase, and the cell cycle. Prog Cell Cycle Res 2: 187-195.

193. Egan ED, Collins K (2012) Biogenesis of telomerase ribonucleoproteins. RNA 18: 1747-1759.

194. Greider CW, Blackburn EH (1989) A telomeric sequence in the RNA of *Tetrahymena* telomerase required for telomere repeat synthesis. Nature 337: 331-337.

195. Hukezalie KR, Wong JMY (2013) Structure–function relationship and biogenesis regulation of the human telomerase holoenzyme. FEBS Journal 280: 3194-3204.

196. Peng Y, Mian IS, Lue NF (2001) Analysis of telomerase processivity: mechanistic similarity to HIV-1 reverse transcriptase and role in telomere maintenance. Mol Cell 7: 1201-1211.

197. Lue NF (2004) Adding to the ends: what makes telomerase processive and how important is it? BioEssays 26: 955-962.

198. Fu D, Collins K (2007) Purification of Human Telomerase Complexes Identifies Factors Involved in Telomerase Biogenesis and Telomere Length Regulation. Molecular Cell 28: 773-785.

199. Reichenbach P, Hoss M, Azzalin CM, Nabholz M, Bucher P, et al. (2003) A Human Homolog of Yeast Est1 Associates with Telomerase and Uncaps Chromosome Ends When Overexpressed. Curr Biol 13: 568-574.

200. Azzalin CM, Reichenbach P, Khoriauli L, Giulotto E, Lingner J (2007) Telomeric Repeat-Containing RNA and RNA Surveillance Factors at Mammalian Chromosome Ends. Science 318: 798-801.

201. Gatfield D, Unterholzner L, Ciccarelli FD, Bork P, Izaurralde E (2003) Nonsense-mediated mRNA decay in Drosophila:at the intersection of the yeast and mammalian pathways. 3960-3970 p.

202. Venteicher AS, Abreu EB, Meng Z, McCann KE, Terns RM, et al. (2009) A human telomerase holoenzyme protein required for Cajal body localization and telomere synthesis. Science 323: 644-648.

203. Stern JL, Zyner KG, Pickett HA, Cohen SB, Bryan TM (2012) Telomerase Recruitment Requires both TCAB1 and Cajal Bodies Independently. Molecular and Cellular Biology 32: 2384-2395.

204. Holohan B, Wright WE, Shay JW (2014) Telomeropathies: An emerging spectrum disorder. The Journal of Cell Biology 205: 289-299.

205. Egan ED, Collins K (2010) Specificity and Stoichiometry of Subunit Interactions in the Human Telomerase Holoenzyme Assembled In Vivo. Molecular and Cellular Biology 30: 2775-2786.

206. Angrisani A, Vicidomini R, Turano M, Furia M (2014) Human dyskerin: beyond telomeres. Biological Chemistry. pp. 593.

207. Chen J-L, Greider CW (2004) Telomerase RNA structure and function: implications for dyskeratosis congenita. Trends in Biochemical Sciences 29: 183-192.

208. Wang C, Meier UT (2004) Architecture and assembly of mammalian H/ACA small nucleolar and telomerase ribonucleoproteins. 23: 1857-1867.

209. Yang PK, Hoareau C, Froment C, Monsarrat B, Henry Y, et al. (2005) Cotranscriptional Recruitment of the Pseudouridylsynthetase Cbf5p and of the RNA Binding Protein Naf1p during H/ACA snoRNP Assembly. Molecular and Cellular Biology 25: 3295-3304.

210. Trahan C, Martel C, Dragon F (2010) Effects of dyskeratosis congenita mutations in dyskerin, NHP2 and NOP10 on assembly of H/ACA pre-RNPs. Human Molecular Genetics 19: 825-836.

211. Vulliamy T, Beswick R, Kirwan M, Marrone A, Digweed M, et al. (2008) Mutations in the telomerase component NHP2 cause the premature ageing syndrome dyskeratosis congenita. Proceedings of the National Academy of Sciences 105: 8073-8078.

212. Chung J, Khadka P, Chung IK (2012) Nuclear import of hTERT requires a bipartite nuclear localization signal and Akt-mediated phosphorylation. Journal of Cell Science 125: 2684-2697.

213. Chen L-Y, Liu D, Songyang Z (2007) Telomere Maintenance through Spatial Control of Telomeric Proteins. Molecular and Cellular Biology 27: 5898-5909.

214. Jády BE, Richard P, Bertrand E, Kiss T (2006) Cell Cycle-dependent Recruitment of Telomerase RNA and Cajal Bodies to Human Telomeres. Mol Biol Cell 17: 944-954.

215. Jády BE, Bertrand E, Kiss T (2004) Human telomerase RNA and box H/ACA scaRNAs share a common Cajal body–specific localization signal. The Journal of Cell Biology 164: 647-652.

216. Cristofari G, Adolf E, Reichenbach P, Sikora K, Terns RM, et al. (2007) Human Telomerase RNA Accumulation in Cajal Bodies Facilitates Telomerase Recruitment to Telomeres and Telomere Elongation. Molecular Cell 27: 882-889.

217. Tycowski KT, Shu M-D, Kukoyi A, Steitz JA (2009) A Conserved WD40 Protein Binds the Cajal Body Localization Signal of scaRNP Particles. Molecular Cell 34: 47-57.

218. Tomlinson RL, Li J, Culp BR, Terns RM, Terns MP (2010) A Cajal body-independent pathway for telomerase trafficking in mice. Experimental Cell Research 316: 2797-2809.

219. Li Z-H, Tomlinson RL, Terns RM, Terns MP (2010) Telomerase trafficking and assembly in Xenopus oocytes. Journal of Cell Science 123: 2464-2472.

220. Lee J, Lee Y, Jeong S, Khadka P, Roth J, et al. (2014) Catalytically active telomerase holoenzyme is assembled in the dense fibrillar component of the nucleolus during S phase. Histochemistry and Cell Biology 141: 137-152.

221. Hiyama E, Hiyama K (2007) Telomere and telomerase in stem cells. Br J Cancer 96: 1020-1024.

222. Hornsby PJ (2007) Telomerase and the aging process. Experimental Gerontology 42: 575-581.

223. Artandi SE, DePinho RA (2010) Telomeres and telomerase in cancer. Carcinogenesis 31: 9-18.

224. Nguyen B, Elmore LW, Holt SE (2003) Telomerase as a Target for Cancer Immunotherapy. Cancer Biology & Therapy 2: 131-136.

225. Zaug AJ, Crary SM, Jesse Fioravanti M, Campbell K, Cech TR (2013) Many disease-associated variants of hTERT retain high telomerase enzymatic activity. Nucleic Acids Research 41: 8969-8978.

226. Dokal I (2011) Dyskeratosis Congenita. ASH Education Program Book 2011: 480-486.

227. Carroll KA, Ly H (2009) Telomere dysfunction in human diseases: the long and short of it! Int J Clin Exp Pathol 2: 528-543.

228. Hreidarsson S, Kristjansson K, Johannesson G, Johannsson JH (1988) A Syndrome of Progressive Pancytopenia with Microcephaly, Cerebellar Hypoplasia and Growth Failure. Acta Pædiatrica 77: 773-775.

229. Sznajer Y, Baumann C, David A, Journel H, Lacombe D, et al. (2003) Further delineation of the congenital form of X-linked dyskeratosis congenita (Hoyeraal-Hreidarsson syndrome). European Journal of Pediatrics 162: 863-867.

230. Batista LFZ, Pech MF, Zhong FL, Nguyen HN, Xie KT, et al. (2011) Telomere shortening and loss of self-renewal in dyskeratosis congenita induced pluripotent stem cells. Nature 474: 399.

231. Mason PJ, Bessler M (2011) The genetics of dyskeratosis congenita. Cancer Genetics 204: 635-645.

232. Walne AJ, Vulliamy T, Marrone A, Beswick R, Kirwan M, et al. (2007) Genetic heterogeneity in autosomal recessive dyskeratosis congenita with one subtype due to mutations in the telomerase-associated protein NOP10. Human Molecular Genetics 16: 1619-1629.

233. Cronkhite JT, Xing C, Raghu G, Chin KM, Torres F, et al. (2008) Telomere Shortening in Familial and Sporadic Pulmonary Fibrosis. American Journal of Respiratory and Critical Care Medicine 178: 729-737.

234. Gross TJ, Hunninghake GW (2001) Idiopathic Pulmonary Fibrosis. New England Journal of Medicine 345: 517-525.

235. (2002) American Thoracic Society/European Respiratory Society International Multidisciplinary Consensus Classification of the Idiopathic Interstitial Pneumonias. American Journal of Respiratory and Critical Care Medicine 165: 277-304.

236. Tsakiri KD, Cronkhite JT, Kuan PJ, Xing C, Raghu G, et al. (2007) Adult-onset pulmonary fibrosis caused by mutations in telomerase. Proceedings of the National Academy of Sciences 104: 7552-7557.

237. Diaz de Leon A, Cronkhite JT, Katzenstein A-LA, Godwin JD, Raghu G, et al. (2010) Telomere Lengths, Pulmonary Fibrosis and Telomerase *TERT* Mutations. PLoS ONE 5: e10680.

238. Tsang AR, Wyatt HDM, Ting NSY, Beattie TL (2012) hTERT mutations associated with idiopathic pulmonary fibrosis affect telomerase activity, telomere length, and cell growth by distinct mechanisms. Aging Cell 11: 482-490.

239. Zhong Franklin L, Batista Luis FZ, Freund A, Pech Matthew F, Venteicher Andrew S, et al. (2012) TPP1 OB-Fold Domain Controls Telomere Maintenance by Recruiting Telomerase to Chromosome Ends. Cell 150: 481-494.

240. Steele MP, Speer MC, Loyd JE, Brown KK, Herron A, et al. (2005) Clinical and Pathologic Features of Familial Interstitial Pneumonia. American Journal of Respiratory and Critical Care Medicine 172: 1146-1152.

241. Kropski JA, Mitchell DB, Markin C, Polosukhin VV, Choi LA, et al. (2014) A novel dyskerin (dkc1) mutation is associated with familial interstitial pneumonia. CHEST Journal.

242. Young NS (2002) Acquired Aplastic Anemia. Annals of Internal Medicine 136: 534-546.

243. Dai WJ, Jiang HC (2001) Advances in gene therapy of liver cirrhosis: a review. World J Gastroenterol 7: 1-8.

244. Invernizzi P, Bernuzzi F, Lleo A, Pozzoli V, Bignotto M, et al. (2014) Telomere dysfunction in peripheral blood mononuclear cells from patients with primary biliary cirrhosis. Digestive and Liver Disease 46: 363-368.

245. Carulli L, Anzivino C (2014) Telomere and telomerase in chronic liver disease and hepatocarcinoma. World J Gastroenterol 20: 6287-6292.

246. Xin Z-T, Beauchamp AD, Calado RT, Bradford JW, Regal JA, et al. (2007) Functional characterization of natural telomerase mutations found in patients with hematologic disorders. Blood 109: 524-532.

247. Ziegler P, Schrezenmeier H, Akkad J, Brassat U, Vankann L, et al. (2012) Telomere elongation and clinical response to androgen treatment in a patient with aplastic

anemia and a heterozygous hTERT gene mutation. Annals of Hematology 91: 1115-1120.

248. Blackburn EH, Greider CW, Szostak JW (2006) Telomeres and telomerase: the path from maize, Tetrahymena and yeast to human cancer and aging. Nat Med 12: 1133-1138.

249. Gorovsky MA (1980) Genome Organization and Reorganization in Tetrahymena. Annual Review of Genetics 14: 203-239.

250. Greider CW, Blackburn EH (1985) Identification of a specific telomere terminal transferase activity in *Tetrahymena* extracts. Cell 43: 405-413.

251. Greider CW, Blackburn EH (1987) The telomere terminal transferase of *Tetrahymena* is a ribonucleoprotein enzyme with two kinds of primer specificity. Cell 51: 887-898.

252. Szostak JW, Blackburn EH (1982) Cloning yeast telomeres on linear plasmid vectors. Cell 29: 245-255.

253. Shampay J, Szostak JW, Blackburn EH (1984) DNA sequences of telomeres maintained in yeast. Nature 310: 154-157.

254. Lundblad V, Szostak JW (1989) A mutant with a defect in telomere elongation leads to senescence in yeast. Cell 57: 633-643.

255. Dancis BM, Holmquist GP (1979) Telomere replication and fusion in eukaryotes. Journal of Theoretical Biology 78: 211-224.

256. Walmsley RW, Chan CSM, Tye B-K, Petes TD (1984) Unusual DNA sequences associated with the ends of yeast chromosomes. Nature 310: 157-160.

257. Boeke J, La Croute F, Fink G (1984) A positive selection for mutants lacking orotidine-5′-phosphate decarboxylase activity in yeast: 5-fluoro-orotic acid resistance. Molecular and General Genetics MGG 197: 345-346.

258. Lustig AJ, Petes TD (1986) Identification of yeast mutants with altered telomere structure. ProcNatlAcadSciUSA 83: 1398-1402.

259. Greenwell PW, Kronmal SL, Porter SE, Gassenhuber J, Obermaier B, et al. (1995) *TEL1*, a gene involved in controlling telomere length in *S. cerevisiae*, is homologous to the human ataxia telangiectasia gene. Cell 82: 823-829.

260. Ritchie KB, Mallory JC, Petes TD (1999) Interactions of TLC1 (Which Encodes the RNA Subunit of Telomerase), TEL1, and MEC1 in Regulating Telomere Length in the Yeast Saccharomyces cerevisiae. Molecular and Cellular Biology 19: 6065-6075.

261. Forstemann K, Hoss M, Lingner J (2000) Telomerase-dependent repeat divergence at the 3' ends of yeast telomeres. Nucleic Acids Res 28: 2690-2694.

262. Lendvay TS, Morris DK, Sah J, Balasubramanian B, Lundblad V (1996) Senescence mutants of *Saccharomyces cerevisiae* with a defect in telomere replication identify three additional *EST* genes. Genetics 144: 1399-1412.

263. Hieter P, Mann C, Snyder M, Davis RW (1985) Mitotic stability of yeast chromosomes: A colony color assay that measures nondisjunction and chromosome loss. Cell 40: 381-392.

264. Spencer F, Gerring SL, Connelly C, Hieter P (1990) Mitotic chromosome transmission fidelity mutants in Saccharomyces cerevisiae. Genetics 124: 237-249.

265. Ugolini S, Bruschi CV (1996) The red/white colony color assay in the yeast Saccharomyces cerevisiae: epistatic growth advantage of white ade8-18, ade2 cells over red ade2 cells. Current Genetics 30: 485-492.

266. Singer MS, Gottschling DE (1994) *TLC1*: Template RNA component of *Saccharomyces cerevisiae* telomerase. Science 266: 404-409.

267. Lundblad V, Blackburn EH (1993) An alternative pathway for yeast telomere maintenance rescues *est1*$^{-}$ senescence. Cell 73: 347-360.

268. Nugent CI, Hughes TR, Lue NF, Lundblad V (1996) Cdc13p: A single-strand telomeric DNA binding protein with a dual role in yeast telomere maintenance. Science 274: 249-252.

269. Evans SK, Lundblad V (1999) Est1 and Cdc13 as comediators of telomerase access. Science 286: 117-120.

270. Wood JS, Hartwell LH (1982) A dependent pathway of gene functions leading to chromosome segregation in Saccharomyces cerevisiae. The Journal of Cell Biology 94: 718-726.

271. Wellinger RJ, Zakian VA (2012) Everything You Ever Wanted to Know About Saccharomyces cerevisiae Telomeres: Beginning to End. Genetics 191: 1073-1105.

272. Lingner J, Hughes TR, Shevchenko A, Mann M, Lundblad V, et al. (1997a) Reverse transcriptase motifs in the catalytic subunit of telomerase. Science 276: 561-567.

273. Lingner J, Cech TR, Hughes TR, Lundblad V (1997b) Three Ever Shorter Telomere (*EST*) genes are dispensable for *in vitro* yeast telomerase activity. PNAS USA 94: 11190-11195.

274. Zhou J, Hidaka K, Futcher B (2000) The Est1 subunit of yeast telomerase binds the Tlc1 telomerase RNA. Mol Cell Biol 20: 1947-1955.

275. Seto AG, Livengood AJ, Tzfati Y, Blackburn EH, Cech TR (2002) A bulged stem tethers Est1p to telomerase RNA in budding yeast. Genes Dev 16: 2800-2812.

276. Lubin JW, Tucey TM, Lundblad V (2012) The interaction between the yeast telomerase RNA and the Est1 protein requires three structural elements. RNA 18: 1597-1604.

277. Laterreur N, Eschbach SH, Lafontaine DA, Wellinger RJ (2013) A new telomerase RNA element that is critical for telomere elongation. Nucleic Acids Research 41: 7713-7724.

278. Talley JM, DeZwaan DC, Maness LD, Freeman BC, Friedman KL (2011) Stimulation of yeast telomerase activity by the Ever Shorter Telomere 3 (Est3) subunit is dependent on direct interaction with the catalytic protein Est2. J Biol Chem 286: 26431-26439.

279. Tuzon CT, Wu Y, Chan A, Zakian VA (2011) The *Saccharomyces cerevisiae* telomerase subunit Est3 binds telomeres in a cell cycle- and Est1-dependent manner and interacts directly with Est1 *in vitro*. PLoS Genet 7: e1002060.

280. Evans SK, Lundblad V (2002) The Est1 subunit of *Saccharomyces cerevisiae* telomerase makes multiple contributions to telomere length maintenance. Genetics 162: 1101-1115.

281. DeZwann DC, Freeman BC (2009) The conserved Est1 protein stimulates telomerase DNA extension activity. PNAS USA 103: 17337-17342.

282. Wu Y, Zakian VA (2011) The telomeric Cdc13 protein interacts directly with the telomerase subunit Est1 to bring it to telomeric DNA ends *in vitro*. PNAS 108: 20362-20369.

283. Snow BE, Erdmann N, Cruickshank J, Goldman H, Gill RM, et al. (2003) Functional Conservation of the Telomerase Protein Est1p in Humans. Curr Biol 13: 698-704.

284. Beernink HTH, Miller K, Deshpande A, Bucher P, Cooper JP (2003) Telomere Maintenance in Fission Yeast Requires an Est1 Ortholog. Curr Biol 13: 575-580.

285. Moser BA, Chang Y-T, Kosti J, Nakamura TM (2013) $Tel1^{ATM}$ and $Rad3^{ATR}$ kinases promote Ccq1-Est1 interaction to maintain telomeres in fission yeast. Nat Struct Mol Biol 18: 1408-1413.

286. Ferguson JL, Chao WCH, Lee E, Friedman KL (2013) The Anaphase Promoting Complex contributes to the degradation of the *S. cerevisiae* telomerase recruitment subunit Est1p. PLoS ONE 8: e55055.

287. Peterson SE, Stellwagen AE, Diede SJ, Singer MS, Haimberger ZW, et al. (2001) The function of a stem-loop in telomerase RNA is linked to the DNA repair protein Ku. Nat Genet 27: 64-67.

288. Stellwagen AE, Haimberger ZW, Veatch JR, Gottschling DE (2003) Ku interacts with telomerase RNA to promote telomere addition at native and broken chromosome ends. Genes & Development 17: 2384-2395.

289. Fisher TS, Taggart AKP, Zakian VA (2004) Cell cycle-dependent regulation of yeast telomerase by Ku. Nat Struct Mol Biol 11: 1198-1205.

290. Taggart AKP, Teng S-C, Zakian VA (2002) Est1p as a cell cycle-regulated activator of telomere-bound telomerase. Science 297: 1023-1026.

291. Gallardo F, Olivier C, Dandjinou AT, Wellinger RJ, Chartrand P (2008a) TLC1 RNA nucleo-cytoplasmic trafficking links telomerase biogenesis to its recruitment to telomeres. EMBO J 27: 748-757.

292. Chappell AS, Lundblad V (2004) Structural Elements Required for Association of the Saccharomyces cerevisiae Telomerase RNA with the Est2 Reverse Transcriptase. Molecular and Cellular Biology 24: 7720-7736.

293. Gallardo F, Laterreur N, Cusanelli E, Ouenzar F, Querido E, et al. (2011) Live cell imaging of telomerase RNA dynamics reveals cell cycle-dependent clustering of telomerase at elongating telomeres. Mol Cell 44: 819-827.

294. Teixeira MT, Foerstemann K, Gasser SM, Lingner J (2002) Intracellular trafficking of yeast telomerase components. EMBO Rep 3: 652-659.

295. Blackburn EH (1994) Telomeres: No end in sight. Cell 77: 621-623.

296. Hughes TR, Evans SK, Weilbaecher RG, Lundblad V (2000) The Est3 protein is a subunit of yeast telomerase. Curr Biol 10: 809-812.

297. Livengood AJ, Zaug AJ, Cech TR (2002) Essential regions of *Saccharomyces cerevisiae* telomerase RNA: separate elements for Est1p and Est2p interaction. Mol Cell Biol 22: 2366-2374.

298. Chan A, Boule J-B, Zakian VA (2008) Two pathways recruit telomerase to *Saccharomyces cerevisiae* telomeres. PLoS Genet 4: e1000236.

299. Gravel S, Larrivee M, Labrecque P, Wellinger RJ (1998) Yeast Ku as a regulator of chromosomal DNA end structure. Science 280: 741-744.

300. Ferrezuelo F, Steiner B, Aldea M, Futcher B (2002) Biogenesis of yeast telomerase depends on the importin Mtr10. Mol Cell Biol 22: 6046-6055.

301. Ghaemmaghami S, Huh W, Bower K, Howson R, Belle A, et al. (2003) Global analysis of protein expression in yeast. Nature 425: 737-741.

302. Huh W-K, Falvo JV, Gerke LC, Carroll AS, Howson RW, et al. (2003) Global analysis of protein localization in budding yeast. Nature 425: 686-691.

303. Sambrook J, Russel DW (2001) Molecular cloning: A laboratory manual. Cold Spring Harbor, NY: Cold Spring Harbor Laboratory Press.

304. Goldstein AL, McCusker JH (1999) Three new dominant drug resistance cassettes for gene disruption in *Saccharomyces cerevisiae*. Yeast 15: 1541-1553.

305. Irniger S, Nasmyth K (1997) The anaphase-promoting complex is required in G1 arrested yeast cells to inhibit B-type cyclin accumulation and to prevent uncontrolled entry into S-phase. J Cell Sci 110: 1523-1531.

306. Senger B, Simos G, Bischoff FR, Podtelejnikov A, Mann M, et al. (1998) Mtr10p functions as a nuclear import receptor for the mRNA-binding protein Npl3p. EMBO J 17: 2196-2207.

307. Lange A, McLane LM, Mills RE, Devine SE, Corbett AH (2010) Expanding the definition of the classical bipartite nuclear localization signal. Traffic 11: 311-323.

308. Ferrigno P, Posas F, Koepp D, Saito H, Silver PA (1998) Regulated nucleo/cytoplasmic exchange of HOG1 MAPK requires the importin beta homologs *NMD5* and *XPO1*. EMBO J 17: 5606-5614.

309. Stage-Zimmermann T, Schmidt U, Silver PA (2000) Factors affecting nuclear export of the 60S ribosomal subunit *in vivo*. Mol Biol Cell 11: 3777-3789.

310. Seedorf M, Silver PA (1997) Importin/karyopherin protein family members required for mRNA export from the nucleus. PNAS 94: 8590-8595.

311. Horton RM, Hunt HD, Ho SN, Pullen JK, Pease LR (1989) Engineering hybrid genes without the use of restriction enzymes: gene splicing by overlap extension. Gene 77: 61-68.

312. Bevis BJ, Hammond AT, Reinke CA, Glick BS (2002) *De novo* formation of transitional ER sites and Golgi structures in *Pichia pastoris*. Nat Cell Biol 4: 750-756.

313. Wach A, Brachat A, Alberti-Segui C, Rebischung C, Philippsen P (1997) Heterologous *HIS3* marker and GFP reporter modules for PCR-targeting in *Saccharomyces cerevisiae*. Yeast 13: 1065-1075.

314. Sikorski RS, Hieter P (1989) A system of shuttle vectors and yeast host strains designed for efficient manipulation of DNA in *Saccharomyces cerevisiae*. Genetics 122: 19-27.

315. Hodel AE, Harreman MT, Pulliam KF, Harben ME, Holmes JS, et al. (2006) Nuclear localization signal receptor affinity correlates with *in vivo* localization in *Saccharomyces cerevisiae*. J Biol Chem 281: 23545-23556.

316. Hacker S, Krebber H (2004) Differential export requirements for shuttling serine/arginine-type mRNA-binding proteins. J Biol Chem 279: 5049-5052.

317. Green DM, Marfatia KA, Crafton EB, Zhang X, Cheng X, et al. (2002) Nab2p Is required for Poly(A) RNA export in *Saccharomyces cerevisiae* and is regulated by arginine methylation via Hmt1p. J Biol Chem 277: 7752-7760.

318. Zhang Z, An X, Yang K, Perlstein DL, Hicks L, et al. (2006) Nuclear localization of the *Saccharomyces cerevisiae* ribonucleotide reductase small subunit requires a karyopherin and a WD40 repeat protein. PNAS 103: 1422-1427.

319. Schneider CA, Rasband WS, Eliceiri KW (2012) NIH Image to ImageJ: 25 years of image analysis. Nat Meth 9: 671-675.

320. Hoffman CS, Winston F (1987) A ten-minute DNA preparation from yeast efficiently releases autonomous plamids for transformation of *Escherichia coli*. Gene 57: 267-272.

321. Ji H, Adkins CJ, Cartwright BR, Friedman KL (2008) Yeast Est2p affects telomere length by influencing association of Rap1p with telomeric chromatin. Mol Cell Biol 28: 2380-2390.

322. Bairley RCB, Guillaume G, Vega LR, Friedman KL (2011) A mutation in the catalytic subunit of yeast telomerase alters primer–template alignment while promoting processivity and protein–DNA binding. J Cell Sci 124: 4241-4252.

323. Wright AP, Bruns M, Hartley BS (1989) Extraction and rapid inactivation of proteins from *Saccharomyces cerevisiae* by trichloroacetic acid precipitation. Yeast 5: 51-53.

324. Kito S, Shimizu K, Okamura H, Yoshida K, Morimoto H, et al. (2003) Cleavage of nucleolin and argyrophilic nucleolar organizer region associated proteins in apoptosis-induced cells. Biochem Biophys Res Comm 300: 950-956.

325. Mozdy AD, Cech TR (2006) Low abundance of telomerase in yeast: Implications for telomerase haploinsufficiency. RNA 12: 1721-1737.

326. Teng S-C, Zakian VA (1999) Telomere-telomere recombination is an efficient bypass pathway for telomere maintenance in *Saccharomyces cerevisiae*. Mol Cell Biol 19: 8083-8093.

327. Seibel NM, Eljouni J, Nalaskowski MM, Hampe W (2007) Nuclear localization of enhanced green fluorescent protein homomultimers. Analyt Biochem 368: 95-99.

328. Nakai K, Kanehisa M (1992) A knowledge base for predicting protein localization sites in eukaryotic cells. Genomics 14: 897-911.

329. Nakai K, Horton P (1999) PSORT: a program for detecting sorting signals in proteins and predicting their subcellular localization. Trends in Biochem Sci 24: 34-35.

330. Cokol M, Nair R, Rost B (2000) Finding nuclear localization signals. EMBO Rep 1: 411-415.

331. Kosugi S, Hasebe M, Tomita M, Yanagawa H (2009) Systematic identification of cell cycle-dependent yeast nucleocytoplasmic shuttling proteins by prediction of composite motifs. PNAS USA 106: 10171-10176.

332. Kosugi S, Hasebe M, Matsumura N, Takashima H, Miyamoto-Sato E, et al. (2009) Six classes of nuclear localization signals specific to different binding grooves of importin alpha. J Biol Chem 284: 478-485.

333. Pemberton LF, Rosenblum JS, Blobel G (1997) A distinct and parallel pathway for the nuclear import of an mRNA-binding protein. J Cell Biol 139: 1645-1653.

334. Titov AA, Blobel G (1999) The karyopherin Kap122p/Pdr6p imports both subunits of the transcription factor IIa into the nucleus. J Cell Biol 147: 235-246.

335. Wu X, Huang M (2008) Dif1 controls subcellular localization of ribonucleotide reductase by mediating nuclear import of the R2 subunit. Mol Cell Biol 28: 7156-7167.

336. Görlich D, Kostka S, Kraft R, Dingwall C, Laskey RA, et al. (1995) Two different subunits of importin cooperate to recognize nuclear localization signals and bind them to the nuclear envelope. Curr Biol 5: 383-392.

337. Görlich D, Vogel F, Mills AD, Hartmann E, Laskey RA (1995) Distinct functions for the two importin subunits in nuclear protein import. Nature 377: 246-248.

338. Yano R, Oakes ML, Tabb MM, Nomura M (1994) Yeast Srp1p has homology to armadillo/plakoglobin/beta-catenin and participates in apparently multiple nuclear functions including the maintenance of the nucleolar structure. PNAS USA 91: 6880-6884.

339. Koepp DM, Wong DH, Corbett AH, Silver PA (1996) Dynamic localization of the nuclear import receptor and its interactions with transport factors. J Cell Biol 133: 1163-1176.

340. Romano GH, Harari Y, Yehuda T, Podhorzer A, Rubinstein L, et al. (2013) Environmental stresses disrupt telomere length homeostasis. PLoS Genet 9: e1003721.

341. Underwood M, Fried H (1990) Characterization of nuclear localizing sequences derived from yeast ribosomal protein L29. EMBO J 9: 91-99.

342. Schaap P, van't Ried J, Woldringh C, Raue H (1991) Identification and functional analysis of the nuclear localization signals of ribosomal protein L25 from *Saccharomyces cerevisiae*. J Mol Biol 221: 225-237.

343. Burich R, Lei M (2003) Two bipartite NLSs mediate constitutive nuclear localization of Mcm10. Curr Genet 44: 195-201.

344. Theimer CA, Feigon J (2006) Structure and function of telomerase RNA. Current Opinion in Structural Biology 16: 307-318.

345. Ribeyre C, Shore D (2013) Regulation of telomere addition at DNA double-strand breaks. Chromosoma 122: 159-173.

346. Jang B-C, Muñoz-Najar U, Paik J-H, Claffey K, Yoshida M, et al. (2003) Leptomycin B, an Inhibitor of the Nuclear Export Receptor CRM1, Inhibits COX-2 Expression. Journal of Biological Chemistry 278: 2773-2776.